
Theses

Dissertations and Theses


2021

Laser-Scribed Graphene Electrodes as Inflammatory Biosensors (LASERFLAME)

Pei Shee Tan

Department of Biological and Pharmaceutical Science, Munster Technological University, Kerry, Ireland.

Follow this and additional works at: <https://sword.cit.ie/allthe>

 Part of the [Biology Commons](#), and the [Biotechnology Commons](#)

Recommended Citation

Shee Tan, Pei, "Laser-Scribed Graphene Electrodes as Inflammatory Biosensors (LASERFLAME)" (2021).
Theses [online].

Available at: <https://sword.cit.ie/allthe/780>

This Master Thesis is brought to you for free and open access by the Dissertations and Theses at SWORD - South West Open Research Deposit. It has been accepted for inclusion in Theses by an authorized administrator of SWORD - South West Open Research Deposit. For more information, please contact sword@cit.ie.

Laser-Scribed Graphene Electrodes as Inflammatory Biosensors (LASERFLAME)

Pei Shee Tan

A Thesis Submitted in Fulfilment of the Requirements for
The Degree of Masters of Science

Research Supervisors

Dr. Joanna B. Tierney

Dr. Niall Burke

Dr. Daniela Iacopino

Department of Biological and Pharmaceutical Science
School of Science, Technology, Engineering and Mathematics

MTU Kerry



Submitted

April 2021

Abstract

Laser-scribed graphene electrodes (LSGE) are a low cost, portable, flexible and ideal electrochemical platform approach as point of care biosensors. It is anticipated that integrating the detection of immune cell inflammatory cytokines with LSGEs may present a useful diagnostic platform for managing the risk of inflammatory diseases as early detection of inflammatory molecules could significantly improve the treatment and outcome of diseases induced by protracted inflammation, such as cancer, asthma and rheumatoid arthritis.

This study proposed LSGE first time novel use in the detection of an inflammatory cytokine released by immune cells (monocyte THP-1 cell line), with high sensitivity and short response time compared to conventional detection techniques like ELISA. Monocyte THP-1 cells were differentiated into macrophages using phorbol 12-myristate 13-acetate and polarised into classically activated macrophages (M1), responsible for pro-inflammatory responses, with interferon-gamma (IFN- γ) and lipopolysaccharide (LPS). THP-1 macrophages were additionally polarised into alternatively activated macrophages (M2), responsible for anti-inflammatory responses, with interleukin-4 (IL-4) and interleukin-13 (IL-13). To confirm inflamed cell states, cytokine and surface marker expression were assessed by ELISA and flow cytometry respectively. It was confirmed that M1 macrophage phenotype secreted the inflammatory cytokine IL-6 and expressed CD80 surface marker. M2 macrophage phenotypes secreted fibronectin and expressed mannose receptor CD206.

IL-6 antigen was biofunctionalised onto the LSGE as the bioreceptor to enable the biosensor to detect IL-6 antibody. The LSGE was functionalised with 1-pyrenebutyric acid (PBA) and EDC/NHS to create a linker that immobilised the bioreceptor, IL-6 antigen onto the surface of LSGE. The linear detection range of the LSGE biosensor was from 10 pg/mL to 500 pg/mL in physiological buffer solutions with interfering agents such as serum albumin showing no effect on biosensor detection ability.

Acknowledgments

Firstly, I would like to thank the Institute of Technology Tralee for providing financial support throughout the postgraduate research degree scholarship program. I would also like to thank Shannon Applied Biotechnology Centre and Tyndall National Institute, University College Cork for having the facilities to assist the course.

Special thanks to my supervisors, Dr. Joanna Tierney, Dr. Niall Burke from Shannon ABC, and Dr. Daniella Iacopino from Tyndall National Institute, UCC for all the support, guidance and valuable knowledge. Not only academic support, I also want to thank my supervisors for encouraging me through this master study, especially during COVID-19 period.

I would like to express my gratitude to Shannon ABC research scientists including Dr. Aoife Curran and Dr. Najla Jouini for all their help in the lab throughout this research. I would like to express my gratitude to Tyndall National Institute Phd students, Jahidul Islam and Eoghan Vaughan for fabricating Laser Scribed Graphene Electrode and also provide the training to use the Laser Scribed Graphene Electrode and Origin Software.

Special thanks to Daniel Riordan from IMaR who lent me the potentiostat and Joanne Holmes from Metrohm who provided training to use the potentiostat. I would also like to express my gratitude to the centre manager of Shannon ABC, Tim Yeomans to help with organising out of hours access to Shannon ABC lab.

List of Abbreviations

AuNP - Gold Nanoparticles

BSA – Bovine Serum Albumin

CAP - Community-acquired Pneumonia

CRP – C-Reactive Protein

CV - Cyclic Voltammetry

DPV – Differential Pulse Voltammetry

EDC - 1-Ethyl-3-(3-dimethylaminopropyl)carbodiimide

EIS - Electrochemical Impedance Spectroscopy

ELISA - Enzyme-linked Immunosorbent Assay

FETs - Field-Effect Transistors

IFN- γ - Interferon-Gamma

IL-6 – Interleukin 6

iNOS - inducible Nitric Oxide Synthase

JAK - Janus Kinase

LPS – Lipopolysaccharide

LSGE – Laser Scribed Graphene Electrode

M0 – Differentiated Macrophage

M1- Classically Activated Macrophage

M2 – Alternatively Activated Macrophage

MCD - Minimal Change Disease

MIP - Molecularly-Imprinted Polymer

NF- κ B - Nuclear Factor Kappa B

NHS - N-hydroxysuccinimide

PBA – 1-Pyrenebutyric Acid

PBMC - Peripheral Blood Mononuclear Cell

PBS – Phosphate Buffered Saline

PMA - Phorbol-12-Myristate-13-Acetate

QCM - Quartz Crystals Biosensors

RA - Rheumatoid Arthritis

SAM - Surface Acoustic Wave

SOCS - Suppressor of Cytokine Signaling

SPE - Screen Printed Carbon Electrode

SPR - Surface Plasmon Resonance

STAT - Signal Transducer and Activator of Transcription

TAM - Tumour-Associated Macrophages

TNF- α - Tumour Necrosis Factor-Alpha

Table of Contents

Abstract	i
Acknowledgments	ii
List of Abbreviations	iii
List of Figures	ix
List of Tables	xi
Chapter 1. Introduction	1
1.1 Introduction to the Biosensor Market.....	2
1.2 Research Needs.....	3
1.3 Aim	4
1.4 Objectives.....	4
Chapter 2. Literature Review	5
2.1 Immune System	6
2.2. Macrophages.....	7
2.3 Macrophage Activation	10
2.3.1 Classically Activated Macrophages; (M1)	11
2.3.2 Alternatively Activated Macrophages (M2).....	12
2.4. Inflammation	13
2.4.1 Atherosclerosis	14
2.4.2 Osteoarthritis	15
2.4.3. Asthma.....	15
2.4.4. Tumour Associated Macrophages (TAM)	16
2.5. Biomarkers for Chronic Inflammation	17
2.5.1 C-Reactive Protein.....	17
2.5.2 IL-6.....	18
2.5.3 CD206.....	20

2.5.4 CD80.....	21
2.5.5 Fibronectin	22
2.5.6 Other	22
2.6. Immune Effector Cell Models	22
2.7 Biosensors.....	24
2.8. Types of Bioreceptors.....	27
2.9. Methods of Detection	28
2.9.1 Optical-Based Biosensor	28
2.9.2 Mass-Based Biosensor.....	28
2.9.3 Electrochemical-Based Biosensor	29
2.10. IL-6 Biosensor	31
2.11. Graphene	33
2.12. Laser Scribed Graphene Electrode	34
2.12.1 LSGE Glucose Biosensors	36
2.12.2 Aptamer-Based LSGE Biosensor	38
2.12.3 Others	39
Chapter 3. Materials and Methods.....	41
3.1 Culture of THP-1 Cells.....	42
3.1.1 Cell Resuscitation	42
3.1.2 Cell Viability Counts	42
3.1.3 Cell Subculture	43
3.1.4 Cell Cryopreservation	43
3.2. Differentiation and Polarisation of THP-1 Cells	43
3.2.1 Differentiation of THP-1 cells to Macrophage; M0	43
3.2.2 Polarisation to Classically Activated Macrophage; M1	44
3.2.3 Polarisation to Alternative Activated Macrophage; M2.....	44
3.3. Characterisation of THP-1 Cell Polarisation to Macrophage	45

3.3.1 Macrophage Cell Secretion; ELISA	45
3.3.2 Flow Cytometry of Macrophage Surface Markers.....	46
3.4. Antibody Selection for Biofunctionalisation of LGSE	47
3.5. Fabrication of LSGE	47
3.6. Characterisation of LSGE.....	48
3.7. LSGE BioFunctionalisation.....	49
3.7.1 Preparation of LSGE for BioFunctionalisation.....	50
3.7.2 Optimisation of LSGE Biosensor	51
3.8. Calibration of LSGE Biosensor.....	53
3.9. Method Comparison; LSGE Biosensor vs ELISA.....	53
3.10. Specificity and Selectivity of LSGE Biosensor.....	53
Chapter 4. Results	55
4.1 THP-1 Cells Differentiation and Polarisation	56
4.2 Macrophage Cell Secretion; ELISA	57
4.3 Cell Surface Marker Expression by Flow Cytometry	59
4.5. Characterisation of LSGE.....	63
4.6. LSGE BioFunctionalisation.....	64
4.7. Optimisation of LSGE Modification.....	67
4.7.1 PBA Optimisation.....	67
4.7.2 EDC/NHS Optimisation.....	68
4.7.3 IL-6 Antigen Optimisation.....	70
4.8. Calibration Curve for IL-6 LSGE Biosensor.....	71
4.9. Method Comparison; Biosensor vs ELISA.....	72
4.9. Specificity and Selectivity of LSGE.....	73
Chapter 5. Discussion and Conclusion	76
5.1 ELISA	78
5.2. Flow Cytometry	79

5.3. Fabrication and Characterisation of LSGE	80
5.4. LSGE Functionalisation	80
5.5. Optimisation for Modification of LSGE.....	82
5.6. Calibration curve for IL-6 with LSGE	83
5.7. Specificity and Selectivity of LSGE.....	84
5.8. Future Work.....	85
5.9. Conclusion.....	86
Bibliography	88

List of Figures

Figure Title	Page
Figure 2.1. Cells in the innate and adaptive immune system, (Sharpe and Mount, 2015).....	7
Figure 2.2. The development of monocytes to macrophages in the human body, (Gordon, 2003).....	9
Figure 2.3. Activation pathway of macrophage into different phenotypes with various stimulants, (Two Types of Macrophages: M1 and M2 Macrophages - Cusabio, 2019).....	12
Figure 2.4. Biological activities of IL-6, (MouseDoctor, 2013).	19
Figure 2.5. THP-1 cells, (THP-1 ATCC® TIB-202TM, 2016).	24
Figure 2.6. Biosensor components, (Zhou, Fang and Ramasamy, 2019).....	25
Figure 2.7. Classification of biosensors based on bioreceptors and transducer system, (Hassani et al., 2017).....	26
Figure 2.8. SPR optical biosensor, (Patricia, 2004)	28
Figure 2.9. Image of A) a packaged device for electrochemical testing, and B) needle-shaped electrode, (Russell et al., 2019).....	31
Figure 2.10. Schematic process for modification of the glassy carbon electrode, (Tertis et al., 2019).....	32
Figure 2.11. Structure of Graphene, (Science, 2017).	34
Figure 2.12. Schematic progress of fabrication and modification of DVD-laser scribed graphene (LSG), (Lin et al.2018).....	37
Figure 2.13. LSGE fabrication and functionalisation process, (Fenzl et al., 2017).	38
Figure 2.14. Electrochemical detection mechanism of thrombin, (Fenzl et al., 2017).....	39
Figure 3.1. A) Schematic of the LIG fabrication process, (Vaughan et al., 2020). B) Fabricated LSG electrode (3mm).	48
Figure 3.2. Electrochemical Cell Setup. including LSGE as working electrode, Ag/AgCl as reference electrode and Platinum wire as the counter electrode. ...	49
Figure 3.3. Biofunctionalisation of LSGE.	51
Figure 3.4. Graphene functionalisation with PBA.....	52

Figure 3.5. EDC/NHS coupling reaction mechanism, (Thermoscientific, 2012).	52
Figure 4.1. Differentiation and polarisation of THP-1 cells; from monocytes (A) into; (B) macrophages (M0); (C) classically activated macrophages (Inflammatory) (M1); and (D) Alternatively activated phenotypes (anti-inflammatory) (M2).	56
Figure 4.2. IL-6 secretion by different THP-1 cell phenotypes.	57
Figure 4.3. Fibronectin secretion by different THP-1 cell phenotypes.....	58
Figure 4.4. Flow cytometry analysis of cell size (SSC-A) and granularity (FSC-A) of different THP-1 phenotypes; M0, M1 and M2.	60
Figure 4.5. Flow cytometry analysis of surface marker expression A) CD80-FITC and B) CD206-PE of different THP-1 cell monocytes, M0, M1 and M2 macrophages.	62
Figure 4.6. Cyclic Voltammograms.	63
Figure 4.7. Randles-Sevcik plot;	64
Figure 4.8. Differential Pulse Voltammograms of LSGE A) without and B) with functionalisation..	65
Figure 4.9. Cyclic Voltammogram of LSGE after each functionalisation step..	66
Figure 4.10. Cyclic Voltammogram of LSGE functionalised with various concentrations of 1-pyrenebutyric acid (PBA).....	68
Figure 4.11. Change in DPV peak with various IL-6 antigen concentrations on LSGE.	70
Figure 4.12. Calibration curve for IL-6 Biosensor.....	72
Figure 4.13. Method Comparison of LSGE Biosensor versus ELISA.	73
Figure 4.14. Specificity of LSGE Biosensor for IL-6 in A) 10% Fetal Bovine Serum B) 10% Bovine Serum Albumin (BSA) from 10 to 500 pg/mL.	74
Figure 4.15. Change in peak current for IL-6 detection in PBS, 10% Serum and 10% BSA with three replicates for IL-6 antibody concentrations across 10 and 500 pg/mL.....	75

List of Tables

Table Title	Page
Table 2.1. Table of the inducers, cell markers, cytokines and chemokines secreted and the functions of different subtypes of alveolar macrophages. Table taken from (Jiang and Zhu, 2016).	16
Table 2.2. Different types of electrochemical biosensors for the detection of IL-6, (Khan and Mujahid, 2020).	33
Table 2 3. Comparison of different methods to fabricate graphene, (Huang et al., 2020).	35
Table 4.1. CD80 and CD 206 surface marker expression in different THP-1 cell phenotypes.	61
Table 4.2. CV and DPV of LSGE with different EDC and NHS concentrations.	69

Chapter 1. Introduction

1.1 Introduction to the Biosensor Market

The press released by iHealthcareAnalyst, Inc on 30 June 2020 estimated that by 2027, the global market for biosensor devices will reach 27.1 Billion USD due to the wider usage of low cost non-invasive medical products and the increasing acceptance by health practitioners and the general public. A huge number of investments have been poured into biosensor technology worldwide. The electrochemical biosensors segment accounted for more than 70% of the total market and is widely used for most glucose diagnostic biosensor devices (IHealthcareAnalyst, 2020).

The recent Coronavirus pandemic has put the world into lockdown. This further strengthens the importance of early diagnostics for the control and spread of diseases. There is an increasing need for the early diagnosis of chronic diseases such as early-stage cancer and for the detection of infection/pathogens, supporting the development of point-of-care biosensors. Instead of using RT-PCR which takes at least 3 hours for testing excluding samples transfer to the laboratory and sample preparation time to get accurate results, researchers have been working hard to find alternative biosensors that can save time and provide accurate results.

Graphene has attracted researchers' attention as the material for electrodes due to its excellent electrical properties, mechanical strength and large surface area. Research has been published using various types of graphene biosensors such as graphene-based fluorescent biosensor, graphene-based electrochemistry biosensor and graphene-based surface plasmon resonance biosensor (Bai, Xu and Zhang, 2020). Graphene biosensors hold great potential as graphene can produce a highly sensitive biosensor due to the porous surface that increases the surface area for antibody attachment.

Different methods have been developed to fabricate graphene and Laser Scribed Graphene Electrodes (LSGE) stand out due to their high porosity which increases the surface area for bioreceptor immobilisation. As well as this they have good electrical and thermal conductivity, good flexibility and are mechanically robust, making LSGEs a potential candidate for the development of miniaturised biosensors. The size and shape of the LSGEs can be also easily controlled by

computer design (Huang et al., 2020). This process is cost-effective and time-saving making them suitable as a point of care biosensor electrodes (Kumar et al., 2015).

The LSGE biosensor is constantly employed by researchers to incorporate different bioreceptors and different transducers. However, no antibody-based LSGE has been reported yet in the literature and specifically the use of LSGEs for the detection of inflammation.

1.2 Research Needs

Inflammation is the response of our body's immune system to injury and infection. Inflammation can be subcategorised as either acute or chronic inflammation. Acute inflammation typically lasts anywhere between a number of hours and a few days while chronic inflammation can last for weeks, months and even years. Examples of chronic inflammation include cancer, atherosclerosis, osteoarthritis, rheumatoid arthritis and Alzheimer's diseases.

The macrophage cell is one of the early key effector cell types during an inflammation response. The main functions of macrophages are to maintain homeostasis in the body which depends on the local microenvironments for example, resident macrophages regulate tissue homeostasis by responding to physiology changes (Thomas A. Wynn, Ajay Chawla, 2014). The macrophage also initiates the adaptive immune response through antigen-presenting activities, assists in tissue repair and clearing dead cells. Hence, early detection of activated macrophages is essential to diagnose, and offer treatment supports for inflammatory diseases (Murray et al., 2014).

The most common clinical biomarker for inflammation is C-reactive protein and involves tests using different techniques such as ELISA (Salvo et al., 2017). However, this is time-consuming and requires trained personnel to perform the test, while laser-scribed graphene electrodes represent a low-cost, portable and flexible electrochemical platform, ideal for use in point of care biosensors. It is anticipated that the LSGE will enable the detection of inflammation with higher

sensitivity and shorter response times compared to other conventional techniques (Kumar et al., 2015).

1.3 Aim

The aim of the present study was to develop a prototype laser-scribed graphene electrode sensor (LSGE) to detect the inflammatory marker, IL-6, secreted by inflamed macrophages for early diagnosis of inflammatory diseases.

1.4 Objectives

The objectives of this study were to:

- Induce inflammatory cell markers in an *in vitro* human macrophage cell model under various inflammatory conditions.
- Characterise the human macrophage cell model under various inflammatory conditions.
- Characterise the Laser Scribed Graphene Electrode (LSGE).
- Bio-functionalisation of the LSGE to detect macrophage inflammatory markers.

Chapter 2. Literature Review

2.1 Immune System

Amongst other things, our immune system responds against harmful pathogens invading the human body. The immune system can be separated into the innate and adaptive immunity. The first line of defence is the innate immune system, also known as the non-specific defence system. The innate immune system responds immediately to non-self targets within minutes or hours (Sharpe and Mount, 2015). Adaptive immunity is the antigen-specific reaction of T-lymphocytes and B-lymphocytes that takes up to days or weeks to develop. Adaptive immunity recognises and remembers specific pathogens. Vaccination induces adaptive immunity without the risk of disease (Parkin and Cohen, 2001).

The innate immune system is composed of antimicrobial proteins and complement, natural killer (NK) cells, dendritic cells (DCs) and phagocytic systems (Medina, 2016). Antimicrobial proteins are small molecules of proteins with common structural features for antimicrobial activity but lack of specificity such as interferon (Batycka-Baran et al., 2014). The inflammatory cytokines IL-1 and IL-6 are secreted by phagocytes and stimulate hepatocytes. The hepatocytes trigger the secretion of protein in the complement system associated with neutrophils, monocytes, macrophages, mast cells, dendritic cells, B cells and T cells. Antimicrobial proteins opsonise pathogens to facilitate phagocytosis and recruitment of phagocytes to host infection sites (Medina, 2016).

Natural killer (NK) cells make up 5 to 15% of human peripheral blood. Natural killer cells can distinguish healthy cells from cells infected by viruses, bacterial or cancer cells. Healthy cells have the Major Histocompatibility Complex (MHC-I), which is the inhibitor for NK cells, while cancer cells or infected cells have over-expressed activating ligands that can be recognised by the NK cells. NK cells trigger apoptosis of these cells with specific enzymes (Sharrock, 2019).

Dendritic Cells (DC) are antigen-presenting cells that induce adaptive immune responses. DC cells secrete TNF- α and Nitric Oxide (NO) to help clear pathogens and also activate NK cells (Mbongue et al., 2014).

The phagocytic system consists of macrophages and granulocytes i.e. basophils, eosinophils and neutrophils. Neutrophils are the most abundant type of white blood cell but they are very short-lived. They phagocytose and self-destruct after

engulfing the pathogen at the site of tissue injury (Medina, 2016). Macrophages play the most essential function in innate immunity and will be further discussed in section 2.2.

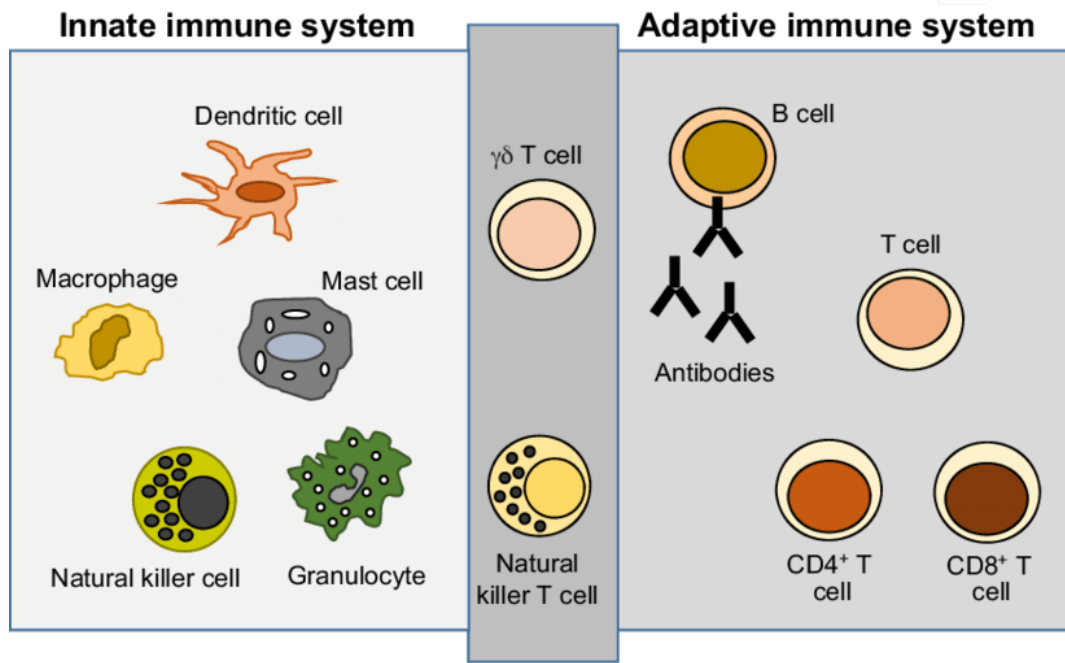


Figure 2.1. Cells in the innate and adaptive immune system, (Sharpe and Mount, 2015).

2.2. Macrophages

Macrophages are effector cells for the innate immune system. They have large vacuoles to phagocytose pathogens (Kozloski, 2019). The main functions of macrophages include maintaining tissue homeostasis, initiating adaptive immune response through antigen-presenting molecule, tissue repair and dead cell clearance (Murray et al., 2014). Hence, macrophages are considered as a potential target for disease treatment and hold potential in early detection for immune response.

By observing white blood cells engulfing bacteria, macrophages were first discovered by Ilya Mechnikov in 1884. Ilya Mechnikov proposed that phagocytosis is part of the body's defence mechanism and initiates inflammation

responses (Cavaillon, 2011). In the 20th century, researchers (Ebert and Florey, n.d.; Clark and Clark, 1930) identified the origin of macrophages. It was shown that monocytes enter damaged tissues, increase in size and become macrophages.

Monocytes are converted to different types of macrophages when they travel into the blood and migrate to different tissues. Monocytes arise in the bone marrow from myeloid stem cells and circulate in the blood for 1 to 3 days under homeostatic conditions. During infection or inflammation, the monocytes will be activated into macrophages and attracted to the infected sites due to the chemokines released locally (Mantovani, 2014).

Since macrophages are distributed throughout the body, they act as an effective first line of defence against invading pathogens. Once distributed in the bloodstream, monocytes migrate to different tissues and develop into a different population of resident macrophages according to the microenvironment such as alveolar macrophages in the lung, Kupffer cells in the liver, Osteoclasts in the bone and microglia in the central nervous system.

Kupffer cells can be found within the lumen of liver sinusoids. Kupffer cells adhere to the endothelial cells in blood vessel walls and act as the first innate immune cells that protect the liver from gut bacterial. Kupffer cells are also responsible for the metabolism of lipids, removing apoptotic cells from circulation and metabolism of protein complexes. Malfunction of Kupffer cells can cause liver diseases such as alcoholic liver disease, viral hepatitis and steatohepatitis which is the fatty liver disease (Nguyen-Lefebvre and Horuzsko, 2015).

Microglia is the macrophage resident in the brain and spinal cord. Microglia are responsible for the clearance of defective or immature neuronal synapses. Dysfunction of the microglia can cause neurological diseases such as Alzheimer's disease (Gordon and Martinez-Pomares, 2017).

Alveolar macrophages in the lung have close interactions with alveolar epithelial cells. Alveolar macrophages express scavenger receptors, SR-A for the clearance of foreign particles and also express CD 206 that recognise the microbial carbohydrates (Gordon and Plüddemann, 2017).

Osteoclasts are also known as bone macrophages are involved in skeletal growth, development and remodeling through calcium metabolism. Osteoclasts interact with the adaptive immune system and also the hematopoietic system. Hence, osteoporosis malfunction can cause diseases such as rheumatoid arthritis and osteoporosis (Italiani and Boraschi, 2014).

Resident macrophages can re-enter the bloodstream and develop into dendritic cells depends on the stimuli, (Gordon, 2003). Figure 2.2 shows the development of monocytes to the different types of macrophages based on the microenvironment.

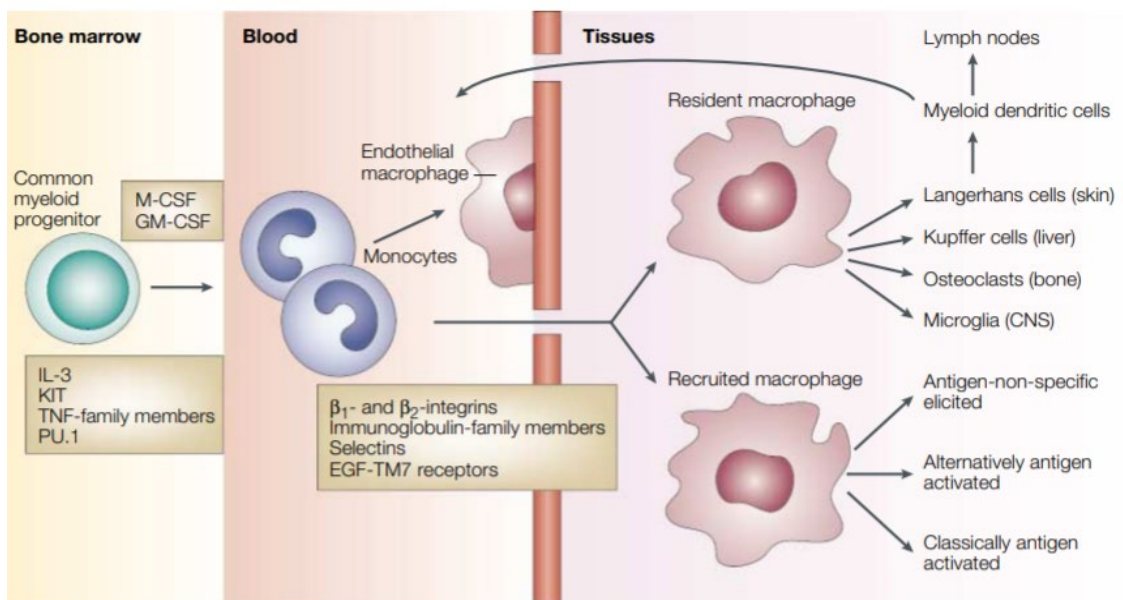


Figure 2.2. The development of monocytes to macrophages in the human body, (Gordon, 2003).

However, recently the point of view that tissue macrophages are derived from monocytes has been challenged by increasing evidence showing that tissue macrophages are originated before birth and maintained throughout adulthood (Mantovani, 2014).

2.3 Macrophage Activation

Macrophages are heterogeneous cells that respond to their microenvironment and change their response accordingly. Macrophages can be polarised into either classically activated macrophages (M1) for pro-inflammatory responses, or the alternatively activated macrophage (M2) for anti-inflammatory responses with different functional and phenotypic properties (Mills et al., 2000). However, the M1 and M2 classification of macrophages is now considered as an oversimplified approach that does not describe the full spectrum of macrophages (Kozloski, 2019).

Based on their surface markers, secretion of inflammatory cytokines and gene signatures, macrophages have been categorised into classically activated (M1) and alternatively activated (M2) macrophages. Differences between different macrophage activation pathways are possible with studies of murine macrophages to identify important genes and chemokines. However, murine models poorly mimic human macrophages due to the differences in physiology and immunology. The murine markers also have limited use for human macrophage studies. Few differences had been listed (Tarique et al., 2015).

First, murine studies are usually performed using bone marrow-derived macrophages whereas human studies are usually performed using human monocytes-derived macrophages. Bone marrow-derived murine macrophages are widely used due to their ability to be transfected, longer lifespan, homogeneity and proliferation capacity (Wang et al., 2013). The human monocytes-derived monocytes are used for human macrophage study to overcome the difficulty to access tissue and the inability of the macrophage to survive *in vitro* after isolation (Kelly, Grabiec and Travis, 2018). The surface marker expression for the murine model is different from humans. For example, the CD206 mannose receptor is highly expressed in murine M2 macrophages but only expressed at low levels in humans. Thirdly, in the murine model, IL-4 induces the production of CD163 surface marker, not IL-10 in humans.

It was reported that human macrophages had no INOS, Ym1, Arginase and FIZZ1 genes that were signature genes of murine macrophages (Tarique et al., 2015). A study showed that murine macrophages produce the obligatory cofactor

tetrahydrobiopterin (BH4) that is used to stabilise and enable the function of the INOS enzyme protein. INOS induces produce Nitric Oxide. Human macrophages do not synthesise BH4 and hence lack INOS enzyme to produce Nitric Oxide (Schneemann and Schoeden, 2007). According to the study shown by (G, R and P, 2005), IL-4 regulates the expression of Ym1 and the Arginase gene in murine macrophages is not expressed by human macrophages.

Besides, the metabolic responses of murine and human macrophages to lipopolysaccharide are reported to be different. The study showed that LPS activated human monocytes-derived macrophages rely on oxidative phosphorylation for the generation of ATP while LPS activated bone marrow-derived murine macrophages experience an increase in glycolysis and decrease oxidative phosphorylation. This is further confirmed by the treatment of activated human and murine macrophages with 2-deoxyglucose which is an inhibitor of glycolysis leading to the death of murine macrophages but not human macrophages (Vijayan et al., 2019). This study proved the different responses of human and murine macrophages towards LPS stimulation.

2.3.1 Classically Activated Macrophages; (M1)

Based on Mackaness's work in 1960 that revealed enhanced antimicrobial activities in the presence of certain stimuli, more recent studies have shown that macrophage activation depends on the presence of interferon-gamma (IFN- γ), IL-12 and IL-18 cytokines which are secreted by the T-helper 1 type (Th1) lymphocytes and natural killer cells. Th1 cells cause an increased level of cell-mediated response against bacteria while natural killer cells work to control viral infection (Gordon, 2003).

Macrophages are polarised towards the M1 phenotype with bacterial lipopolysaccharide (LPS) and interferon-gamma. This induces the secretion of many types of cytokines such as IL-1beta, tumor necrosis factors (TNF), IL-12, IL-6 as well as low levels of IL-10. IFN- γ induces Janus Kinase (JAK)-mediated phosphorylation and activates the Signal Transducer and Activator of Transcription (STAT 1) pathway. JAK activation causes cell proliferation, cell differentiation and migration which is crucial for the immune response (Rawlings, Rosler and Harrison, 2004).

STAT 1 pathway promotes M1 macrophage phenotypes and stimulates the secretion of cytokine IL-12 and chemokines CXCL10. LPS activates the TRIF-dependent TLR4 pathway. This results in the activation of the IFN Regulatory Factor 3 (IRF3) and hence induces the expression of Interferon-beta (IFN- β). IFN- β activates STAT 1 and STAT 2 pathways. Besides IRF3, IRF 5 is also triggered in M1 cells which regulate the expression of IL-12, IL-23 and TNF (Mantovani, 2014). Figure 2.3 shows a schematic diagram for the activation pathway of M1 macrophage polarisation.

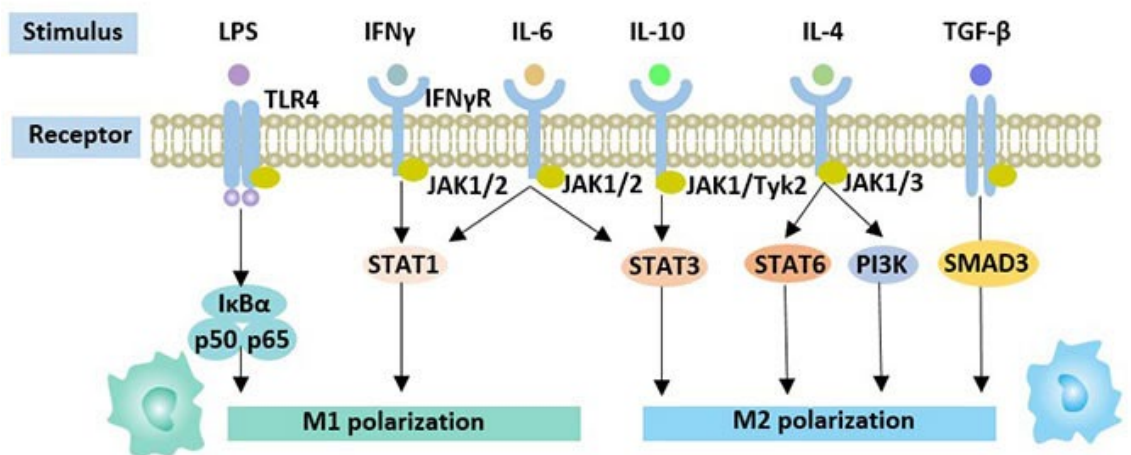


Figure 2.3. Activation pathway of macrophage into different phenotypes with various stimulants, (Two Types of Macrophages: M1 and M2 Macrophages - Cusabio, 2019).

2.3.2 Alternatively Activated Macrophages (M2)

Evidence shows that alternatively activated macrophages induce changes that are distinct from classically activated macrophages. Based on the work of (Nathan et al., 1983) it was shown that macrophages stimulated with IL-4 express different genes compared to macrophages stimulated with IFN- γ and LPS. The alternatively activated macrophage is activated by IL-4 and IL-13 that are secreted by the T-helper 2 (Th2) cells. Macrophages with M2 phenotypes have a high expression level of mannose receptors, scavenger receptors, galactose type receptors and Arginase-1 for nitric oxide production. Mannose receptors such as

CD206 are responsible for endocytosis, phagocytosis and immune homeostasis. Hence, M2 cells promote tissue repair and remodeling, the development of new blood vessels (angiogenesis), immunoregulation and tumour progression (Mantovani, 2014).

The presence of IL-4 and IL-13 activates STAT 6 phosphorylation and initiates the transcription of M2-associated genes such as mannose receptor and inhibits the transcription of inflammatory genes. Besides, IL-4 and IL-13 also upregulate the suppressor of cytokine signalling (SOCS) family including SOCS 1 and SOCS 2 which blocks the STAT 1 and STAT 2 pathway by negative feedback which interferes with the polarisation of M1 cells (Mantovani, 2014).

It is worth noting that available human data for polarisation of human macrophages is limited and lacks consistency due to different experimental conditions, different cell lines used and different stimuli for the differentiation and polarisation of macrophages (Tarique et al., 2015). More research is needed to fully understand the plasticity and phenotypes of macrophage populations *in vivo*.

2.4. Inflammation

Inflammation is part of the body's defence system and can be divided into acute inflammation and chronic inflammation. Acute inflammation is induced by injury, tissue damage or microbial invasion and can last for hours up to a few days. Acute inflammation prevents injury and helps in the healing process. Chronic inflammation is a long-term inflammation that can last for several months or even years ((Stone, Basit and Burns, 2020).

Chronic inflammation can be caused by the infectious organisms that can resist host defences such as *Mycobacterium tuberculosis*, parasites, fungi and protozoa (an organism that can resist phagocytosis), and autoimmune disorders where the body starts to attack normal body components, causing inflammatory diseases such as Rheumatoid Arthritis (RA), Inflammatory Bowel Disease, diabetes, cardiovascular diseases, obesity and cancer (Pahwa R, Goyal A, Bansal P, 2020). According to the World Health Organisation, chronic diseases were predicted to account for three-quarters of all deaths worldwide by 2020,

(Background, 2007). Hence, it is important to be able to diagnose inflammatory diseases as early as possible for early treatment.

Macrophages have been identified as the major factor contributing to chronic inflammation. M1 macrophages elicit a pro-inflammation response by the production of nitric oxide, a pro-inflammatory mediator converted from arginine by inducible nitric oxide synthase (iNOS) that is toxic for invading organisms. Nitric oxide also inhibits cell proliferation and induces cancer cell death. M2 macrophages conversely work by promoting cell proliferation and cell repair by metabolising the arginine, (Ponzoni et al., 2018). Examples of inflammatory diseases caused by macrophage will be discussed in the following section.

2.4.1 Atherosclerosis

Atherosclerosis is associated with the formation of plaque on inside of the arterial wall and results in the narrowing and sometimes occlusion of arteries. This is the result of plaque initiation and progression by pro-inflammatory macrophages. The formation of plaque decreases the migration causing failure to prevent inflammation. The macrophages that undergo necrosis or apoptosis will lead to unstable plaques because these macrophages will release the tissue factor and lipid contents. Tissue factor and lipid contents will lead to the formation of the pro-thrombotic necrotic core which is the component that causes the unstable plaques to rupture and promote intravascular blood clots (Moore, Sheedy and Fisher, 2013).

Hence, therapies that alter the macrophage content such as promoting macrophage apoptosis, reducing the recruitment of macrophage to atherosclerotic plaques or altering the macrophage inflammation by increasing the polarisation to M2 phenotype macrophage can be beneficial to treat atherosclerosis. Unlike M1 macrophage phenotypes that promote plaque inflammation, M2 phenotypes resolve plaque inflammation (Moore, Sheedy and Fisher, 2013).

M2 macrophages that secrete anti-inflammatory cytokines can promote tissue repair by the formation of collagen and clearance of dying cells and debris. Research has shown that in the plaque regression animal model, M2 phenotype

macrophage enrichment was found and indicated that M2 macrophage polarisation reduces the atherosclerotic plaques (Bi et al., 2019).

2.4.2 Osteoarthritis

Osteoarthritis occurs when the protective cartilages that act as cushions at the end of bones become worn out, which damages the joints and causes pain. The secretion of TNF- α and IL-1 β by macrophages can cause synovial inflammation that is commonly observed in patients with osteoarthritis, (Ponzoni et al., 2018). The severity of osteoarthritis of a patient is assessed by the level of CD14 and CD163, (Daghestani, Pieper and Kraus, 2015).

2.4.3 Asthma

Several studies show the role of alveolar macrophages in asthma. Asthma is an allergic lung disorder. During early infection, the resident alveolar macrophages play a protective role, (Zasłona et al., 2014). According to (Jiang and Zhu, 2016)'s work, alveolar macrophages are polarised to M1 and M2 phenotypes when exposed to pathogens where M1 cells express pro-inflammatory cytokines which will induce lung inflammation and cause the damage of tissues such as Tumour necrosis factor-alpha (TNF- α), iNOS and IL-1 β . M2 cells can be further divided into different subsets that are M2a, M2b and M2c. Table 2.1 shows the inducers, cell markers, cytokines and chemokines secreted and the functions of different subtypes of alveolar macrophages. When lung injury occurs, M1 cells present predominantly from day 1 to day 3, while M2 cells significantly increase at 28 days. The low expression of MHC II, CD86, iNOS2 but the high level of arginase-1 and macrophage mannose receptor CD206. The high level of CD206 helps phagocytosis and scavenging of M2 cells, (Jiang and Zhu, 2016).

Table 2.1. Table of the inducers, cell markers, cytokines and chemokines secreted and the functions of different subtypes of alveolar macrophages. Table taken from (Jiang and Zhu, 2016).

Subtypes	Inducers	Cell markers	Cytokines	Chemokines	Function
M1	IFN- γ , LPS, bacteria	CCR7, CD25, CD86,	TNF- α , IL-1 β ,	RANTES,	Proinflammatory function
	GM-CSF, oxidative fatty acid/LDL, HMGB1	CD127, MHCII, ROS, iNOS, arginase-2	NO, IP-10, IL-6/8/12/15/17/23	CCL-8/15/19/20, CXCL-9/10/11/13	Pathogen clearance, tissue damage
M2a	IL-4, IL-13, M-CSF, NLRP3	CD206, CD209, Fizzl, Ym1/2, RELM- α , arginase-1	IL-4/10/13/33/35, MMP-9, MMP-14, IGF-1	CCL-8/13/14, CCL-17/18/23/26	Allergic inflammation
M2b	LPS, IL-1 β , immune complex/IL-1Ra	CD206, CD209, Fizzl, Ym1/2, RELM- α , arginase-1	IL-10, TGF- β , CCL-1/20, CXCL-1/2/3	CCL-1/20,	Tissue remodeling, fibrosis
M2c	TGF- β , IL-10, PGE2, Tregs, BM-MSc, ADSCs, IDO	CD163, CD206, Fizzl, Ym1/2, arginase-1, PPAR- δ , SRA-1 TLR1/8	IL-10, TGF- β , IGF-1, PGE-2	CCL-8/17/18/22/24	Anti-inflammatory function Phagocytosis, tissue remodeling, fibrosis

2.4.4. Tumour Associated Macrophages (TAM)

Inflammation can be the cause of many cancers where the tumour-associated macrophages (TAM) releases inflammatory mediators that promote tumour growth by angiogenesis. Angiogenesis is the growth of new blood vessels. The metastasis of tumours occurs and the tumour cells begin to travel through the bloodstream. The tumour cells invade other tissues which causes decrease of anti-tumor immunity. This could happen once the tumour progresses to malignancy. Tumour-associated macrophages can also change their phenotypes to adapt and survive in different tissues (Liu et al., 2014).

Tumour-associated macrophages initially produce low levels of nitric oxide which is an indication for the M1 phenotype. After exposure to LPS and TNF- α , TAM shows a low level of IL-12, IL-6 and IL-1 β which are the cytokines released by M1-like macrophages, while a marker for M2-like macrophages such as MRC1, Arg 1, FIZZ1 and Ym1 are expressed on TAM. However, it is widely accepted that the phenotype of TAMs change according to the microenvironment, such as infiltrating leukocytes, mediators and signals, (Liu et al., 2014).

2.5. Biomarkers for Chronic Inflammation

Current laboratory based tests available for inflammation include serum protein electrophoresis (SPE), high-sensitivity C-reactive protein (hs-CRP) test, fibrinogen test and pro-inflammatory cytokines test. SPE measures concomitant hypoalbuminemia and polyclonal gammopathy (a hypergammaglobulinemia that results the increased in the increased of immunoglobulin) in blood where the increase in these proteins indicates inflammation. Pro-inflammatory cytokine tests include cytokine tumor necrosis factor-alpha (TNF-alpha), interleukin-1 beta (IL-1beta), interleukin-6 (IL-6), and interleukin-8 (IL-8). These are expensive tests but are able to identify the factors of chronic inflammation (Fleit, 2014).

Blood tests for biomarkers to detect chronic inflammation include high sensitivity CRP, fibrinogen, IL-6, IL-1 β , TNF- α and IL-8. The optimal ranges for hs-CRP in men are under 0.55 mg/L and below 1.0 mg/L in women. The fibrinogen optimal ranges are within 200 to 300 mg/dL. Cytokine testing includes TNF- α with normal ranges below 8.1 pg/mL, IL-1 β below 15 pg/mL, IL-8 below 32 pg/mL and IL-6 between 2 to 29 pg/mL (Chronic Inflammation - Life Extension, 2020). Different types of inflammatory cytokines and surface markers hold great potential as biomarkers for the diagnosis and progression monitoring of inflammatory diseases.

2.5.1 C-Reactive Protein

C-Reactive Protein (CRP) was discovered by Tillet and Francis (1930) after it was isolated from patients infected by pneumococcus ((WS and T, 1930). In 1999, evidence had shown that CRP can be a biomarker for vascular risk and can be used as a method to prevent and treat cardiovascular diseases (WK et al., 1999). However, the threshold level of CRP causing vascular risk is in the range from 5 to 10 mg/L which is lower than the detection limit of the standard CRP immunoassay, the hsCRP, high sensitive CRP was developed for commercial tests with reproducible results (Wang et al., 2017).

CRP is an acute-phase reactant liver protein, released in blood quickly (hours) after tissue injury, infection, or other forms of inflammation. The level of CRP can increase a thousand-fold in response to inflammatory conditions. The laboratory

test measures the amount of CRP in the blood which can rise from 0.8 mg/L to 600-1000 mg/L in hours after insult (Anon, 2021). The peak concentration can be observed after 48 hours. The concentration of the CRP in the blood rapidly returns to normal after the inflammation is resolved (Salvo et al., 2017).

The CRP test is not diagnostic, but provides information to a health practitioner as to whether inflammation is present. This information can be used in conjunction with other symptoms and tests performed by the health practitioner. CRP has emerged as one of the most important novel inflammatory biomarkers. The commercial availability of high sensitive CRP assays has made screening for this marker simple, reliable and reproducible, meaning it can be used as a clinical guide for the diagnosis, management, and prognosis of coronary heart disease, (Ridker, 2009).

2.5.2 IL-6

IL-6 is a small glycoprotein, 21 kDa in size and is produced by innate immune cells such as macrophages, mast cells and dendritic cells. IL-6 is also secreted by non-leukocytes such as endothelial cells, epithelial cells, fibroblast and astrocytes. IL-6 is secreted during the activation of nuclear factor (NF) commonly when tissue damage occurs, (Jiang and Zhu, 2016). Hence, the elevation of IL-6 levels is associated with inflammatory diseases. IL-6 plays different roles in different tissues and organs (figure 2.4) (MouseDoctor, 2013).

Biological activities of interleukin-6

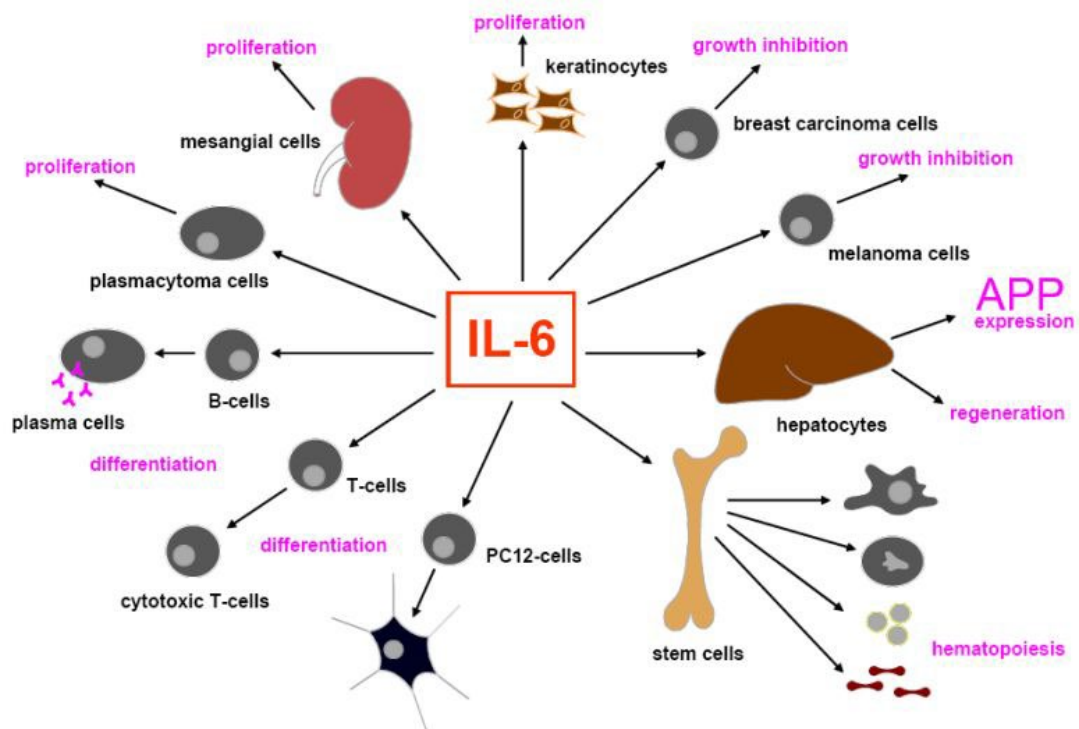


Figure 2.4. Biological activities of IL-6, (MouseDoctor, 2013).

It was reported that the elevation of IL-6 can be observed in the serum and synovial tissues of patients with rheumatoid arthritis. However, the IL-6 level for the patient with osteosclerosis is not increased indicating that IL-6 does not increase in all types of inflammatory conditions, (Kishimoto, 2010). IL-6 is synthesised during the initial stage of inflammation and moves to the liver through the bloodstream. This induces the secretion of acute-phase proteins, such as fibrinogen and CRP, that will increase or decrease in plasma level due to inflammation. IL-6 also inhibits the production of albumin, fibronectin and transferrin (Tanaka, Narazaki and Kishimoto, 2014).

Since IL-6 is a pro-inflammatory cytokine, circulating IL-6 can be a potential diagnostic tumour biomarker or prognostic tumour biomarker. A diagnostic tumour biomarker can detect the stage of a tumour or the response of the tumour to its treatment, while prognostic tumour biomarker tests indicate the risks of the cancer-related event. (Vainer, Dehlendorff and Johansen, 2018) reviewed thirty-six papers regarding the diagnostic use of IL-6 and twenty-seven studies of

prognostic use of IL-6 to diagnose gastric cancer, bile duct cancer, pancreatic cancer and colorectal cancer. This paper concludes that IL-6 can only be used as a bedside test in general practice for patients with unspecified cancer symptoms. IL-6 can be used as the prognostic biomarker for gastric and pancreatic cancer and is not suitable as a diagnostic tumour biomarker. In other words, IL-6 is not cancer specific but the detection of IL-6 in the blood can help to diagnose cancer in the early stage (Vainer, Dehlendorff and Johansen, 2018).

Studies have shown that IL-6 is a highly accurate biomarker for the diagnosis of sepsis (Song et al., 2019). IL-6 concentration in the blood of healthy people ranges from 5 to 25 pg/mL and increases as much as 1000 pg/mL for people with sepsis (Hou et al., 2015). IL-6 is an upstream inflammatory marker that leads to the production of downstream CRP. Hence, it has the potential to predict the risk of the future inflammatory event. One clinical study has demonstrated the independent association of IL-6, with the risk of major coronary events such as cardiovascular death, myocardial infection, cancer and heart failure, suggesting that IL-6 can potentially be a more specific biomarker compared to CRP (Held et al., 2017).

IL-6 is not tested in patients as frequently as CRP. However, doctors might require patients to get tested to evaluate the risk of stroke, heart disease and diabetes. Recently, the role of cytokines was being investigated for their association with COVID-19 positive patients. COVID-19 patients experience a “Cytokine Storm” or Macrophage Activation Syndrome (MAS) including IL-6, IL-1, IL-2, IL-10, TNF- α and IFN- γ . Data suggests that many COVID-19 patients die due to the excessive immune response due to the abnormal circulation of cytokines (also known as cytokine release syndrome). IL-6 has been chosen as a potential target for COVID-19 targeted therapy. This shows the importance of a biosensor that will be able to detect cytokine levels rapidly and accurately, (EnzoSciences, 2020).

2.5.3 CD206

CD206 is a mannose receptor and C-type lectin which is a receptor to initiate adaptive immune responses. CD206 is expressed on the surface of alternatively

activated macrophage and immature dendritic cells. Besides being able to recognise the glycoprotein and glycolipid on the surfaces of viruses, bacteria, fungi and pathogens, CD206 also functions to clear the glycoprotein released due to pathological events, (Suzuki et al., 2018). Community-acquired pneumonia (CAP) is an infectious disease mostly caused by *Streptococcus pneumoniae* (pneumococcus) and respiratory viruses that can lead to death. Immunomodulatory molecules have the potential to act as markers for infectious diseases as demonstrated in (Kazuo et al., 2019).

Macrophages in the lung act as the first line of defence against the invasion of airborne pathogens and CD206 on the surface of macrophages recognise and scavenge unwanted glycoprotein and glycolipids. CD206 can also bind to the polysaccharides of *Streptococcus pneumoniae* and the lipopolysaccharide from *Klebsiella pneumoniae*. This promotes phagocytosis and subsequently leads to the destruction of these pathogens. It increases in the CD206 positive macrophages in the lung and an increased level of soluble CD206 can be observed in the CAP fatal patients. Hence, CD206 incorporated into a biosensor could be a good diagnostic tool for CAP, (Kazuo et al., 2019).

2.5.4 CD80

CD80 is a B7 type I membrane protein that is closely related to CD86. CD80 can be found on the surface of various immune cells such as classically activated macrophages, B cells, dendritic cells and monocytes. CD80 is the receptor for CD28 which is the protein for autoregulation and the CTLA-4 for cellular dissociation that can be found on the surface of T-cells. The binding of CD80 to CD28 and CTLA-4 results in the activation of B-cells and T-cells, (Nolan et al., 2009). The binding of CD80 to CD 8 stimulates the dendritic cells and increases the production of cytokine IL-6 (see 2.3.3) (Peach et al., 1995).

CD80 can be used as an indicator to monitor the efficiency of chemotherapeutic treatment for cancer. P53 is a tumour suppressor gene and necessary for late-stage cancer (National Center for Biotechnology Information, 1998). Expression of CD80 mRNA in human lung cancer cells can be observed when the stimuli for p53 activation is increased. This indicated that CD 80 can act as the biomarker

for p53 action and indicates the efficacy of the anti-cancer therapy, (David et al., 2013)

Urinary CD80 can potentially be used as the prognostic marker for Minimal Change Disease (MCD). MCD is a primary nephrotic syndrome in children. Expression of CD80 in podocytes for children with steroid-sensitive MCD is reported, (Ling et al., 2018).

2.5.5 Fibronectin

Fibronectin is a glycoprotein with a molecular weight of 440 kDa of the extracellular matrix which can bind to the integrins and other extracellular matrix proteins such as fibrin and collagen. Fibronectin is responsible for cell growth, cell adhesion, cell migration and differentiation, wound healing and also embryonic development (Parisi et al., 2020). Tumour development can suppress the expression of fibronectin making fibronectin a candidate biomarker for cancer such as ovarian cancer, breast cancer and prostate cancer (TAS et al., 2016).

2.5.6 Other

Other inflammatory cytokines such as Interleukin-1beta (IL-1 β), TNF- α and IL-8 are potential biomarkers for detecting inflammation, however they are mainly used in research as there are no known “normal” levels in the body. One study shows that IL-1 β and TNF- α can potentially be used as a salivary biomarker for the diagnosis of periodontal diseases, in particular inflammation of the gums. IL-1 β and TNF- α present in the early stages of the disease and the level of both cytokines increases with the progression of the disease, (Gomes et al., 2016). IL-1 β significantly increases in cancer patients and is known to promote tumour growth. However, the level of IL-1 β in different stages of cancers is still unknown, (Idris, Ghazali and Koh, 2015).

2.6. Immune Effector Cell Models

There are few cell lines that have been widely used for immunology research such as the THP-1 cell line, U937 cell line, ML-2 and Mono Mac 6 which are

immortalized human monocyte-macrophage cell lines. U937 cell line is an immature cell line with little or no expression of CD14, (Mantovani, 2014).

THP-1 cell line was derived from the blood of a one-year-old boy with acute monocytic leukaemia and established in 1980, (Tsuchiya et al., 1980). THP-1 cells are suspension cells that have large, round single-cell morphology as shown in Figure 2.5. After differentiating with phorbol-12-myristate-13-acetate (PMA), the THP-1 cells become adherent. Compared to human primary monocytes or macrophages, THP-1 cells have a homogeneous genetic background with minimum variation in cell phenotype. THP-1 cell line also allow simple genetic modifications. THP-1 cells can be cultured *in vitro* up to passage 25, which is approximately three months, without any significant changes in cell activity, (Chanput, Peters and Wichers, 2015).

U937 is another cell line that has been widely used in immunology research. The difference between U937 and THP-1 cell lines is that THP-1 cells are derived from blood and are at a less mature stage compared to U937 cells that are derived from tissue and are more mature (Chanput, Mes and Wichers, 2014). THP-1 cells have a much higher growth rate compared to human peripheral blood mononuclear cell (PBMC)-derived monocytes and macrophages where the average doubling time of the THP-1 monocytes is around 35 to 50 hours. THP-1 cells do not produce any toxic products which makes them safe to use for research purposes. THP-1 cells can be stored in liquid nitrogen for years with an appropriate protocol with no effect on the cell features, where the availability of PBMC is limited since they cannot be stored in the liquid nitrogen, (Chanput, Mes and Wichers, 2014).

To mimic the macrophage in the human body, THP-1 cells can be differentiated into macrophages and then polarised into classically activated macrophages (M1) and alternatively activated macrophages (M2) with different stimulants. According to (Chanput, Mes and Wichers, 2014), THP-1 cells can be differentiated into macrophage-like phenotype using three different reagents which include 25-dihydroxyvitamin D3 (vD3), macrophage colony-stimulating factor (M-CSF) and phorbol 12-myristate 13-acetate (PMA). PMA-differentiated THP-1 cells were used in this present work to study macrophage activity because

they have a more mature phenotype with higher expression of surface markers. PMA differentiated THP-1 cells also adhere better to cell culture plates (Qin, 2012).

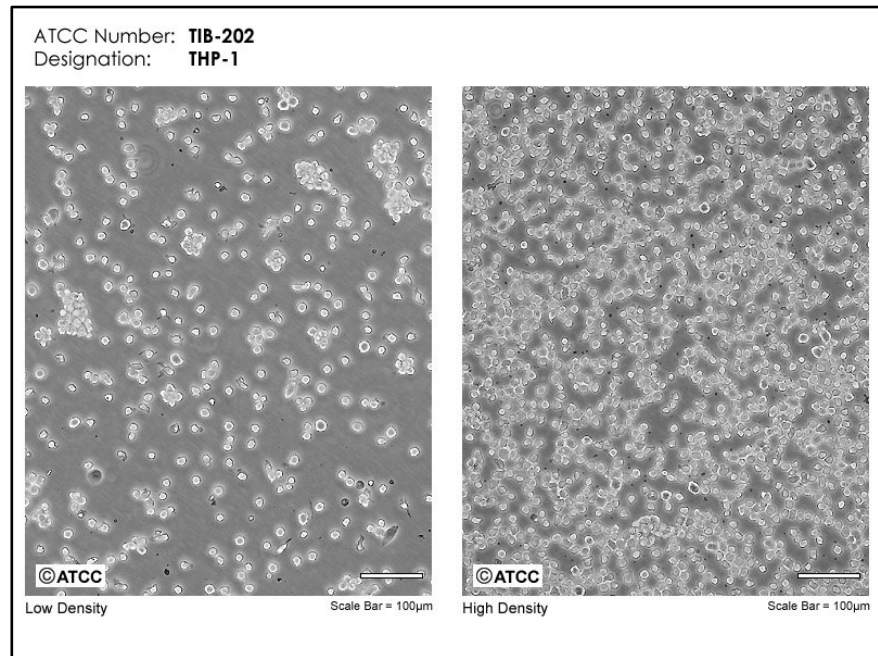


Figure 2.5. THP-1 cells, (THP-1 ATCC® TIB-202TM, 2016).

2.7 Biosensors

A biosensor is defined as “a self-contained analytical device that combines a biological component with a physicochemical device for the detection of an analyte of biological importance”, (Rocchitta et al., 2016). A successful biosensor should be highly specified to analytes with low background noise, and stability under normal storage conditions. In other words, the response of the biosensor should be precise, accurate, reproducible, and linear over a specified concentration range. Clinical biosensors need to be small, biocompatible and non-toxic. Rapid measurement is one of the criteria for real-time analysis with easy operation, (Grieshaber et al., 2008).

The component of a typical biosensor is shown in Figure 2.6. A typical biosensor is made up of three components which are a bioreceptor, transducer and data processor.

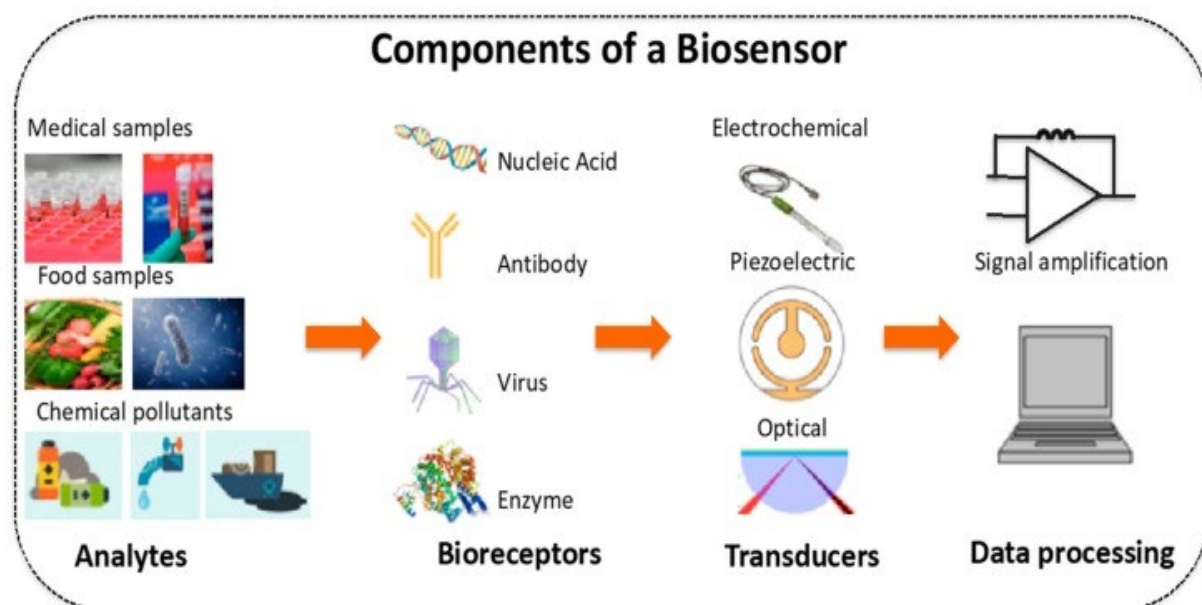


Figure 2.6. Biosensor components, (Zhou, Fang and Ramasamy, 2019).

When the presence of a specific analyte in a tested sample is detected by the bioreceptor through specific binding, the interaction between analyte and bioreceptor is captured by signal transduction using different transducers. The data processor amplifies and processes the signal into readable data.

The performance of a biosensor is accessed by its selectivity, reproducibility, stability, sensitivity and linearity. Selectivity is the most important characteristic of a biosensor. A biosensor with good selectivity should be able to detect specific analytes in a sample with other contaminations. This enables the biosensor to detect analytes in saliva, serum, blood or urine with no further treatment which can reduce labour, time and cost. The reproducibility of a biosensor is characterised by the precision and accuracy of the transducer of a biosensor. The ability of the biosensor to generate identical responses is important for reliable test results.

Stability test the measurement of a biosensor against degradation over a period of time. Disturbance such as incubation time, pH and temperature can potentially drift the signals produced by the biosensor especially the biosensor with sensitive receptors which affinity to analytes can be affected by environmental factors. The

sensitivity of a biosensor is normally accessed by the limit of detection (LOD) which quantified the minimum amount of analytes that can be detected by a biosensor. To detect the trace amount of analytes in a sample, a biosensor is required to be able to detect as low as ng/ml or pg/ml depends on the targeted analytes. High sensitivity biosensors also able to detect analytes with a smaller amount of sample required. Linearity shows the accuracy of biosensor response for different concentrations of analytes. Linear range determines the range of analytes concentration that the biosensor response changes linearly (Bhalla et al., 2016).

Biosensors can be categorised according to the type of bioreceptors, the target molecules bind to, or transducers to detect the signal, as shown in Figure 2.7. Biosensors can be categorised according to the type of bioreceptors used to detect the biological response such as enzyme-based biosensors, cell-based biosensors, DNA biosensors, biomimetic-based biosensors, phage-based biosensor and antibody-based biosensors (also known as immunosensors), (Hassani et al., 2017) (Mehrotra, 2016). Biosensors can also be characterised based on their transducers. Different methods such as optical method, electrochemical method, mass sensitivity method and nanomaterial-based sensors are available as the transducers for biosensors.

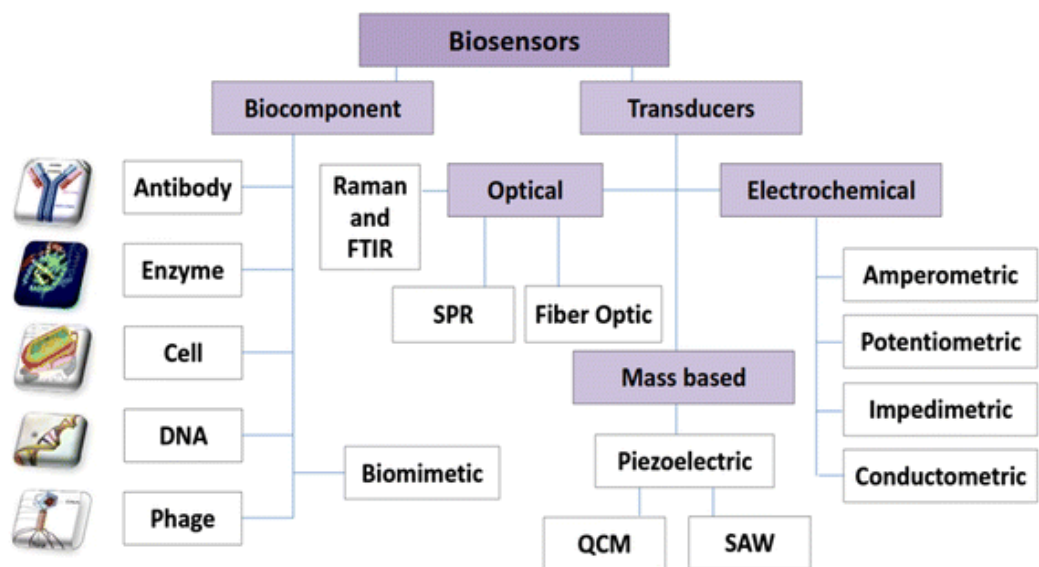


Figure 2.7. Classification of biosensors based on bioreceptors and transducer system, (Hassani et al., 2017).

2.8. Types of Bioreceptors

Enzyme-based chemical biosensors work by using an enzyme to catalyse a specific biochemical reaction. Hence, the enzyme must be stable and able to maintain its quaternary protein structure under operating conditions. The enzyme-based biosensor was the first type of biosensor invented. In 1956, Leland C. Clark invented the oxygen electrode for oxygen detection followed by an amperometric enzyme electrode for the detection of glucose in 1962 (LC and C, 1962) (Heineman and Jensen, 2006) In 1967, Updik and Hicks developed the enzyme-based biosensor using enzyme oxidase by immobilisation (SJ and GP, 1967). The main disadvantages of an amperometric enzyme-based biosensor are the interferences from other chemicals present in the samples, (Rocchitta et al., 2016).

Cell-based biosensors use entire cells or components of the cells such as mitochondrial, chloroplast or cell membrane as the bioreceptors. The first cell-based sensor was invented for the determination of amino acid arginine using plant and animal sources, (Rocchitta et al., 2016). DNA biosensors utilised the single-strand nucleic acid molecules to bind with the complementary strand in the samples by the formation of hydrogen bonds. Biomimetic-based biosensors utilise artificial receptors as the bioreceptors to mimic a biological receptor, (Alahi and Mukhopadhyay, 2017). Phage-based biosensors for bacterial pathogen detection work with the principle where phage recognises specific bacterial strains which assist the detection of bacterial contamination. Phage retains physiological activities and bacterial cells capture efficiencies for a long period. Compared to existing bacterial detection methods such as microscopic techniques and conventional culture, phage-based biosensors are less time consuming and less labour intense (Farooq et al., 2019). Immunosensors work based on the specificity of the antibodies to the antigens. Immunosensors detect the binding of antigens to antibodies to generate signals.

2.9. Methods of Detection

2.9.1 Optical-Based Biosensor

Optical-based biosensors have been widely utilised in many fields such as the medical field to detect antibodies and tumour biomarkers, food safety to detect pathogens, and the environment for virus detection. The most commonly used optical-based biosensor is the surface plasmon resonance (SPR) based biosensor. Biosensors based on the optical method utilise characteristics of light such as refraction, reflection, absorption and dispersion, to produce the signal that is proportional to the concentration of the analytes. Figure 2.8 shows the SPR biosensor where the analyt causes refraction and shifts the SPR angle. Optical based biosensors are highly selective, sensitive for a wide range of analytes and can be used as a real-time detection system (Damborský, Švitel and Katrlík, 2016).

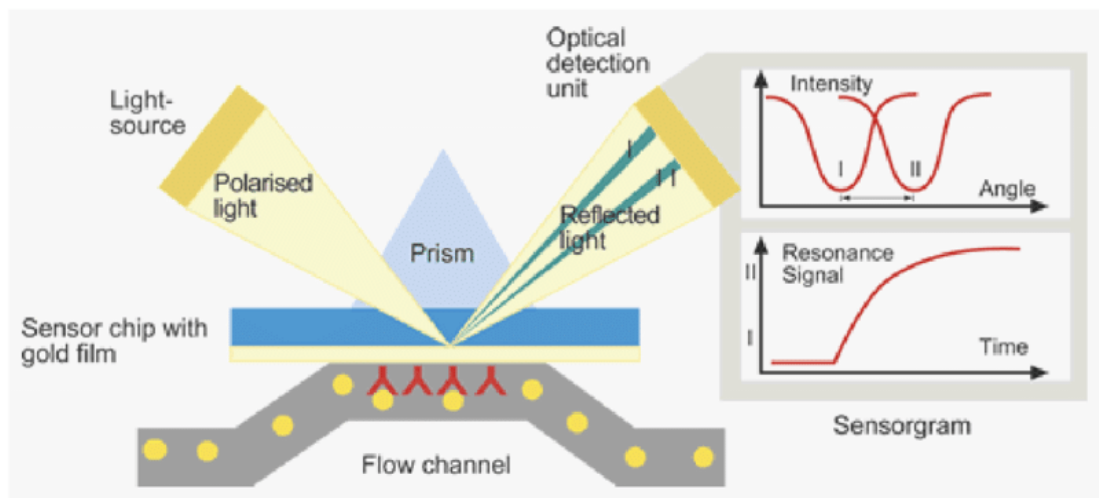


Figure 2.8. SPR optical biosensor, (Patricia, 2004)

2.9.2 Mass-Based Biosensor

Mass-based biosensors measure the mass change due to the biomolecular interaction. Quartz Crystals Biosensors (QCM) and Surface Acoustic Wave (SAM) biosensors are examples of mass-based biosensors and operate based on a piezoelectric crystal surface that vibrates at specific frequencies creating piezoelectricity. Piezoelectricity is the electricity resulting from mechanical stress.

The bioreceptors are immobilised on the quartz oscillator surface. When binding occurs between analytes and bioreceptors, the effective mass increases and the frequency of vibration decrease. These changes are detected by the transducers and presented as readable signals.

QCM-based biosensors are very sensitive and are capable of measuring up to sub-nanogram levels (Prakrankamanant, 2014). QCM biosensors are also able to measure the binding affinity and thus allow the study of the interaction between large biomolecules such as with whole cell immobilisation (Ogi, 2013).

The Surface Acoustic Wave (SAM) biosensor is a biosensor that can detect gaseous, chemical and biological analytes. The high-frequency acoustic wave, which is the wave generated by the displacement of atoms in the piezoelectric material, that travel close to the piezoelectric surface experience frequency shift during molecular absorption or adsorption (Zhang, 2009). Mass-based biosensors are cheaper and easy to operate compared to other methods. Mass-based biosensors can also perform real-time detection. However, the specificity of mass-based biosensors is low with a longer incubation time. The major drawback of mass-based biosensors is the problem to regenerate the crystal surface (Alahi and Mukhopadhyay, 2017).

2.9.3 Electrochemical-Based Biosensor

An electrochemical-based biosensor converts the biological events to electronic signals directly by measuring the change in potential or current when the analytes interact with the electrodes. Potentiometric biosensors, impedimetric biosensors, amperometric biosensors and conductometric biosensors are different types of electrochemical biosensors (Alahi and Mukhopadhyay, 2017). The major drawback of the electrochemical biosensor is the lack of surface architectures for high sensitivity and specific responses for desired analytes. The effect of pH on the bioreceptors of immunosensor is one of the examples. pH can affect the conformation of the antibodies and affect its complementarity with the antigens.

The electrodes play a vital role in electrochemical biosensors where the surface modifications, materials and dimensions of the electrode can greatly influence their detection ability. Three electrodes are required in electrochemical sensing

which include the working electrode, the counter electrode and the reference electrode. Figure 3.2 showed the example of three electrodes system in electrochemical cells. The biochemical reaction occurs on the surface of the working electrode. The counter electrode acts as the connection for the electrolytic solution for the current to be applied to the working electrode. Silver/Silver Chloride is the most common material used for the reference electrode to maintain a known and stable potential. The electrodes used for biosensors need to be chemically stable and conductive. Hence, carbon, gold, platinum and silicon are the compounds that are commonly used as the material for the electrodes, depending on the type of analytes (Grieshaber et al., 2008).

Potentiometric biosensors measure the potential difference between the Ion-Selective Electrode (ISE) and the reference electrode in the electrochemical cell due to ion activity with zero or not significant current. The concentration of the ion can be determined with the Nernst equation. The potentiometric biosensor has a very low detection limit which is suitable for very tiny sample volumes (Grieshaber et al., 2008).

Electrochemical Impedance Spectroscopy (EIS) is the most common technique used for impedance-based biosensors. Electrochemical impedance is measured by applying the alternating potential to the electrode and the current flowing through the cell is measured (Alahi and Mukhopadhyay, 2017).

Amperometric biosensors measure the change in current resulting from the oxidation and reduction that occurs during the biochemical reaction with a constant potential. Amperometry is a voltametric method where a constant potential is applied between the reference electrode and the working electrode. The current that flows between the working and the counter electrode is measured. An amperometric biosensor can be a two or three electrodes system. However, the two electrode system has a shortened linear range due to the limiting control for the potential and a higher current is required (Mohammed Asef Iqbal, 2012). If the controlled variations of potential are applied instead of constant potential, the current is measured and referred to as the voltammetry technique (Grieshaber et al., 2008). If the current is measured as a function of time, it is referred to as the chronoamperometry technique. In this technique, a

drastic change in the potential is applied to the working electrode with the current constantly measured (Pupim Ferreira et al., 2013).

2.10. IL-6 Biosensor

IL-6 biosensors are of particular interest, especially as IL-6 has been identified as the inflammatory biomarker that indicates the severity of COVID-19 infection, together with CRP, Procalcitonin and Ferritin (Garg, Sharma and Singh, 2021).

(Russell et al., 2019) described a needle-shaped biosensor to detect sepsis using IL-6 as the biomarker. It shortened the analysis time roughly from between 12 and 72 hours to only 2.5 minutes. The needle-shaped silicon substrate was fabricated with arrays of eight microelectrodes, as shown in Figure 2.9. Differential Pulse Voltammetry (DPV) was carried out to detect the binding of IL-6. This work showed the novelty of microfabricating multi-electrode arrays to detect biomarkers in real-time.

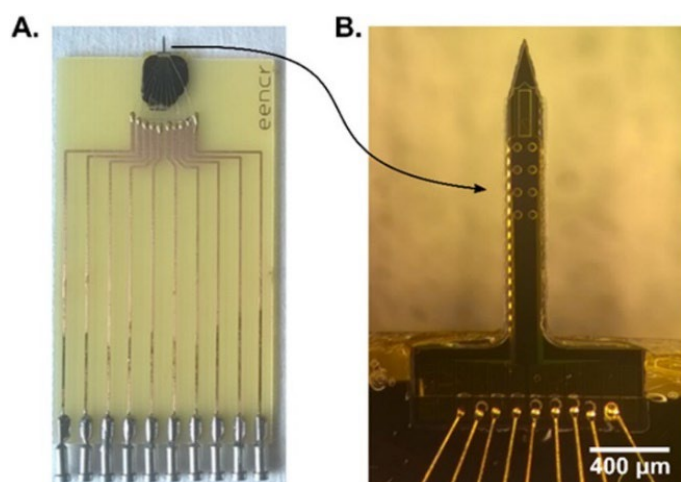


Figure 2.9. Image of the biosensor to detect sepsis using IL-6 as the biomarker A) a packaged device for electrochemical testing, and B) needle-shaped electrode, (Russell et al., 2019).

Another study used IL-6 for colorectal cancer screening. This paper modified the glassy carbon electrode with p-aminobenzoic acid, p-amino thiophenol and gold

nanoparticles (Figure 2.10). The thio-terminated IL-6 aptamer was immobilised on the surface of the modified electrode as the bioreceptors to detect IL-6. Electrochemical Impedance Spectroscopy (EIS) was performed as the sensing technique. This biosensor successfully detected the presence of IL-6 in the blood samples collected from colorectal cancer patients with great recovery (Tertis et al., 2019).

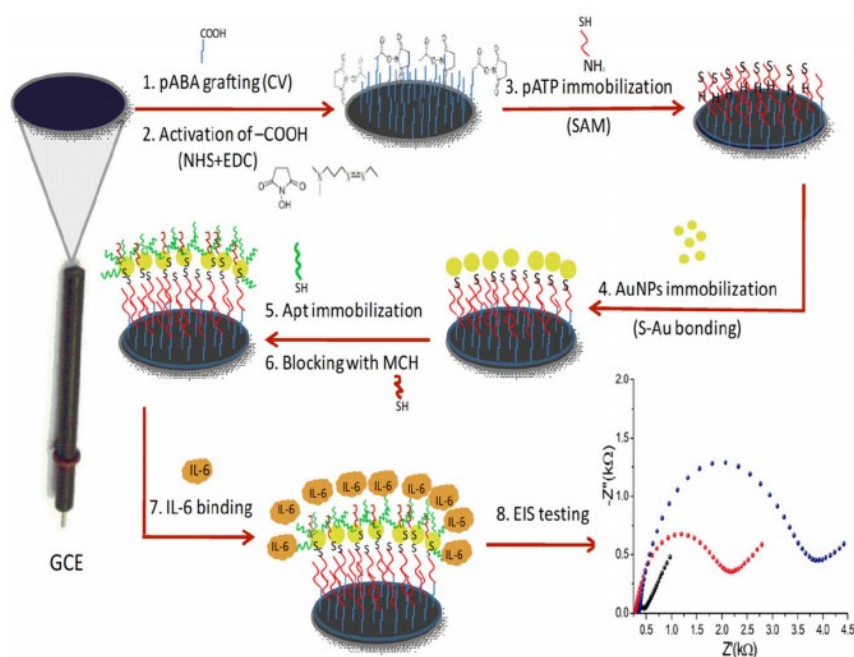


Figure 2.10. Schematic process for modification of the glassy carbon electrode, (Tertis et al., 2019).

(Khan and Mujahid, 2020) reviewed recent advances of electrochemical and optical biosensors to detect IL-6 and (Garg, Sharma and Singh, 2021) development of IL-6 biosensors. A table to summarise the different electrochemical IL-6 biosensor linear ranges and detection limits based on these two papers are shown in Table 2.2.

2.11. Graphene

Graphene has been widely studied recently due to its physical and chemical compatibility as a suitable material for biosensors. Graphene has a large surface-to-volume ratio, excellent thermal and electric conductivity, strong mechanical strength and low cost. Due to the high enzyme loading capacity, graphene provides good sensitivity, which is an ideal characteristic for a biosensor.

Table 2.2. Different types of electrochemical biosensors for the detection of IL-6, (Khan and Mujahid, 2020).

References	Linear Range	Limit of Detection
Russell et al., 2019	20 pg/mL – 100 pg/mL	-
Tertis et al., 2019	5 pg/mL – 100 ng/mL	1.6 pg/mL
Khosravi, Loeian and Panchapakesan, 2017	1 pg/mL – 100 pg/mL	1 pg/mL
Chen et al., 2016	1 pg/mL – 100 pg/mL	1.37 pg/mL
Lou et al., 2014	0.1 pg/mL – 100 ng/mL	0.059 pg/mL
Yang et al., 2013	0.00001 pg/mL – 0.1 pg/mL	0.00001 pg/mL
Peng et al., 2011	0.00001 pg/mL – 10 ng/mL	0.1 pg/mL
Li and Yang, 2011	2 pg/mL – 20 ng/mL	1 pg/mL
Deng et al., 2011	5 pg/mL – 50 ng/mL	2 pg/mL
Wang et al., 2012	0.2 pg/mL – 20 pg/mL	0.05 pg/mL
Wang et al., 2011	4 pg/mL – 800 pg/mL	1 pg/mL
Li and Yang, 2011	0.5 pg/mL – 30 pg/mL	0.5 pg/mL

Graphene is a very suitable material for electrochemical sensors due to the direct electron transfer between functionalised graphene and the bioreceptor, without the need for a mediator (Kumar et al., 2015). Graphene is a type of allotrope of carbon, with each carbon atom bonded to the neighbouring carbon with sp^2 carbon arrangement with the molecular bond length of 0.142 nanometres. Graphene is a two-dimensional nanomaterial with a closely packed carbon atom arranged in a monolayer hexagonal manner. Figure 2.11 shows the chemical structure of graphene.

Different protocols to synthesise graphene have been developed, such as chemical reduction of graphene oxide, chemical vapour deposition and mechanical exfoliation. However, the scale-up production of these protocols had high energy consumption and low productivity until 2014, where the infrared CO₂ laser was utilised to directly convert the polyimide to porous graphene, also known as Laser Scribed Graphene or Laser-Induced Graphene (Huang et al., 2020).

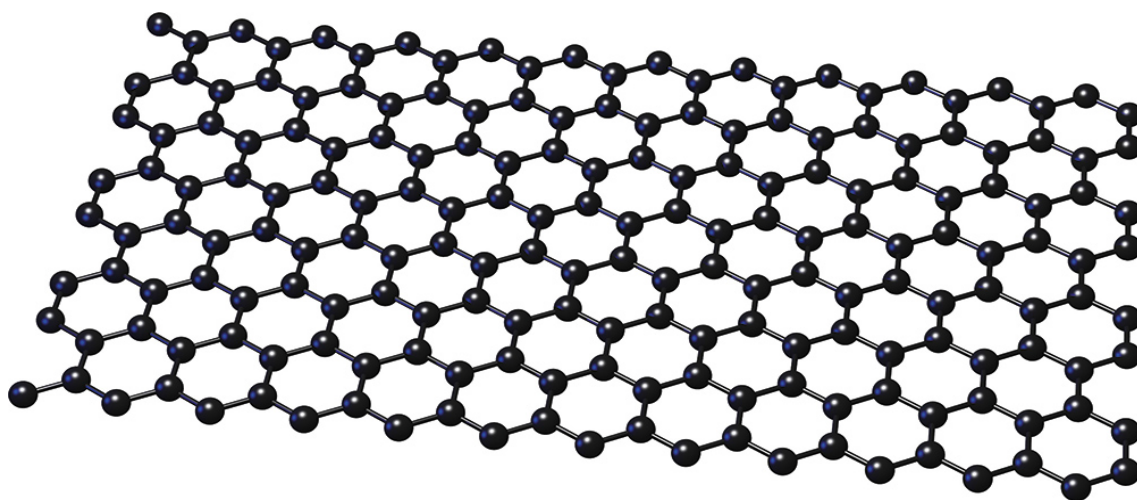


Figure 2.11. Structure of Graphene, (Science, 2017).

Although the physical properties of graphene attract research interest due to its strength, elasticity and mechanical stiffness, the electric properties of graphene should be carefully controlled. Graphene is only one atom thick and hence all the carbon atoms are exposed to the environment. Due to the atomically thin electric properties of graphene, graphene is very sensitive to the foreign atoms or molecules adsorbed on its surface. These features make graphene a better functional material compared to other bulk materials that rely not only on the surface but also on the homogeneous distribution of foreign atoms inside the bulk materials (Kim et al., 2015).

2.12. Laser Scribed Graphene Electrode

In 2014, a paper was published that described a one-step technique, laser scribed graphene (LSG) to produce electrodes where the polyimide substrate is

modified into 3D porous graphene films using carbon dioxide laser irradiation (Lin et al., 2014). This converts the sp^3 carbon atoms arrangement into sp^2 as the energy from the laser induces the vibration of atoms and thus breaks the carbon-oxygen single bond, carbon-oxygen double bond and nitrogen carbon single bonds. The aromatic structure of the polyimide rearranged itself into the graphitic structure which forms the graphene structure (Cardoso et al., 2019).

LSG has high porosity which increases the surface of immobilisation of bioreceptors, good electrical and thermal conductivity, good flexibility and mechanically robust which makes LSG a potential candidate for the development of miniaturised biosensors. Besides, the size and shape of the LSG electrodes can be easily controlled by computer design (Huang et al., 2020). This process is cost-effective and time-saving, making it suitable as a point of care biosensor electrode (Kumar et al., 2015).

Different methods had been invented before LSG technology to fabricate graphene and include 3D printing, screen printing and photolithography. (Huang et al., 2020) summarised the pros and cons of these methods compared to LSG/LIG technology and can be seen in Table 2.3.

Table 2 3. Comparison of different methods to fabricate graphene, (Huang et al., 2020).

	Screen printing	3D printing	Photolithography	LIG
Patternable	✓	✓	✓	✓
Mask/mold-free	×	×	×	✓
High resolution	✓ (40 μ m)	✓ (150 nm)	✓ (atomic)	✓ (12 μ m)
High yield	✓	✓	×	✓
Low cost	✓	✓	×	✓
GO-free	×	×	×	✓
Direct control of surface morphology and properties	×	✓	×	✓

2.12.1 LSGE Glucose Biosensors

A DVD-laser scribed graphene (LSG) with copper nanoparticles electrodeposited as the catalyst was described as a flexible and highly sensitive glucose biosensor for the continuous monitoring of blood glucose of patients with diabetes. This biosensor showed a linear glucose detection range from 1 μM to 4.54 mM with a sensitivity of 1.518 mA mM⁻¹ cm⁻² and a detection limit of 0.35 μM . The detection linear range is important for diagnosis of diseases. For example, a typical blood glucose level for normal people is less than 4.8 mM and more than 11.1 mM for diabetes patient one to two hours after meals (Normal and Diabetic Blood Sugar Level Ranges - Blood Sugar Levels for Diabetes, 2019). The linear range for glucose biosensor should cover the range for both normal and diabetic users. Figure 2.12 shows the schematic process for the fabrication and modification of the LSGE. The graphene paste is coated onto the polyimide foil and converted to graphene by laser. The copper foil is attached to the laser scribed graphene for electric conductivity and encapsulated with silicone rubber to keep a constant reactive area. The LSG electrode is then electrodeposited with the copper nanoparticles to increase the sensitivity of the electrode (Lin et al., 2018).

The paper published by Lin *et al* described the fabrication of the laser-scribed graphene electrode by using 0.4g Graphene Oxide powder, added into 100 mL of water and sonicated for 20 min to produce 4 mg/mL GO aqueous suspension. GO suspension is coated evenly onto a piece of polyimide (PI) foil by the doctor blade method. The copper nanoparticles are decorated on the sensing area via potentiostatic deposition. This biosensor works by the principle that the glucose oxidises the copper and produces electrons that can be quantified by amperometry methods, (Lin et al., 2018).

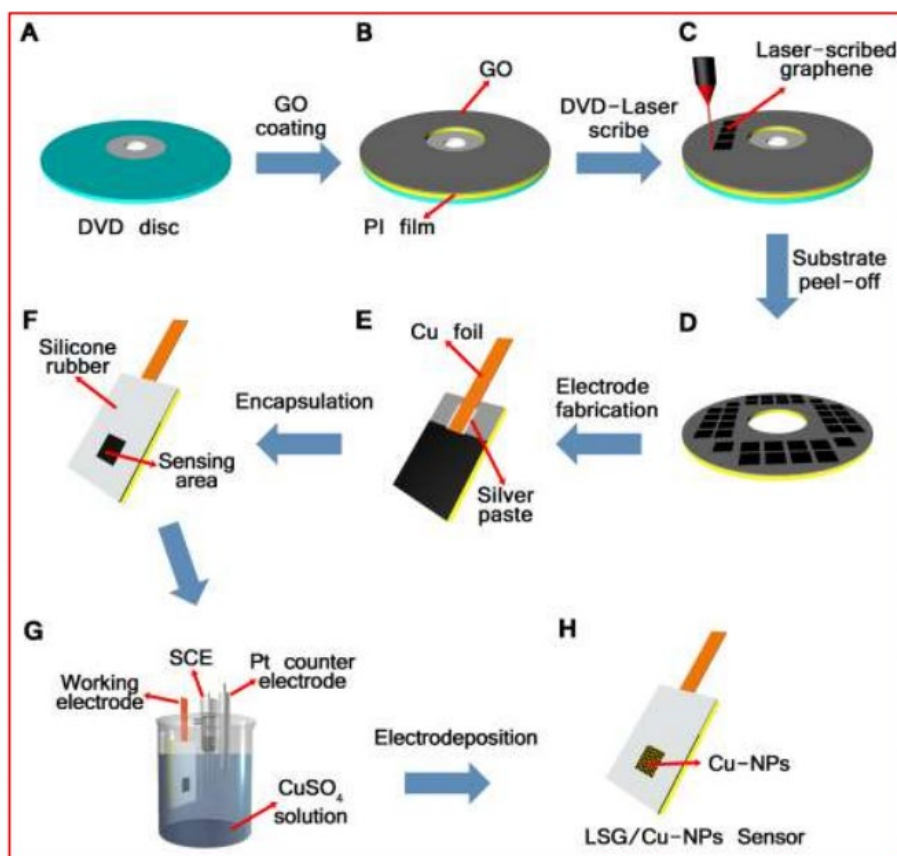


Figure 2.12. Schematic progress of fabrication and modification of DVD-laser scribed graphene (LSG), (Lin et al.2018).

(Tehrani and Bavarian, 2016) described a laser engraved graphene electrode for the detection of glucose using copper nanocubes with a sensitivity of $4532.2 \mu\text{A}/\text{mM}\cdot\text{cm}^2$, a low detection limit of 250 nM and a linear range of 25 μM to 4 mM. (Prabhakaran and Nayak, 2020) described an LSGE sensor that enables the non-enzymatic detection of glucose in human body fluids with copper oxide nanoparticles. This device shows a detection limit of 0.1 μM and a linear range of 1 μM to 5 mM. (Lin et al., 2018).

Commercially available glucose biosensors have assay ranges from 10 to 600 mg/dL which is equivalent to 0.555 mM to 33.3 mM. Hence, graphene-based glucose biosensors have a lower detection limit than the commercially available glucose biosensor.

2.12.2 Aptamer-Based LSGE Biosensor

The LSGE for aptamer-based biosensing is described in the paper published by (Fenzl et al., 2017). Aptamers are short, single stranded oligonucleotides that provide high affinity and bind to specific target molecules. They can be used as the analogs of antibodies, (Adachi and Nakamura, 2019). As shown in Figure 2.13, a universal modification method for LSGE was described where the electrode was modified by 1-pyrenebutyric acid followed by EDC and NHS chemical coupling. This creates a linker to attach the aptamers that act as the bioreceptors to the LSGE.

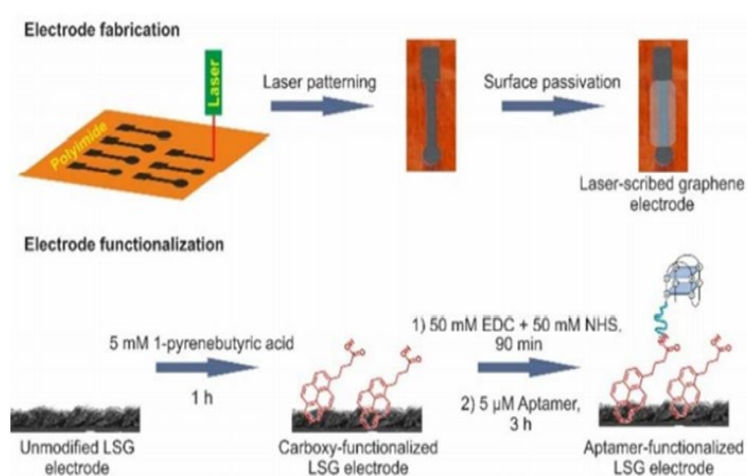


Figure 2.13. LSGE fabrication and functionalisation process, (Fenzl et al., 2017).

The aptamers can then capture the thrombin analytes present in the sample. DPV was performed with the potassium cyanide as electrolytes. With increasing thrombin concentration, the movement of the ferricyanide to the LGS electrode surface is further hindered by the thrombin and hence decrease in peak current can be observed. A schematic representation is shown in Figure 2.14. This electrode showed a low detection limit of 1 pM and high sensitivity of $-5.2 \mu\text{A}\cdot\text{cm}^{-2}$ (Fenzl et al., 2017).

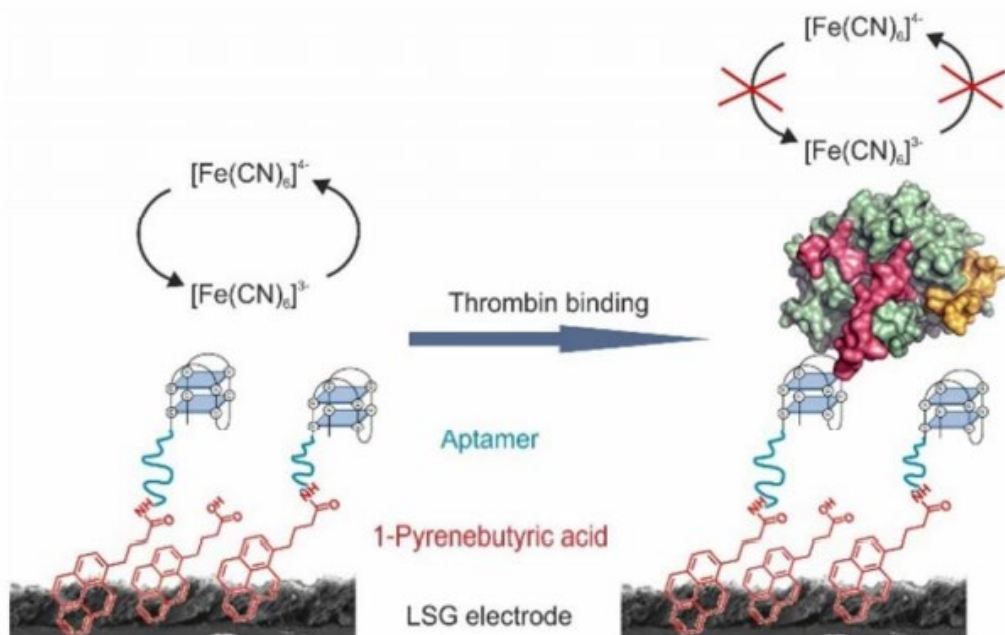


Figure 2.14. Electrochemical detection mechanism of thrombin, (Fenzl et al., 2017).

2.12.3 Others

A laser-induced graphene electrode with molecularly-imprinted polymer (MIP) produced at the working electrode is described in a paper published by (Cardoso et al., 2019). MIP is a type of synthetic receptor that has cavities that act as binding sites and are specific to the target molecules. The MIP was produced by direct electropolymerisation of Eriochrome black T (EBT) which acts as a bioreceptor for chloramphenicol. Chloramphenicol is an antibiotic that is used for the treatment of bacterial infection by binding to the bacterial ribosome and inhibiting protein synthesis. The limit of detection for the electrode described was 0.62 nM with linear behaviour from 1 nM to 1 mM (Cardoso et al., 2019).

Biogenic amines (BA) are basic nitrogenous compounds where the total concentration of BA present in food can be used to indicate food quality and safety. For example, fermented fish products with high levels of BA can be correlated to microbial contamination. (Vanegas et al., 2018) described a method where the LSGE fabricated with the copper nanocubes are used to detect the presence of biogenic amines. The LSGE was biofunctionalized with diamine oxidase encapsulated with cellulose.

PEDOT, also known as poly(3,4-ethylene dioxythiophene) polystyrene sulfonate, is a conductive polymer with low oxidation potential, promotes electron transfer responses, high stability, great biocompatibility and good electrochemical activity. (Xu et al., 2018) described a dopamine sensor with a PEDOT-modified laser scribed graphene. Dopamine is a neurotransmitter that can be used as an indicator for the diagnostic biomarker of a neurological disorder such as Parkinson's disease and Alzheimer's disease. The electrode described in this paper established sensitivity of $0.22 \pm 0.01 \mu\text{A}/\mu\text{M}$ and a low detection limit of $0.33 \mu\text{M}$.

The LSGE is constantly explored by researchers to incorporate different bioreceptors and different transducers. However, no antibody-based LSGE is reported in the literature, specifically for LSGE detection of inflammation markers which was the basis of this present study.

Chapter 3. Materials and Methods

3.1 Culture of THP-1 Cells

All cell culture procedures were carried out aseptically in a biosafety cabinet¹ which had been UV sterilised for 30 minutes prior to use.

3.1.1 Cell Resuscitation

The THP-1 cell line¹ was thawed in a 37°C water bath for 5 minutes and the outer vial sprayed with 70% ethanol². The cell suspension was aseptically and gently transferred to a T-25 red cap flask³ with 9 mL of complete medium (RPMI media⁴, 20% FBS⁵, 0.05 mM β -mercaptoethanol⁶). The T-25 flask with resuscitated THP-1 cell suspension was incubated at 37°C, 5% CO₂ overnight. After 24 hours, 5 mL of cell suspension was spun at 125 g for 5 minutes at 37°C and resuspended in 5 mL of fresh complete medium with 10% FBS instead of 20% FBS (RPMI media, 10 % FBS, 0.05 mM β -mercaptoethanol). The remaining 5 mL of cell suspension was transferred to a new T-25 flask and incubated at 37°C, 5% CO₂. When the cell count reached 1 x 10⁶ cells/mL, the cells were expanded into a T-75 flask⁷.

3.1.2 Cell Viability Counts

Cell counting was performed using Trypan Blue⁸ or Erythrosine B⁹ with a 1:1 ratio of cell suspension and stain. The Neubauer Improved haemocytometer¹⁰ was used with the Leica inverted microscope for cell counting. A 10 μ L sample of the cell suspension was mixed with an equal volume of 0.1% dye in a 600 μ L eppendorf tube. Ten microliters of the mixture was carefully transferred under the coverslip of a Neubauer haemocytometer. The cells were counted in four corner quadrants, averaged and multiplied by 10,000 to determine the number of viable

¹ TIB-202, ATCC, LGC, UK.

² 459844, Sigma-Aldrich Ireland Ltd, Arklow, Ireland.

³ 83.3910.002, Sarstedt LTD, Wexford, Ireland.

⁴ A1049101, Gibco: Biosciences Limited, Dublin, Ireland.

⁵ 10500064, Gibco: Biosciences Limited, Dublin, Ireland.

⁶ 21985-023, Gibco: Biosciences Limited, Dublin, Ireland.

⁷ 83.3911.002, Gibco: Biosciences Limited, Dublin, Ireland.

⁸ T8154, Sigma-Aldrich Ireland Ltd, Arklow, Ireland.

⁹ 200964, Sigma-Aldrich Ireland Ltd, Arklow, Ireland.

¹⁰ BR717805, Sigma-Aldrich Ireland Ltd, Arklow, Ireland.

cells per milliliter in the cell suspension. After counting, 1×10^6 THP-1 cells were transferred to a new T-75 flask with 25 mL complete media and placed in the incubator until further use.

3.1.3 Cell Subculture

THP-1 cell was maintained by adding fresh media every second day. THP-1 cell subculture was performed when cell concentration reached 8×10^5 cells/mL. The cells were resuspended in 20 mL of complete medium at 2×10^5 cells /mL cell density and incubated at 37°C, 5% CO₂ for 14 days.

3.1.4 Cell Cryopreservation

Cell freeze medium was aseptically prepared by creating a 95% FBS and 5% DMSO¹¹ solution which was 0.2 µM sterile-filtered and chilled at 4 °C until needed. Cells were frozen at 5×10^6 cell density in 1 mL of freezing medium and added to the cryovial¹². The cryovial was stored in Mr. Frosty¹³ freezing container at -80°C overnight. The cryovial was transferred to long-term liquid nitrogen storage the next day.

3.2. Differentiation and Polarisation of THP-1 Cells

THP-1 cells are monocytes and for inflammation studies, these cells required differentiation into macrophage phenotypes to be fully competent in their immune duties.

3.2.1 Differentiation of THP-1 cells to Macrophage; M0

To achieve differentiation of cells to macrophage phenotypes, 2×10^5 THP-1 suspended cells per miller of media were incubated with 25 nM Phorbol 12-myristate 13-acetate¹⁴ (PMA) for 24 hours in a T-25 flask. After incubation, the

¹¹ D8418, Sigma-Aldrich Ireland Ltd, Arklow, Ireland.

¹² 72.379, Sarstedt Ltd, Wexford, Ireland.

¹³ 5100-0001, Fisher Scientific, Dublin, Ireland.

¹⁴ P8139, Sigma-Aldrich Ireland Ltd, Arklow, Ireland.

cells adhered to the culture flask. The PMA containing media was replaced with fresh media without PMA. Cell counts were performed for the harvested supernatant to ensure a low number of cells left in the supernatant. The differentiated adherent cells were rested for 24 hours. The supernatant was stored in -20°C until further analysis.

3.2.2 Polarisation to Classically Activated Macrophage; M1

Macrophage cells required polarisation (activation) to different inflamed cell states to analyse the inflammatory cytokines secreted and the surface marker expression. Classically activated macrophages are associated with pro-inflammatory responses. The differentiated THP-1 cells were cultured in fresh media with 20 ng/mL purified Mouse Anti-Human IFN- γ ¹⁵ and 20 ng/mL Lipopolysaccharide (LPS)¹⁶ for 24 hours at 37°C, 5% CO₂. The cell supernatants were recovered and stored at -20°C for further analysis to confirm M1 macrophage phenotype by ELISA and flow cytometry.

3.2.3 Polarisation to Alternative Activated Macrophage; M2

Alternatively activated macrophages are responsible for anti-inflammatory responses. The differentiated THP-1 cells were cultured in fresh medium with 20 ng/mL recombinant Human IL-4 Protein¹⁷ and 20 ng/mL recombinant Human IL-13 Protein¹⁸ and incubated for 72 hours at 37°C, 5% CO₂. The cell supernatants were harvested and stored at -20°C until further analysis to confirm M2 cell phenotype by ELISA and flow cytometry.

¹⁵ 550011, BD Biosciences, UK.

¹⁶ L4391, Sigma Aldrich Ireland Ltd, Arklow, Ireland.

¹⁷ 204-IL-010, R&D BioSystems, UK.

¹⁸ 213-ILB-005, R&D BioSystems, UK.

3.3. Characterisation of THP-1 Cell Polarisation to Macrophage

3.3.1 Macrophage Cell Secretion: ELISA

The cytokine levels in the harvested cell culture supernatants were determined with ELISA for IL-6¹⁹, IL-12p70²⁰, IL-8²¹, IL-1 β ²², Fibronectin²³, and TGF- β ²⁴. ELISA tests were carried out according to the manufacture's manual instructions. For example, the IL6 ELISA was performed by coating the 96 well microplate²⁵ with 100 μ L per well of the 2 μ g/ mL IL-6 Capture Antibody²⁶ overnight at room temperature. Each well was aspirated and washed with 400 μ L of wash buffer²⁷. The washing step was performed three times by complete removal of the wash buffer by aspirating and blotting with paper towel. Reagent Diluent²⁸ (300 μ L) was added to each well and incubated for 1 hour at room temperature to block and prevent non-specific binding in the well plate. The washing step was performed again. Standards and samples were added to the plate in 100 μ L aliquots. Human IL-6 Standard²⁹ (100 μ L of 600 pg/mL) was added and double dilution was performed six times with reagent diluent to 9.48 pg/mL as the lowest concentration. The supernatant collected from THP-1 cells in monocyte form, M0, M1 and M2 macrophage phenotypes were added in 100 μ L aliquots and incubated for 2 hours at room temperature. The washing step was performed, thrice. Detection Antibody³⁰ (100 μ L of 50 ng/mL) in reagent diluent was added to wells and incubated for 2 hours at room temperature. The washing step was performed four times. Streptavidin-HRP³¹ (100 μ L) was added to each well and incubated for 20 minutes at room temperature. The plate was covered with tin foil to avoid direct light. The washing step was performed, five times. The substrate solution was prepared by mixing Colour Reagent A and Colour Reagent B³² and

¹⁹ DY206, R&D Biosystems, UK.

²⁰ DY1270, R&D Biosystems, UK.

²¹ DY208, R&D Biosystems, UK.

²² DY201, R&D Biosystems, UK.

²³ DY1918, R&D Biosystems, UK.

²⁴ DY240, R&D Biosystems, UK.

²⁵ 44-2404-21, ThermoFisherScientific, Ireland.

²⁶ HD4818081, R&D Biosystems, UK.

²⁷ WA126, R&D Biosystems, UK.

²⁸ DY995, R&D Biosystems, UK.

²⁹ 151523, R&D Biosystems, UK.

³⁰ SV2918081, R&D Biosystems, UK.

³¹ P188503, R&D Biosystems, UK.

³² CY999, R&D Biosystems, UK.

100 μ L of substrate was added to each well and incubated for 20 minutes with the plate covered with tin foil. Finally 50 μ L of Stop Solution³³ was added and the plate was gently tapped to ensure thorough mixing. The optical density was measured with the plate reader³⁴ at 540 nm and 450 nm. The final optical density was calculated by subtracting the reading at 540 nm from that at 450 nm (Human IL-6 DuoSet ELISA DY206-05: R&D Systems, 2021).

3.3.2 Flow Cytometry of Macrophage Surface Markers.

Macrophage polarised THP-1 cells were confirmed by flow cytometry which examined the expression of cell surface markers. Polarised THP-1 cells were rinsed with 10 mL of Dulbecco Phosphate Saline (DPBS)³⁵. The adherent polarised macrophage cells were detached from the culture vessel surface by incubating with 10 mL Accutase solution³⁶ at 37°C, 5% CO₂ for 10 minutes. The detached cells were resuspended in 10 mL of complete media for flow cytometry analysis. Flow cytometry stain buffer solution was prepared (DPBS with 0.2 % BSA³⁷). 100 μ L of this buffer was added to 1X10⁶ cells and analysed with the flow cytometer as the unstained control sample. To stain cells for surface marker detection, cells were suspended in 50 μ L flow stain buffer at a concentration of 1X10⁶ cells. To prevent non-specific binding, the cells were blocked with 5 μ L of Human BD Fc Block³⁸ at room temperature for 10 mins. To this cell-Fc block suspension, a variety of antibodies were individually added in 20 μ L aliquots; FITC Mouse Anti-Human CD80³⁹, FITC Mouse IgM Isotype C⁴⁰, PE Mouse Anti-Human CD206⁴¹ or Isotype Control⁴² and incubated on ice for 1 hour in the dark. Fluorescein isothiocyanate (FITC) and Phycoerythrin (PE) were fluorophores with fluorescence properties. The washing step with the flow stain buffer was

³³ DY994, R&D Biosystems, UK.

³⁴ Varioskan™ LUX multimode microplate reader, Fisher Scientific, Dublin, Ireland.

³⁵ 14190-094, Gibco: Biosciences Limited, Dublin, Ireland.

³⁶ A6964, Sigma-Aldrich Ireland Ltd, Arklow, Ireland.

³⁷ A4161, Sigma-Aldrich Ireland Ltd, Arklow, Ireland.

³⁸ 564219, BD Biosciences, UK.

³⁹ 555683, BD Biosciences, UK.

⁴⁰ 555583, BD Biosciences, UK.

⁴¹ 555954, BD Biosciences, UK.

⁴² 555749, BD Biosciences, UK.

performed twice to remove unbound antibody and prevent non-specific binding. Cell fixation was performed in 2% paraformaldehyde⁴³ in DPBS on ice for 15 min to prevent cell deterioration and cleavage of surface markers. Post antibody binding, the washing step was performed twice and the cells were resuspended in 100 µL of flow stain buffer before analysis with the flow cytometer, CytoFLEX⁴⁴ with CytExpert software. Quality control for the CytoFLEX was performed with CytoFLEX Daily QC Fluorospheres⁴⁵ for laser alignment to make sure that the flow cytometer was functioning properly.

3.4. Antibody Selection for Biofunctionalisation of LSGE

Based on the secretion of inflammatory cytokines and the expression of surface markers by M1 and M2 macrophage phenotypes, IL-6 was chosen as the target analyte to be detected by the LSGE biosensor. Hence, an antigen antibody (anti IL-6 antibody) was biofunctionalised on to the LSGE to act as the sensor bioreceptor.

3.5. Fabrication of LSGE

This study was performed in collaboration with Tyndall National Institute, UCC who designed and fabricated the LSGE. The fabrication process is described by Burke *et al.*, (2020) and Vaughan *et al.*, (2020). Briefly, polyimide films with a thickness of 80 µm was the starting material for LSG electrode fabrication. Laser written graphitic carbon electrodes and electrode arrays were fabricated by direct laser writing (CO₂ laser, 10.6 µm wavelength) on these polyimide films using methodologies developed by Tyndall. LSG electrodes were fabricated using a mini-speed laser engraving machine (Colemeter DK-8 Pro-5 Square Haste Edition) equipped with a diode laser with a wavelength of 405 nm (Burke *et al.*, 2020). Polyimide tapes fixed on glass microscope slides for support were irradiated at 500 mW laser power and dwell times (dwell times) between 10 and 120 ms/pix. Electrode structures were fabricated by raster scanning of the laser

⁴³ 158127, Sigma-Aldrich Ireland Ltd, Arklow, Ireland.

⁴⁴ Beckman Coulter, UK.

⁴⁵ B53230, Beckman Coulter, UK.

beam to create the electrode pattern on the polyimide surface. Fabricated electrodes (figure 3.1) were washed with acetone and isopropanol and dried with a N₂ gun before use (biofunctionalisation) in the cell culture laboratories in MTU, Kerry.

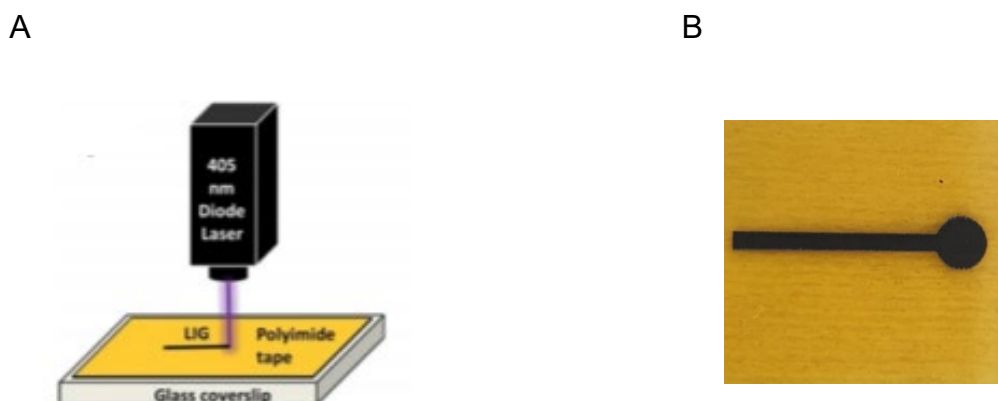


Figure 3.1. A) Schematic of the LIG fabrication process, (Vaughan et al., 2020). B) Fabricated LSG electrode (3mm).

3.6. Characterisation of LSGE

Cyclic Voltammetry (CV) and Differential Pulse Voltammetry (DPV) are electrochemical techniques which measure the current that develops in an electrochemical cell under conditions where voltage is in excess and involves linearly sweeping potential between the working and reference electrodes, i.e., cycling the potential of a working electrode, and measuring the resulting current via a potentiostat, (Allen J. Bard; Larry A. Faulkner, 2001). The measured changing current produces a voltammogram plot where current is plotted against potential.

For this study, the redox-active solution was 5 mM Potassium Ferricyanide⁴⁶ in 1 M KCl in an electrochemical cell (figure 3.2) which consisted of a three-electrode system; a working electrode (the LSGE), a reference electrode (Silver/Silver Chloride⁴⁷) and a counter electrode (platinum wire⁴⁸) and CV was performed with an Autolab PGSTAT 302N potentiostat⁴⁹. Different scan rates, which included

⁴⁶ 702587-50G, Sigma Aldrich Ireland Ltd, Arklow, Ireland.

⁴⁷ CHI 111, IJ Cambria Scientific Ltd.

⁴⁸ CHI 115, IJ Cambria Scientific Ltd.

⁴⁹ Metrohm, UK.

0.01 V/s, 0.025 V/s, 0.5 V/s, 0.1 V/s and 0.2 V/s, were used and the LSGE was scanned from -0.1 V to 0.6 V as the parameter for CV analysis. Differential Pulse Voltammetry was carried out with 0.01 V/s scan rate, 0.025 V modulation amplitude, 0.005 V step potential, 0.5 s interval time and 0.05 s modulation intervals.

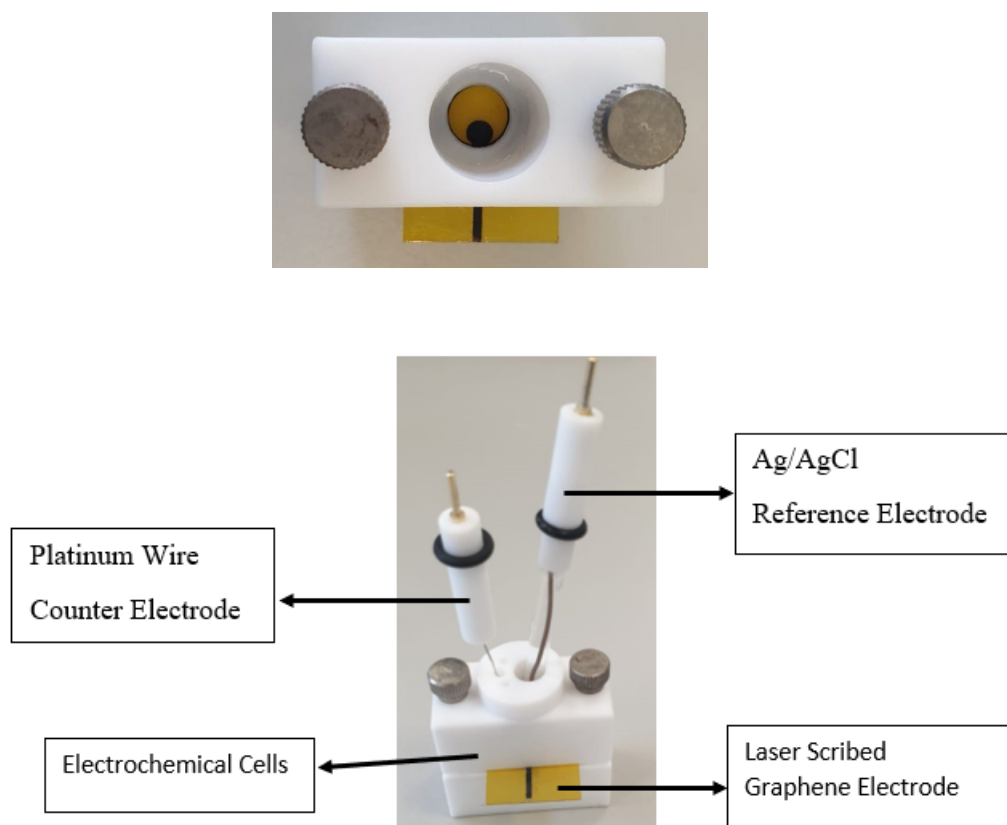


Figure 3.2. Electrochemical Cell Setup; including LSGE as working electrode, Ag/AgCl as reference electrode and Platinum wire as the counter electrode.

3.7. LSGE BioFunctionalisation

To enable the LSGE to function as a biosensor, PBA and EDC:NHS were used to functionalise the LSGE. These two chemicals create the linker for the bioreceptor (IL-6 antigen antibody) to be bound to the electrode surface (biofunctionalisation). The biomodified LSGE with IL-6 antigen which acts as the sensor bioreceptor can bind and detect the IL-6 antibody in solution.

3.7.1 Preparation of LSGE for BioFunctionalisation

The LSGE was washed with acetone⁵⁰, isopropanol⁵¹ and deionised water to remove any residues from the laser engraving process. Cyclic Voltammetry was performed initially before any modification steps. The LSGE was applied with nail polish⁵² as a coating material for passivation to keep the LSGE surface area uniform in structure and activity. The LSGE was incubated in 250 mM 1-Pyrenebutyric Acid (PBA)⁵³ dissolved in DMSO for 60 minutes in a 12 well plate⁵⁴. The LSGE was washed with DMSO, isopropanol and ethanol⁵⁵ in sequence by immersion in 2 mL of the solution for 1 minute in a 6 well plate⁵⁶. The LSGE was then incubated in a one-to-one ratio of 75 mM 1-Ethyl-3-(3-dimethylaminopropyl) carbodiimide (EDC)⁵⁷ and 50 mM (N-Hydroxysuccinimide) NHS⁵⁸ for 90 minutes. The LSGE was immersed in PBS for 15 minutes. The functionalised LSGE was then incubated with 2.5 µg/ml Purified Rat Anti-IL-6⁵⁹ (IL-6 antigen) overnight. The modified LSGE was ready to detect the present of Recombinant Human IL-6 (IL-6 antibody) by incubating the LSGE with the IL-6 antibody for 90 minutes. Cyclic Voltammetry at the scan rate of 0.1 V/s was performed after each modification step in the electrochemical cell. A flow diagram in figure 3.3 shows the overall modification process of the LSGE.

⁵⁰ 100014.5000, Merck Millipore Ltd., Ireland.

⁵¹ 1317HS, Sigma Aldrich Ireland Ltd, Arklow, Ireland.

⁵² Protective Base Coat, Wet n Wild, Ireland.

⁵³ 257354-5G, Sigma Aldrich Ireland Ltd, Arklow, Ireland.

⁵⁴ 83.3921.005, Sarstedt LTD, Wexford, Ireland.

⁵⁵ E392, Sigma Aldrich Ireland Ltd, Arklow, Ireland.

⁵⁶ 83.3920.300, Sarstedt LTD, Wexford, Ireland.

⁵⁷ 39391, Sigma Aldrich Ireland Ltd, Arklow, Ireland.

⁵⁸ 130672, Sigma Aldrich Ireland Ltd, Arklow, Ireland.

⁵⁹ 559068, BD Biosciences, UK.

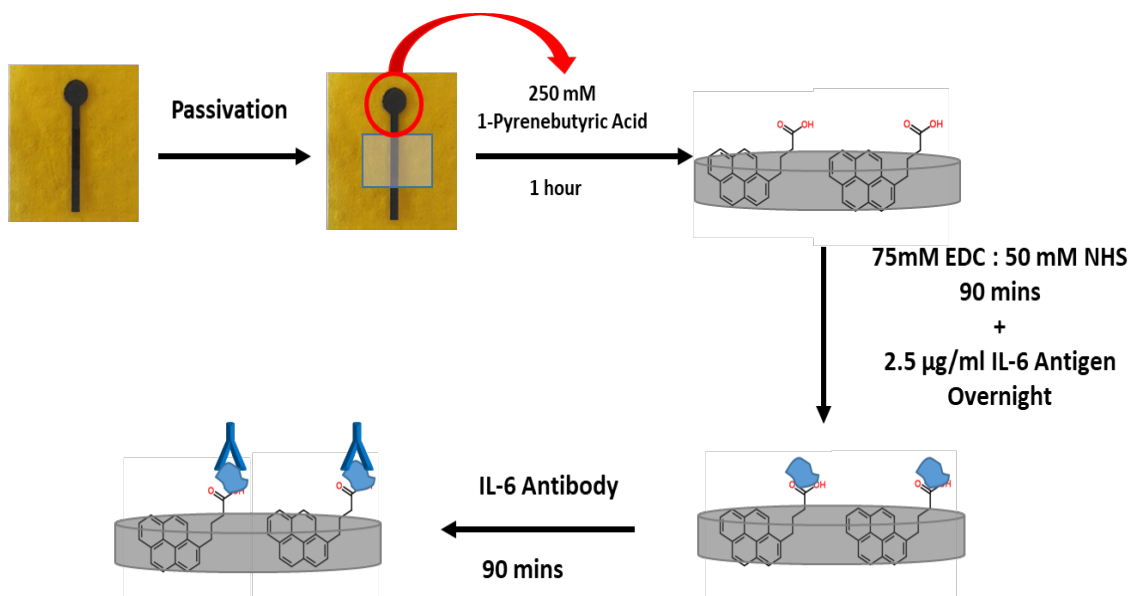


Figure 3.3. Biofunctionalisation of LSGE at room temperature.

3.7.2 Optimisation of LSGE Biosensor

To facilitate binding of the bioreceptor to the LSGE, two chemicals in the form of PBA and EDC:NHS were assessed to facilitate antibody binding to the electrode surface. PBA interacted with the LSGE via π - π -stacking and provided carboxyl groups (figure 3.4) that enable binding of IL-6 antigen to the LSGE. π - π -stacking was a type of non-covalent interaction which occurred between aromatic group containing π bond (Zhuang et al., 2019). PBA concentrations of 10, 100, 250 and 500 mM were used to determine optimum PBA concentration. Cyclic Voltammetry was performed before and after the LSGE was immersed in the PBA to analyse the decrease in peak current.

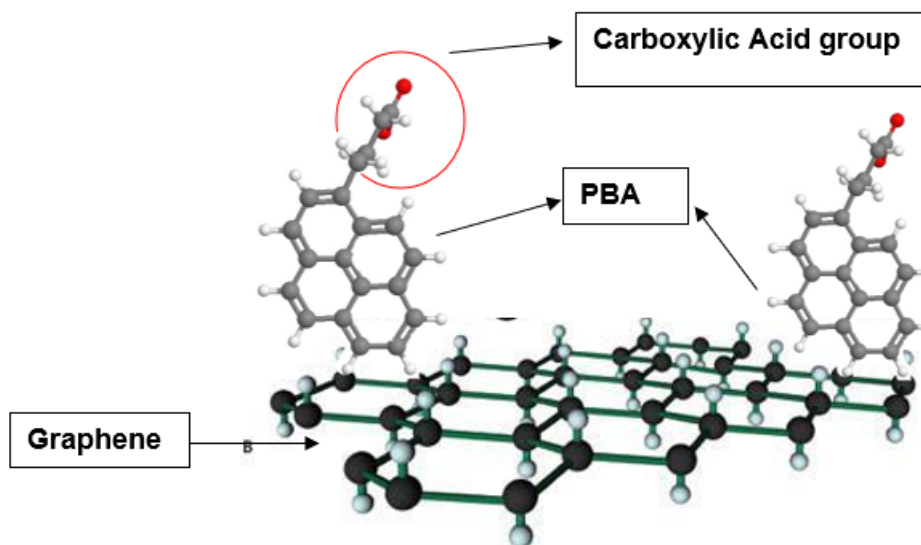


Figure 3.4. Graphene functionalisation with PBA (Domingo, 2010) (Anon, 2019).

Different concentrations of EDC:NHS were used; 5 mM EDC:5 mM NHS, 75 mM EDC:50 mM NHS with 90 minutes incubation and 400 mM EDC:100 mM NHS with 15 minutes incubation time periods based on three different journal paper (Sam et al., 2010) (Thangamuthu, Santschi and Martin, 2018) (Fenzl et al., 2017). The DPV was performed with 1000 pg/mL of IL-6 antigen to confirm enough linker present on the LSGE to bind the IL-6 antigen bioreceptor to the LSGE surface, with figure 3.5 showing the mechanism for the EDC/NHS coupling reaction.

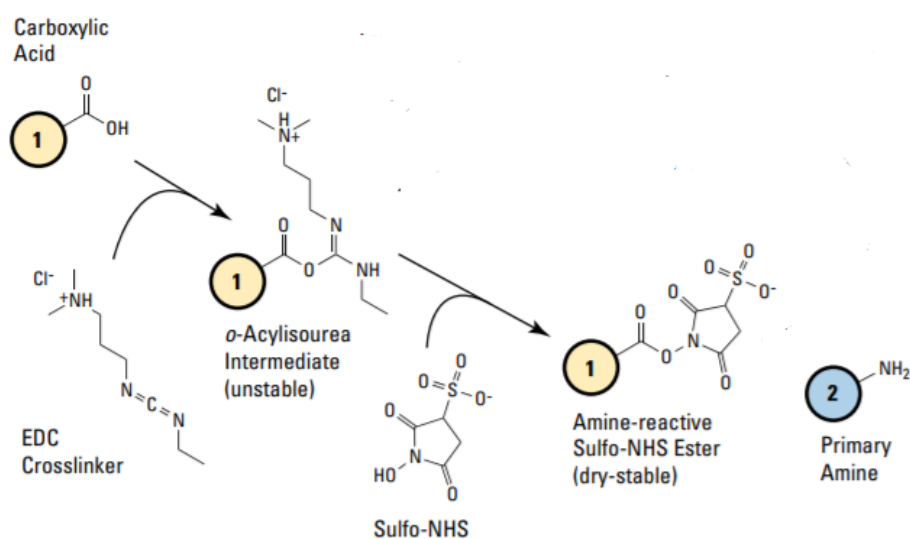


Figure 3.5. EDC/NHS coupling reaction mechanism, (Thermoscientific, 2012).

Different concentrations of the bioreceptor, Purified Rat Anti-IL-6 (IL-6 antigen) were used that included 0.5, 1.0, 2.5 and 5.0 $\mu\text{g/mL}$ with overnight incubation. The changes in DPV peak current were calculated by measuring the peak current before and after IL-6 antigen incubation to determine optimum concentration of IL-6 antigen immobilisation on the LSGE.

3.8. Calibration of LSGE Biosensor

The LSGE biosensor was examined to detect IL-6 antibody concentrations (Recombinant Human IL-6) across a range of 10, 25, 50, 75, 100, 250 and 500 pg/mL prepared in PBS. The IL-6 antibody was dispensed on to the LSGE biosensor in 200 μL aliquots for 90 minutes. The Differential Pulse Voltammetry was performed before and after incubation with IL-6 antibody. The change in peak current before and after incubation with IL-6 antibody on the LSGE was calculated and plotted against the log concentration of IL-6 antibody.

3.9. Method Comparison; LSGE Biosensor vs ELISA

The performance of the LSGE biosensor to detect IL-6 antibody was compared with an IL-6 ELISA. A calibration curve of IL-6 antibody via ELISA detection was plotted with 10, 25, 50, 75, 100, 250, and 500 pg/mL of IL-6 antibody using the protocol in section 3.3.1. A method comparison plot was created to compare both methods with absorbances from ELISA test on x-axis and the change in peak current from LSGE biosensor on the y-axis.

3.10. Specificity and Selectivity of LSGE Biosensor

Recombinant Human IL-6 (IL-6 antibody) over a range of 10 to 500 pg/mL was prepared in 10% of Fetal Bovine Serum (FBS) and 10% BSA in PBS separately. Both biological solutions in 200 μL aliquots were dispensed on to the LSGE biosensor and the DPV was performed after incubation for 90 minutes. The change in peak current before and after incubation with both biological solutions

containing IL-6 antibody was calculated and plotted against the log concentration of IL-6 antibody in 10% FBS and BSA.

Chapter 4. Results

4.1 THP-1 Cells Differentiation and Polarisation

THP-1 monocytes were differentiated into macrophages (M0) and polarised into two different inflamed cell states, a classically activated macrophage (M1) and an alternatively activated macrophage phenotype (M2). THP-1 cell differentiation and polarisation were assessed by microscopy, ELISA and flow cytometry. On microscopic examination, THP-1 cells after differentiation to macrophages appeared to be larger (figure 4.1). The cells changed shape after polarisation from round to irregular shapes. Differentiated cells were adherent in nature opposed to the monocyte precursor which grew in suspension culture.

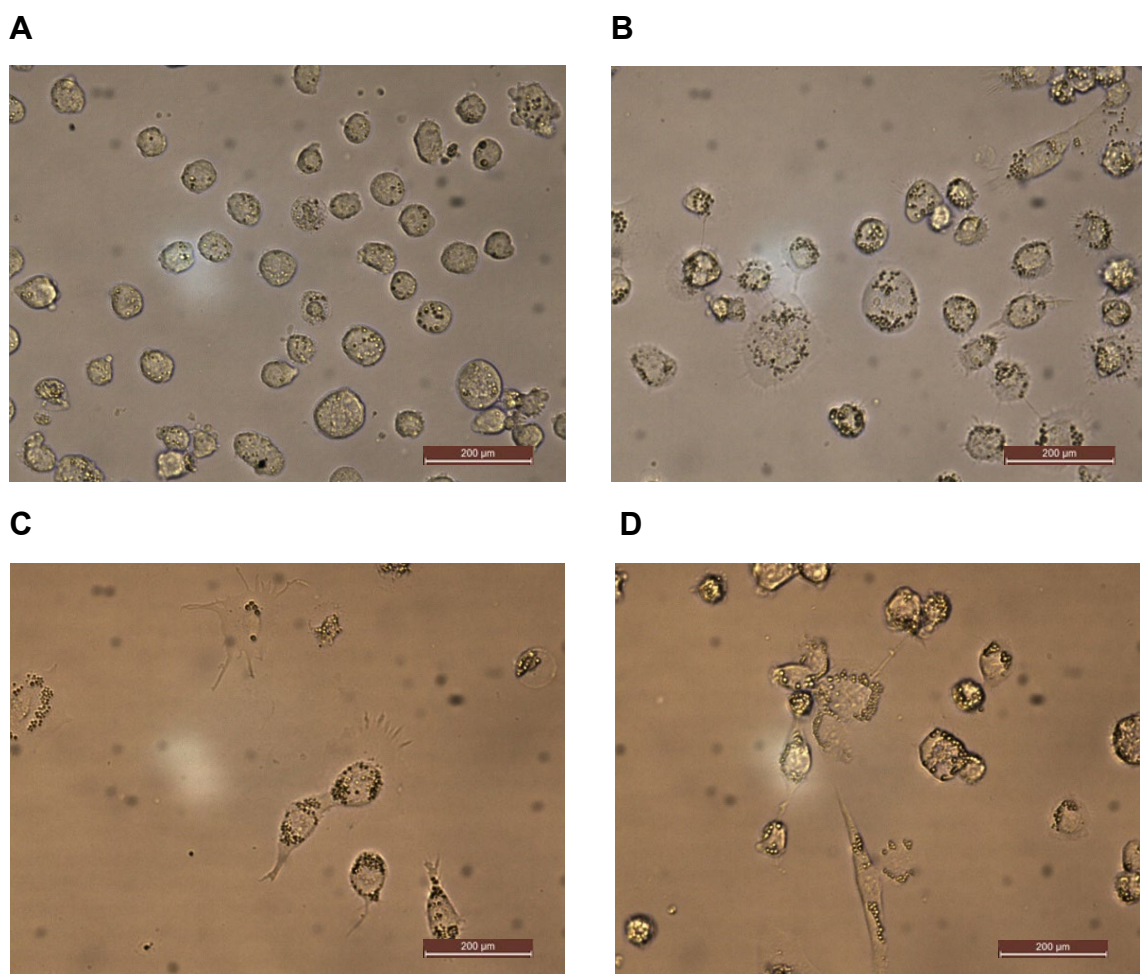


Figure 4.1. Differentiation and polarisation of THP-1 cells; from monocytes (A) into; (B) macrophages (M0); (C) classically activated macrophages (inflammatory) (M1); and (D) Alternatively activated phenotypes (anti-inflammatory) (M2). THP-1 cells were differentiated to macrophages (M0) by incubation in 25 nM PMA for 24 hours. Polarisation to classically activated macrophages (M1) was achieved by incubating macrophages (M0) with LPS and IFN- γ for 24hrs. Alternative activated macrophage phenotypes (M2) were achieved by incubating macrophages (M0) with IL-4 and IL-13 for 72 hours. Images x 1000.

4.2 Macrophage Cell Secretion; ELISA

ELISA was employed to assess the secretory profile of each macrophage phenotype. A variety of interleukin secretions were assayed by ELISA including IL-6, IL-12p70, IL-8 IL-1 β , Fibronectin, PDGF and TGF- β . The THP-1 cell line when differentiated and polarised to macrophage phenotypes did not produce detectable levels of IL-12p70, IL-8 IL-1 β , PDGF and TGF- β (results not presented). However, IL-6 (a proinflammatory interleukin) was detected in high quantities in the classically inflamed macrophage phenotype (M1) (figure 4.2). No IL-6 production was detected for monocytes, M0 and M2 macrophage phenotypes. The secretion of IL-6 by M1 phenotype THP-1 cells was significantly different from monocytes, M0 and M2 phenotype THP-1 cells with $P > 0.001$ and there were no significant differences for the secretion of IL-6 by monocytes, M0 and M2 phenotypes THP-1 cells.

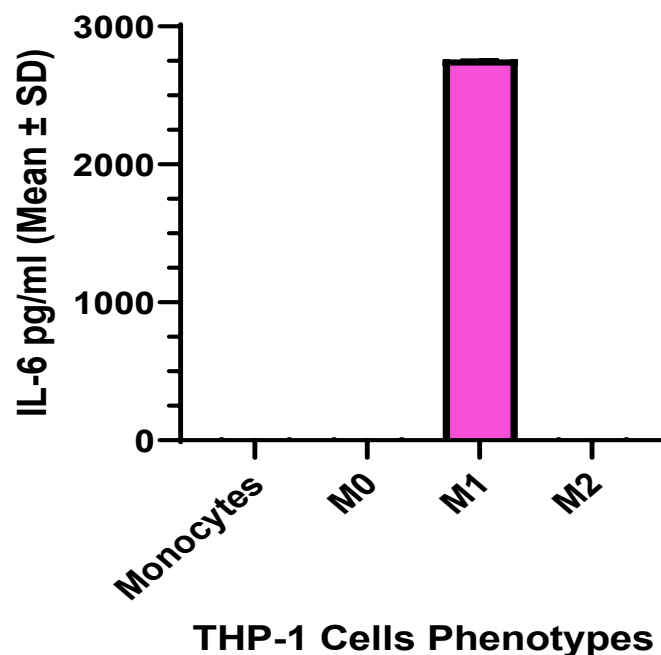


Figure 4.2. IL-6 secretion by different THP-1 cell phenotypes. The supernatant of suspension THP-1 monocytes was collected after centrifugation. THP-1 cells were differentiated to macrophages (M0) by incubation in PMA for 24 hours. Polarisation to classically activated macrophages (M1) was achieved by incubating macrophages (M0) with LPS and IFN- γ for 24hrs. Alternative activated macrophage phenotypes (M2) was achieved by incubating macrophages (M0) with IL-4 and IL-13 for 72 hours. After differentiation, the macrophages (M0, M1 and M2) became adherent to the flask. The cell culture supernatant were collected and cytokines levels in harvested supernatants determined by ELISA. Values represented the mean \pm SD of three replicate samples respectively.

Fibronectin was detected in a variety of macrophage phenotypes (figure 4.3). Alternative activated macrophage phenotypes (M2) secreted the highest level of fibronectin followed by classically activated macrophages (M1), M0 macrophage and finally monocytes. Based on one-way ANOVA analysis with multiple comparisons, the level of fibronectin secreted by M2 phenotype THP-1 cells was significantly higher than monocytes and M1 phenotype THP-1 cells.

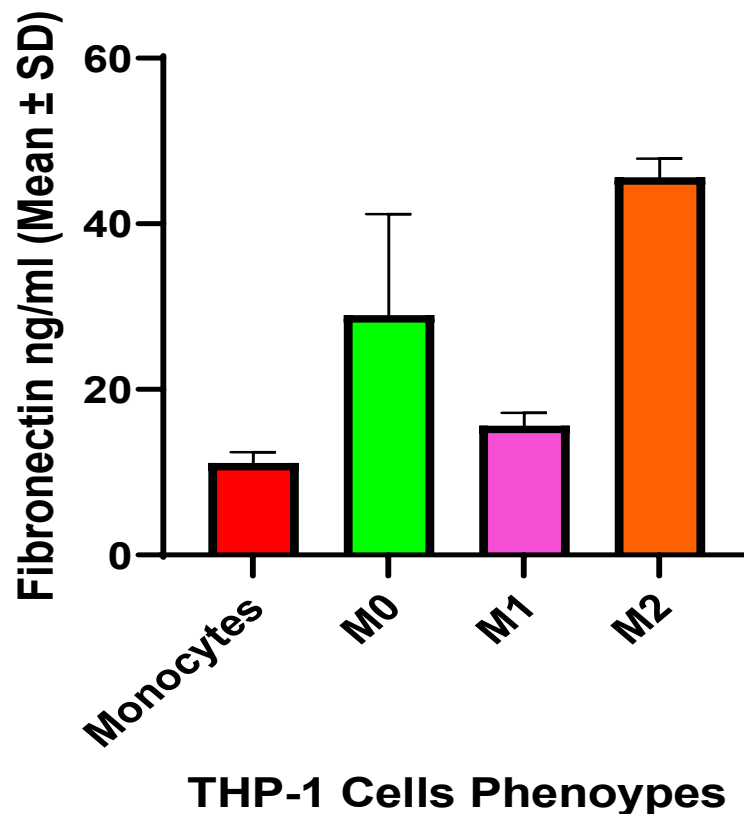


Figure 4.3. Fibronectin secretion by different THP-1 cell phenotypes. The supernatant of suspension THP-1 monocytes was collected after centrifugation. THP-1 cells were differentiated to macrophages (M0) by incubation in PMA for 24 hours. Polarisation to classically activated macrophages (M1) was achieved by incubating macrophages (M0) with LPS and IFN- γ for 24hrs. Alternative activated macrophage phenotypes (M2) was achieved by incubating macrophages (M0) with IL-4 and IL-13 for 72 hours. After differentiation, the macrophages (M0, M1 and M2) were adherent to the flask and cell culture supernatants were harvested for ELISA analysis to determine cytokine levels. Values represented the mean \pm SD of three replicate samples respectively.

4.3 Cell Surface Marker Expression by Flow Cytometry

Flow cytometry was performed on macrophage phenotypes to survey cell size, granularity and surface marker expression. Flow cytometry parameters of forward scatter (FSC) indicated the size of THP-1 cells and side scatter (SSC), granularity of cells. Both size and granularity of the THP-1 cells were increased after differentiation (figure 4.3). No significant increase in size and granularity for M0, M1 and M2 phenotypes was observed.

The surface marker expression of different THP-1 phenotypes was analysed using fluorochrome conjugated antibodies, CD80-FTIC and CD206-PE. CD80 was observed to be expressed only by classically activated macrophages (M1) and CD206 only expressed by alternatively activated macrophages (M2) (Table 4.1).

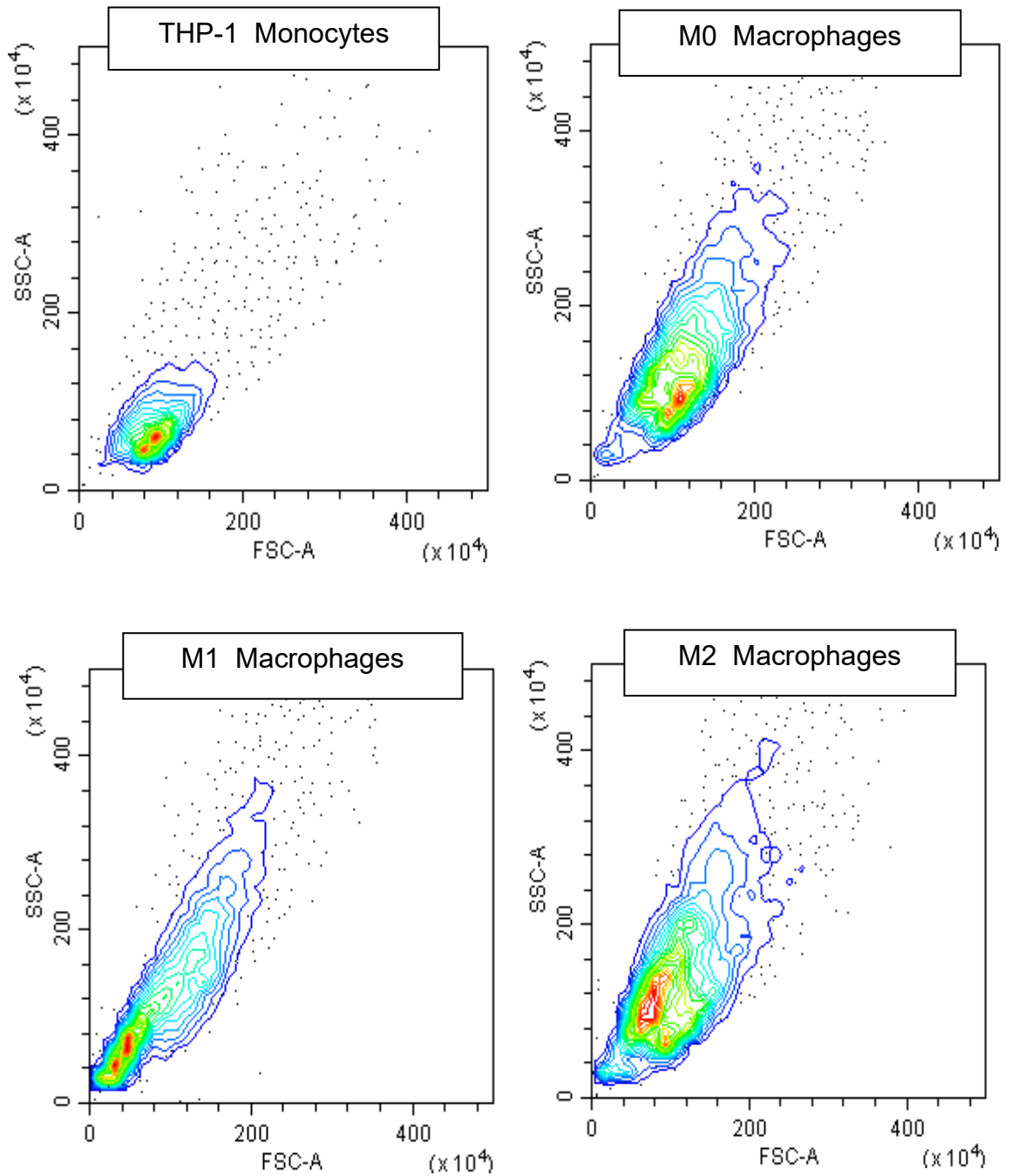
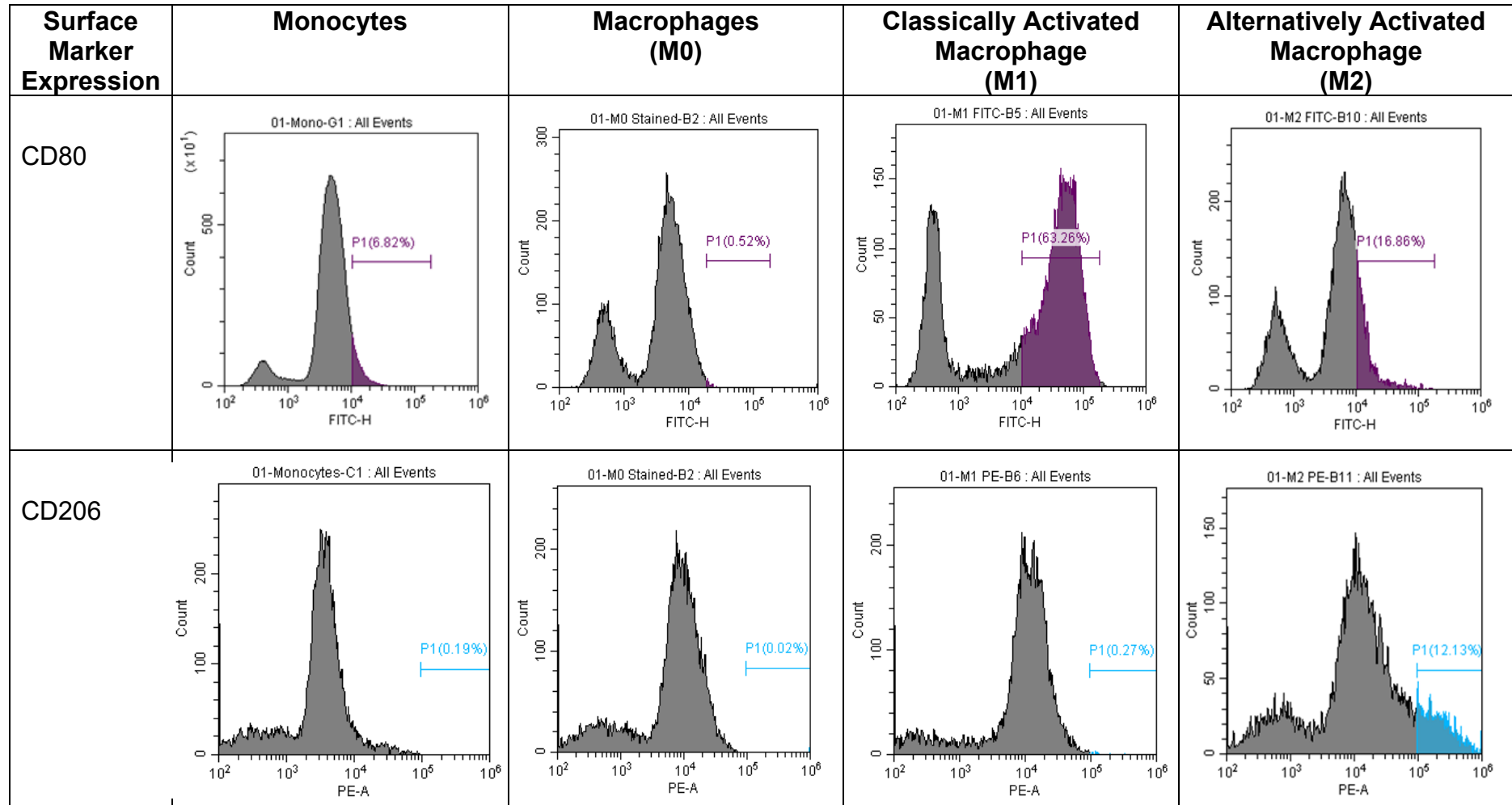


Figure 4.4. Flow cytometry analysis of cell size (SSC-A) and granularity (FSC-A) of different THP-1 phenotypes; M0, M1 and M2. Both size and granularity of the THP-1 cells increased after differentiation. No significant increase in size and granularity after polarisation of M0 macrophages into M1 and M2 macrophage phenotypes was noted.

Table 4.1. CD80 and CD 206 surface marker expression in different THP-1 cell phenotypes.



A

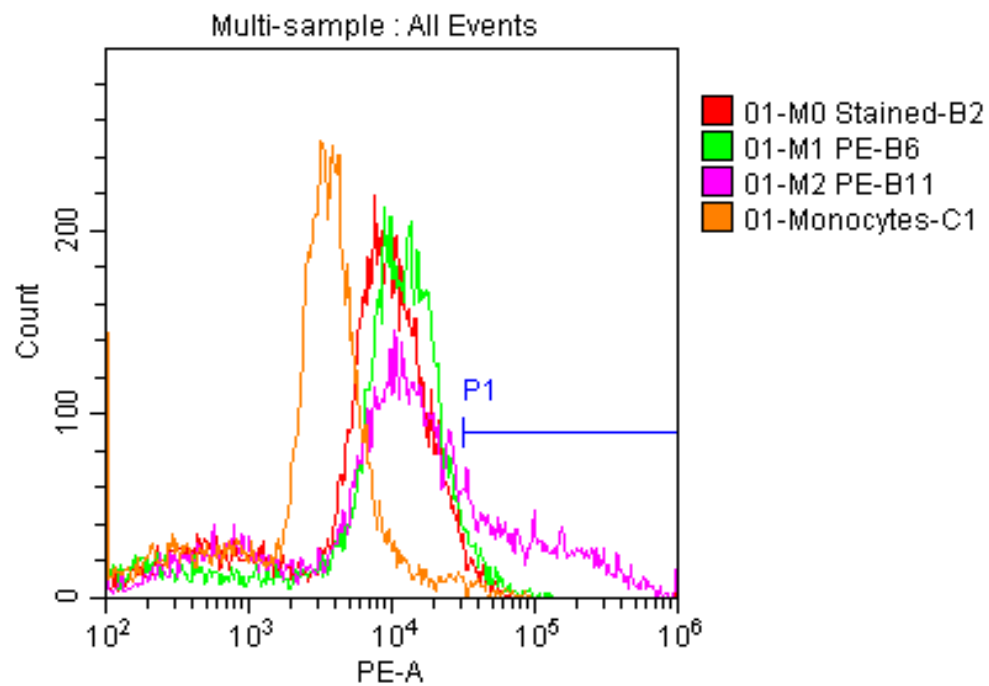
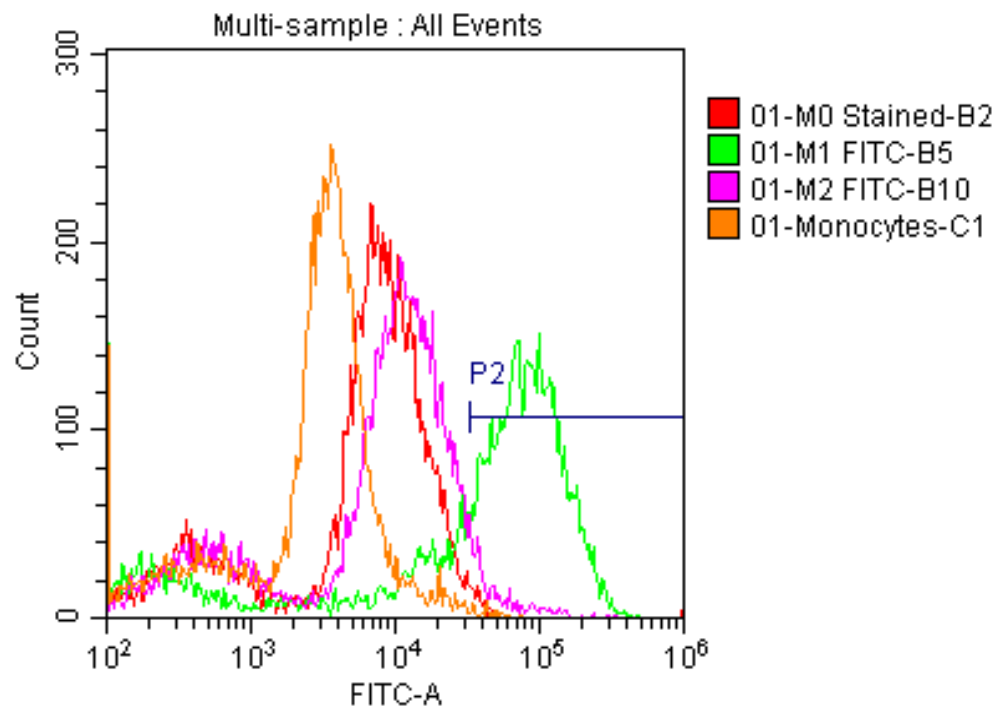


Figure 4.5. Flow cytometry analysis of surface marker expression A) CD80-FITC and B) CD206-PE of different THP-1 cell monocytes, M0, M1 and M2 macrophages. CD80-FITC was expressed only by M1 macrophage phenotypes and CD206 by M2 macrophages.

4.5. Characterisation of LSGE

Cyclic voltammetry (CV) which measures changing current was conducted for the LSGE with different scan rates between 10 and 200 mV/s (figure 4.6). The Randles-Sevcik plot (figure 4.7) of current maxima for the oxidation and reduction processes against the square root of the scan rate showed a linear behaviour, suggesting the occurrence of diffusion-limited electrochemical behaviour, previously reported for these electrodes, (Vaughan et al., 2020). This linear behaviour indicated that the LSGE surface was capable of supporting rapid electron transfer.

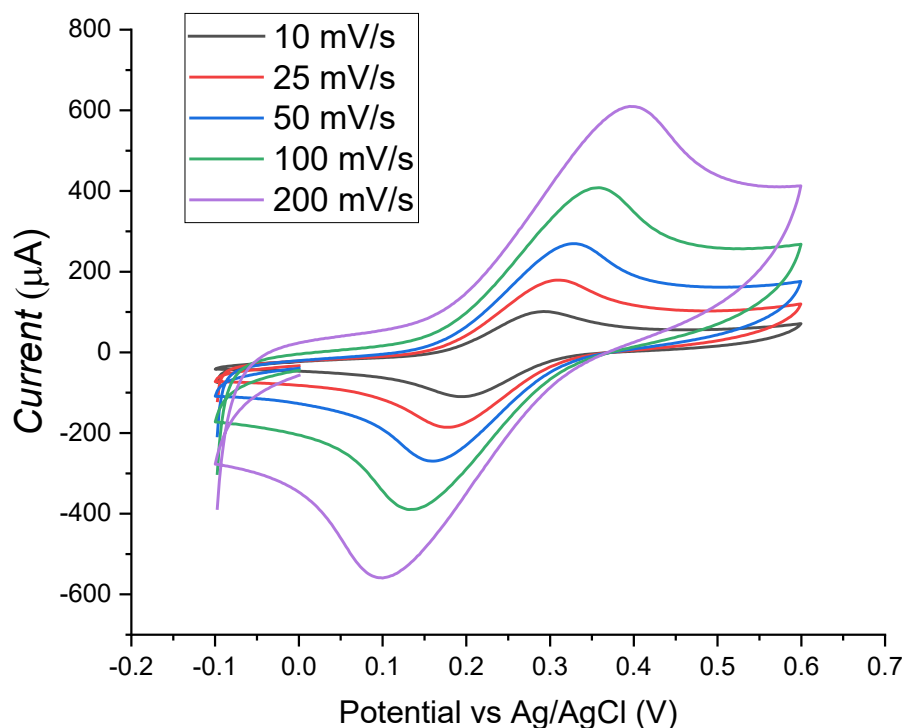


Figure 4.6. Cyclic Voltammograms. CVs of LSGE vs Ag/AgCl in 1M KCl with 5 mM potassium ferrocyanide at scan rates from 10 mV/s to 200 mV/s/ of LSGE. The oxidation and reduction peak current of this graph were plotted against the square root of scan rate in figure 4.7.

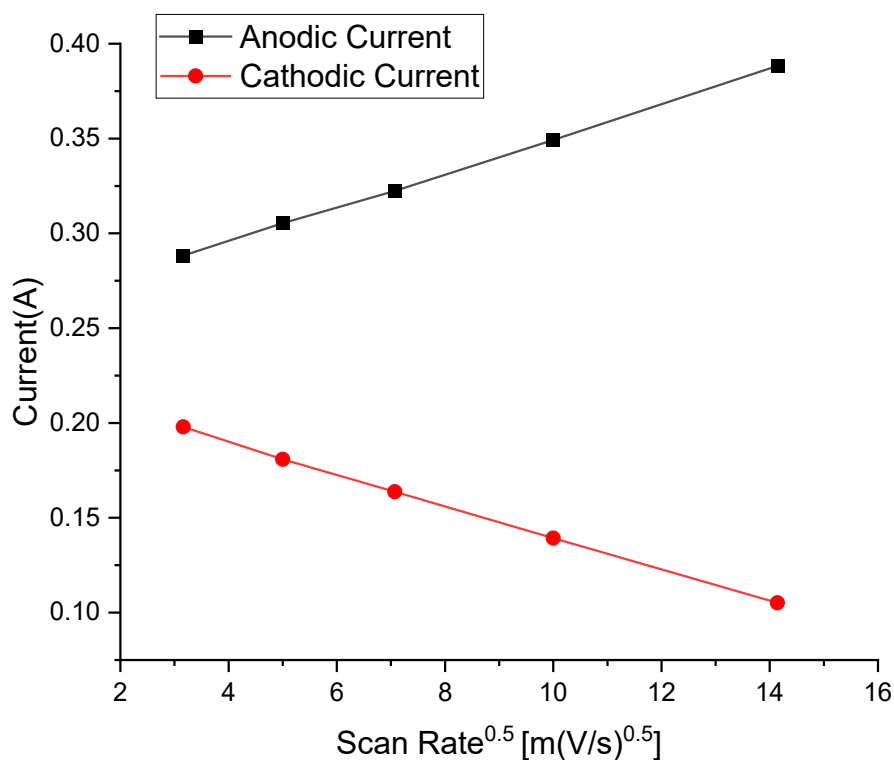
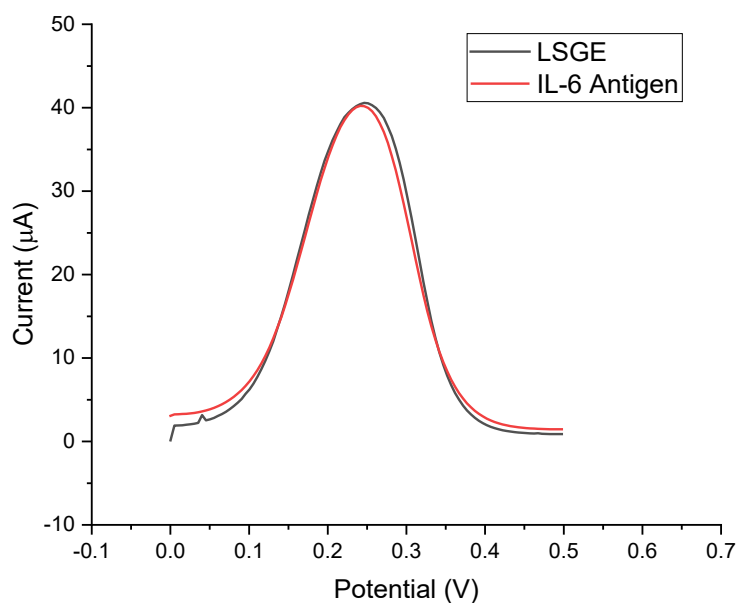


Figure 4.7. Randles-Sevcik plot; LSGE vs Ag/AgCl 1M KCl with 5 mM potassium ferricyanide at scan rates from 10 mV/s to 200 mV/s/ of LSGE based on the oxidation and reduction peak current obtained from figure 4.6. The linear behaviour of this plot indicated that the LSGE surface was capable of supporting rapid electron transfer.

4.6. LSGE BioFunctionalisation

To prove that the functionalisation of LSGE with PBA and EDC:NHS was necessary to enable the attachment of the IL-6 antigen bioreceptor, DPV was performed to show the attachment of IL-6 antigen to LSGE with and without the functionalisation step. Before any modification to the LSGE, the DPV (figure 4.8A) showed no change in peak current. When the LSGE was incubated with the IL-6 antigen bioreceptor and DPV was performed again, no change in current indicated no linking of the IL-6 antigen to the electrode. For biofunctionalisation, the LSGE was modified with PBA and EDC:NHS and subsequent incubation of LSGE with IL-6 antigen bioreceptor. The DPV showed a decrease in peak current which indicated successful attachment of the IL-6 antigen to LSGE (figure 4.8B).

A. LSGE without functionalisation



B LSGE with functionalisation

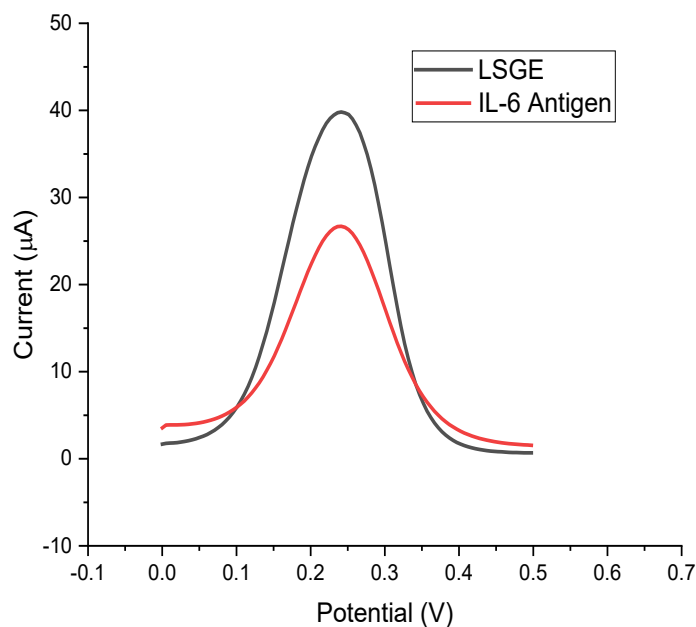


Figure 4.8. Differential Pulse Voltammograms of LSGE A) without and B) with functionalisation. Without functionalisation, the LSGE was incubated with IL-6 antigen bioreceptor with no PBA and EDC:NHS. DPV was performed before and after the immobilisation of IL-6 antigen bioreceptor. For the LSGE with functionalisation with PBA and EDC:NHS, DPV was performed before and after immobilisation of IL-6 antigen.

Cyclic Voltammetry was performed after each modification step and the change in intensity of the peak current was analysed to study the effect of each modification step. After PBA functionalisation, the LSGE surface was coated with the negatively charged carboxyl group (COO⁻). The negatively charged carboxyl group inhibited the movement of redox marker [Fe(CN)₆]^{3-/4-} to the LSGE surface and reduced the peak current giving a smaller CV response. This was demonstrated in the cyclic voltammogram (figure 4.9) where the peak current decreased from 120 μ A of LSGE to 40.5 μ A after PBA functionalisation.

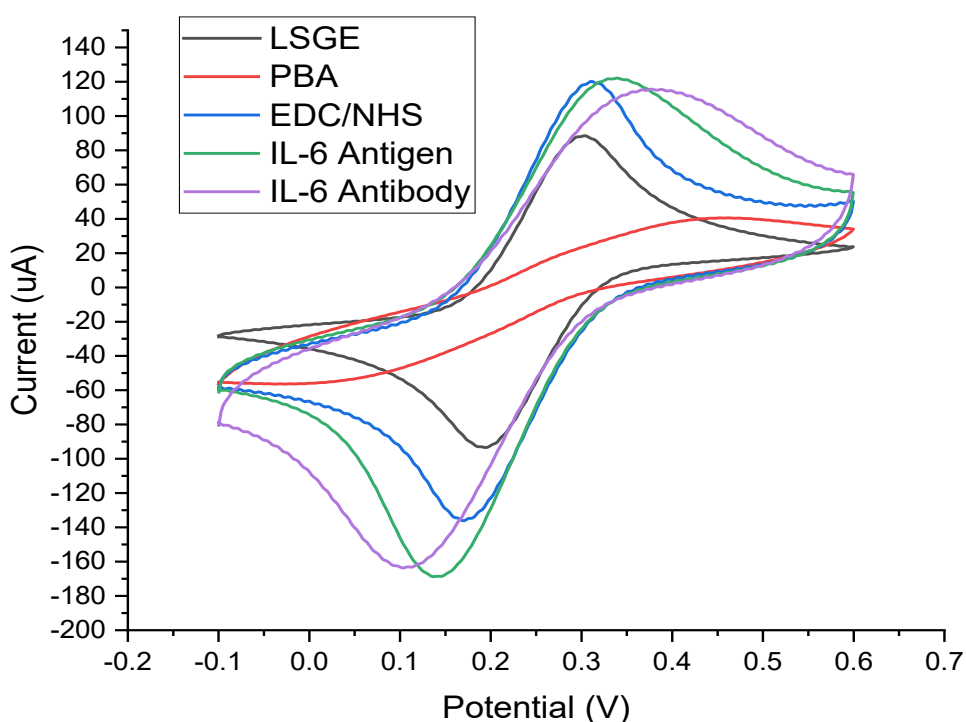


Figure 4.9. Cyclic Voltammogram of LSGE after each functionalisation step. CV was performed for LSGE before any modification step. The LSGE was immersed in 250 mM PBA for 1 hour. After washing step, the LSGE was immersed in 75 mM EDC: 50 mM NHS for 90 minutes and 200 μ L of 2.5 μ g/mL of IL-6 antigen bioreceptor was linked to LSGE. To test, 200 μ L of IL-6 antibody was dispensed onto the LSGE. CV were performed and for each modification step.

The LSGE was also functionalised with EDC/NHS coupling to form the amide bond with the IL-6 antigen. Amide bonds were neutrally charged so that the $[\text{Fe}(\text{CN})_6]^{3-/4-}$ can easily diffuse to the surface of the LSGE giving a larger CV response. DPV is an electrochemical technique with higher sensitivity compared to CV. The peak current of IL-6 antigen and IL-6 antibody were very similar. Hence, the change of peak current was very small. Hence, DPV with higher sensitivity that produced larger change in peak current was used for the analysis of binding of IL-6 antibody to IL-6 antigen for further testing. Collectively these results showed that without the PBA and EDC:NHS functionalisation steps, there is not enough carboxylic groups (PBA) or amide bonds with EDC/NHS coupling, present to act as the linker to promote IL-6 antigen immobilisation (bioreceptor adherence) on the LSGE.

4.7. Optimisation of LSGE Modification

The modification of the LSGE was performed through optimisation with manipulating concentrations of three agents/parameters; (i) 1-pyrenebutyric acid (PBA), (ii) EDC/NHS and (iii) IL-6 antigen bioreceptor concentrations.

4.7.1 PBA Optimisation

Cyclic Voltammetry was carried out for the LSGE before modification with PBA (0 mM PBA). The LSGEs were incubated with various concentrations of PBA and the CV was performed which showed 250 mM PBA as the optimal concentration due to the largest decrease in peak current compared to 0 mM PBA (figure 4.10).

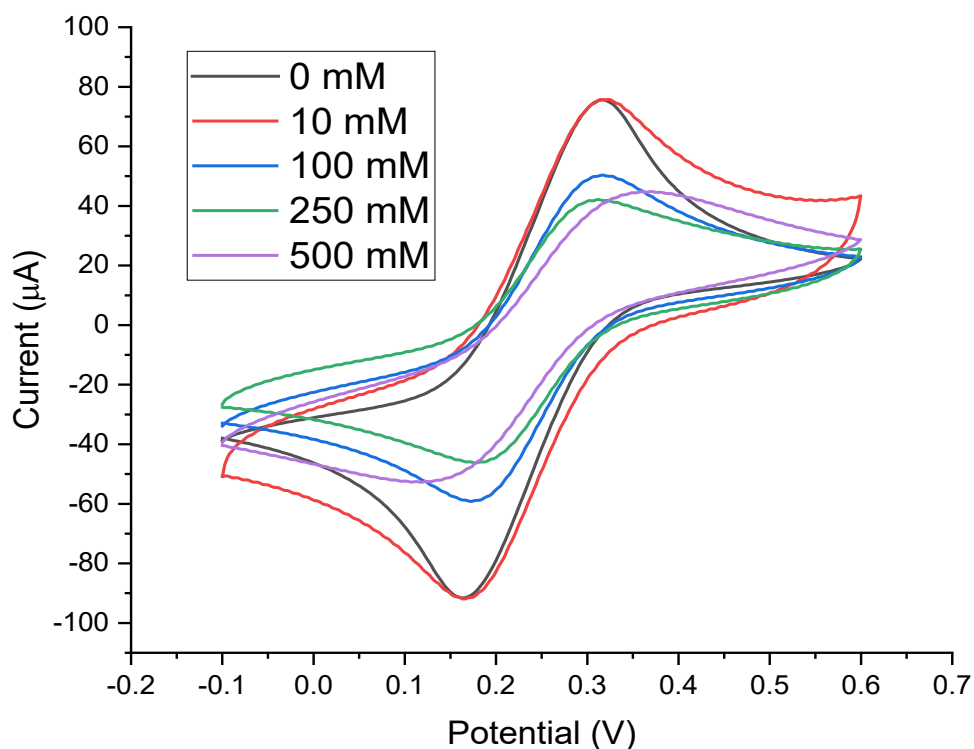
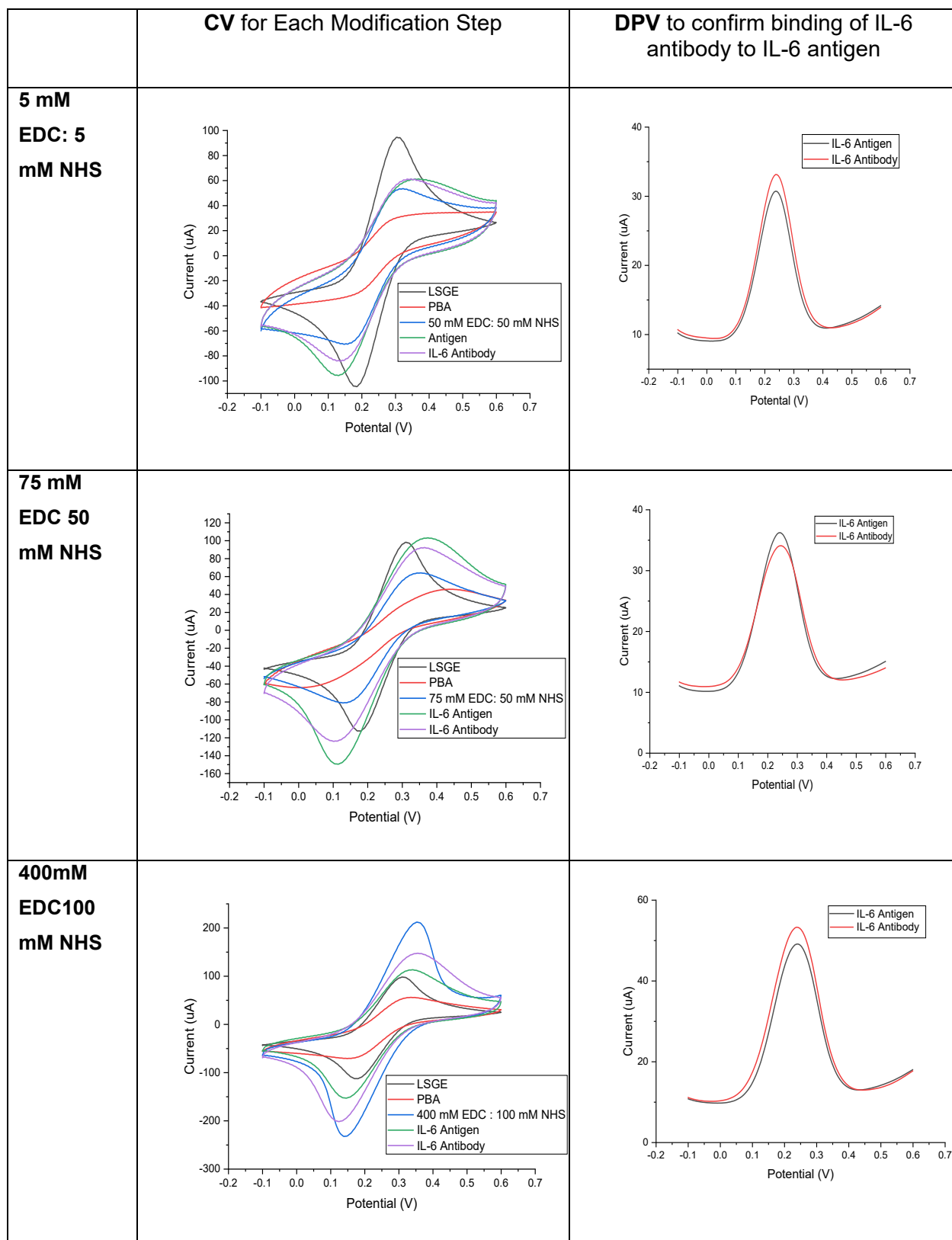


Figure 4.10. Cyclic Voltammogram of LSGE functionalised with various concentrations of 1-pyrenebutyric acid (PBA). CV was performed for LSGE with no PBA functionalisation (0 mM). The LSGEs were immersed in 10 mM, 100 mM, 250 mM and 500 mM PBA for 1 hour. CV was performed after functionalisation with PBA to determine the optimum PBA concentration for LSGE functionalisation.

4.7.2 EDC/NHS Optimisation

After incubation with 250 mM PBA, the LSGE was incubated with three different concentrations of EDC/NHS. The DPV was performed for the biofunctionalization step of IL-6 antigen bioreceptor immobilisation and binding to the target molecule, IL-6 antibody. The DPV was performed instead of CV for this step because DPV had higher sensitivity to show the changes in peak current. The optimal EDC/NHS concentration was chosen based on the decrease in peak current of DPV of IL-6 antigen that indicated successful binding of IL-6 antibody to the antigen. The optimal concentration of 75 mM EDC:50 mM NHS was ascertained and evidenced by the decreased DPV peak current of IL-6 (Table 4.2).

Table 4.2. CV and DPV of LSGE with different EDC and NHS concentrations.



4.7.3 IL-6 Antigen Optimisation

The functionalised LSGE was incubated with various IL-6 antigen concentrations and the change of DPV peak current calculated and plotted (figure 4.11) to determine the optimum IL-6 antigen concentration to be immobilised onto the LSGE. The LSGEs functionalised with PBA and EDC:NHS were incubated with 0.5 $\mu\text{g/mL}$, 1 $\mu\text{g/mL}$, 2.5 $\mu\text{g/mL}$ and 5 $\mu\text{g/mL}$ of IL-6 antigen. The DPV was performed prior and post IL-6 antigen immobilisation. When more IL-6 antigen was attached to the LSGE, the movement of redox marker to the LSGE surface was further hindered and hence a change in peak current increased. The change in peak current was calculated and plotted against the IL-6 antigen concentration. The concentration of 2.5 μM of IL-6 antigen showed the largest change in peak current which indicated the optimal IL-6 antigen bioreceptor concentration.

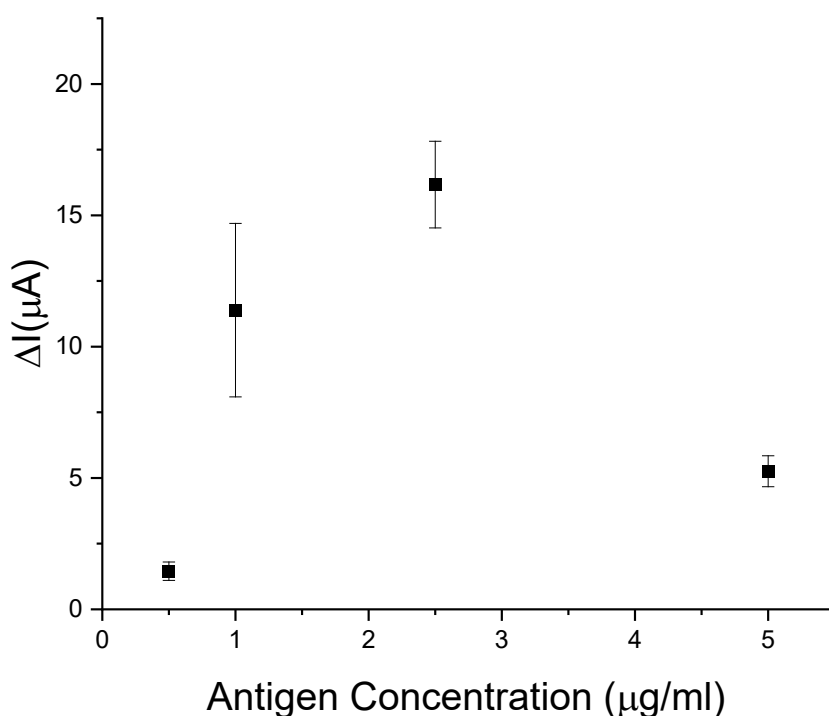
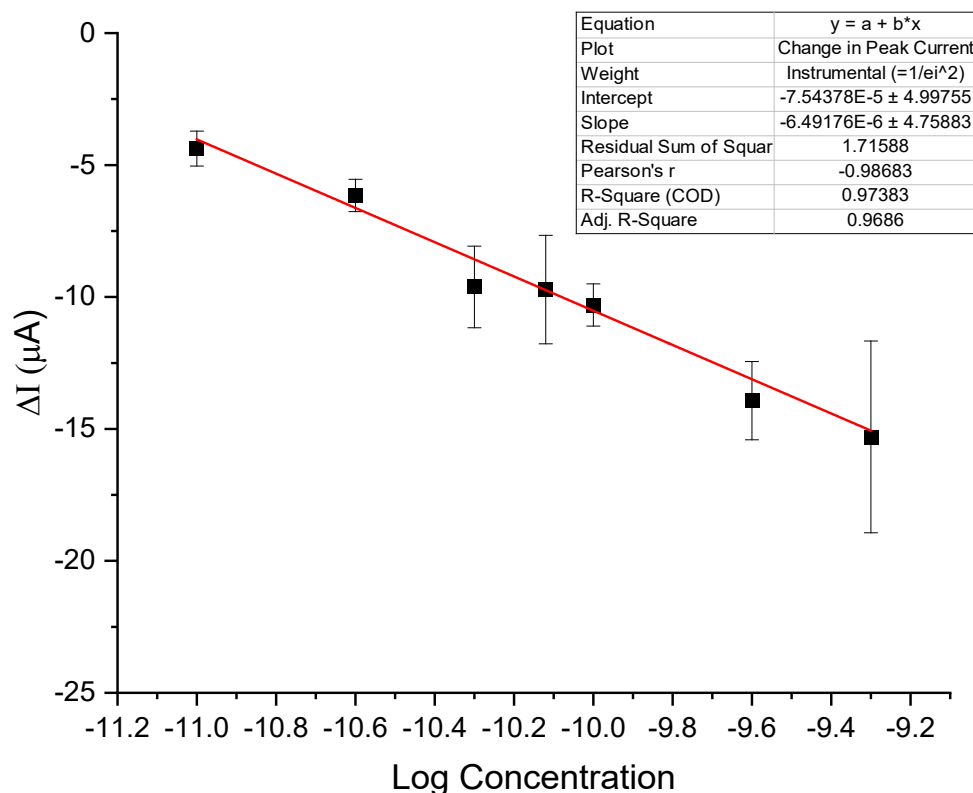


Figure 4.11. Change in DPV peak with various IL-6 antigen concentrations on LSGE. The LSGE functionalised with PBA and EDC:NHS was incubated with 0.5 $\mu\text{g/mL}$, 1 $\mu\text{g/mL}$, 2.5 $\mu\text{g/mL}$ and 5 $\mu\text{g/mL}$ of IL-6 antigen. The DPV was performed before and after the IL-6 antigen immobilisation. Change in peak current was calculated and plotted against the IL-6 antigen concentration.

4.8. Calibration Curve for IL-6 LSGE Biosensor

The functionalised LSGE with IL-6 antigen as the bioreceptor (biosensor), was incubated with various concentrations of the target molecule, IL-6 antibody to assess if the biosensor could detect a variety of antibody concentrations. The DPV was performed for the LSGE biosensor before and after incubation with IL-6 antibody. The change in peak current (Δi) was plotted against the log concentration of IL-6 antibody (figure 4.12A). The change in peak current increased with increased IL-6 antibody concentration with linearity of 0.974 R^2 value. Another calibration curve for IL-6 was produced by ELISA.

A



B

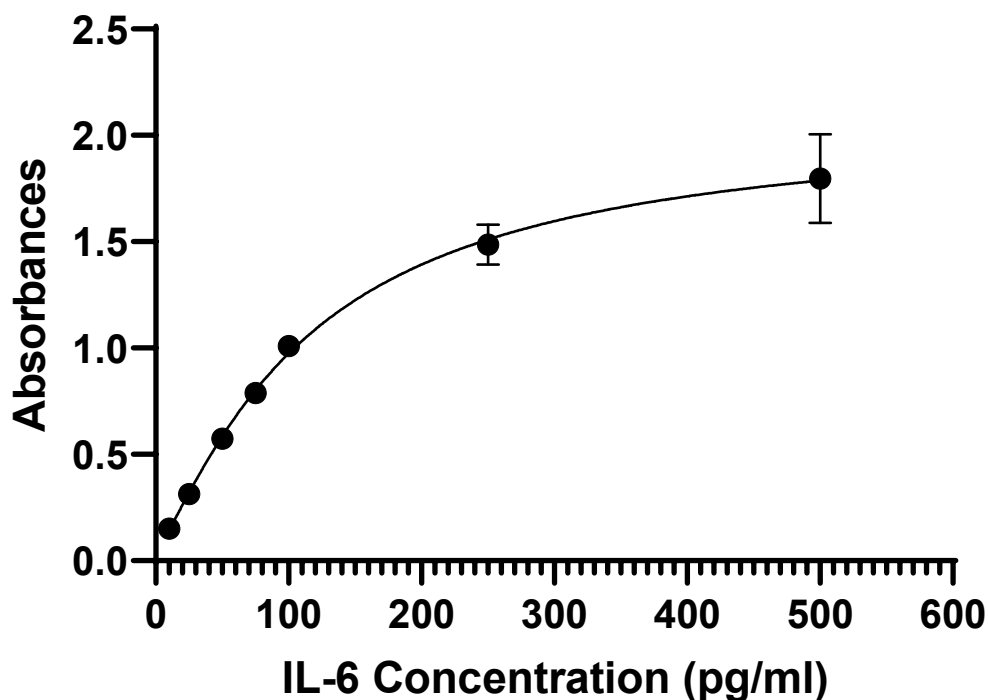


Figure 4.12. Calibration curve for IL-6 Biosensor. A) Change in peak current of LSGE biosensor and B) Absorbances from IL-6 ELISA test using 4 PL non-linear regression as suggested by manufacturer. For the LSGE biosensor, IL-6 antibody concentrations of 10, 25, 50, 75, 100, 250 and 500 pg/mL detection was examined. The IL-6 antibody was aliquoted onto the LSGE biosensor for 90 minutes to enable binding of the IL6 antibody to the IL-6 antigen receptor on the LSGE surface. The change of peak current before and after IL-6 antibody incubation was calculated and plotted against the log concentration of IL-6 antibody. Values represented three replicate samples.

4.9. Method Comparison; Biosensor vs ELISA

A method comparison was performed and plotted (figure 4.13) to compare both IL-6 detection methods with absorbances from ELISA assay on x-axis and the change in peak current from LSGE biosensor on y-axis. The R^2 value of 0.962 showed good comparison between methods.

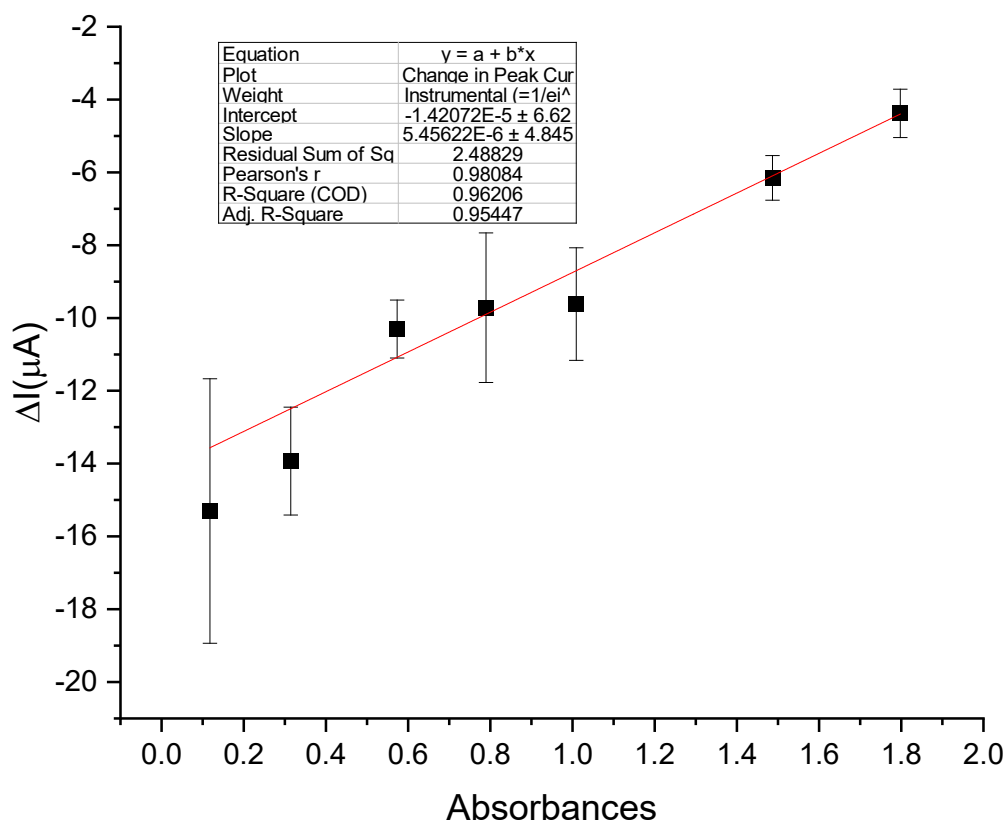
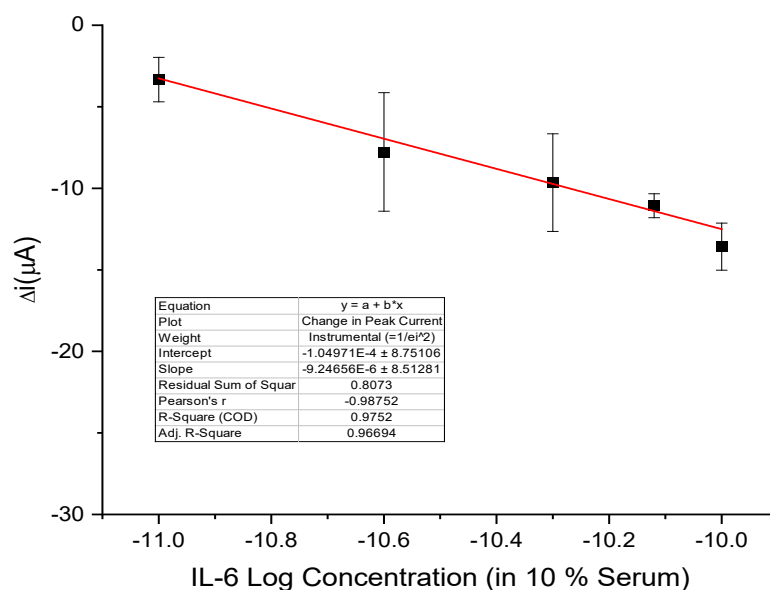


Figure 4.13. Method Comparison of LSGE Biosensor versus ELISA. IL-6 detection across a range of concentrations, 10, 25, 50, 75, 100, 250 and 500 pg/mL was determined by ELISA and LSGE biosensor. The change in peak current LSGE (figure 4.12 A) and absorbances from ELISA test (figure 4.12 B) were plotted to compare both methods. The R² value of 0.962 shows good comparison between methods. Three replicates were tested for each concentration.

4.9. Specificity and Selectivity of LSGE

The selectivity of the LSGE was tested with various concentrations of IL-6 antibody in the presence of interfering agents such as serum proteins and albumin (10% FBS and 10 % BSA). The functionalised LSGE with IL-6 antigen bioreceptor was incubated with various concentrations of the target molecule, IL-6 antibody in the presence of 10 % FBS and 10 % BSA. The DPV was performed for the LSGE biosensor before and after incubation with IL-6 antibody. The change in peak current (Δi) was plotted against the log concentration of IL-6 antibody (figure 4.14).

A



B

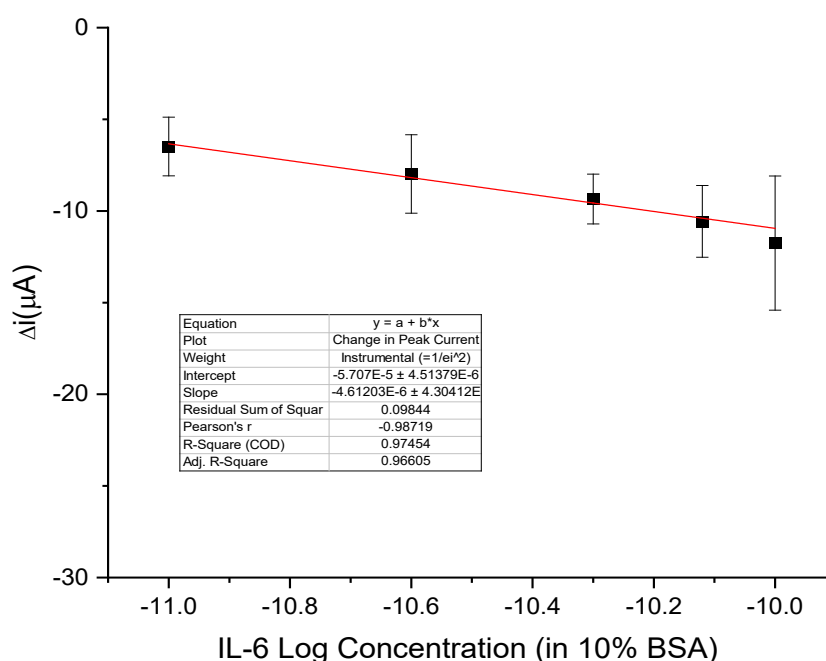


Figure 4.14. Specificity of LSGE Biosensor for IL-6 in A) 10% Fetal Bovine Serum B) 10% Bovine Serum Albumin (BSA) from 10 to 500 $\mu\text{g/mL}$. The IL-6 antibody in 10% serum or BSA was dispensed onto the LSGE biosensor for 90 minutes. The change of peak current before and after IL-6 addition was calculated and plotted against the log concentration of IL-6 antibody. Values represent three sample replicates.

In order to test the performance of LSGE biosensor to detect the IL-6 antibody in different medium a two-way anova analysis showed no significant difference in peak current change between the three different media containing the IL-6 analyte (figure 4.15).

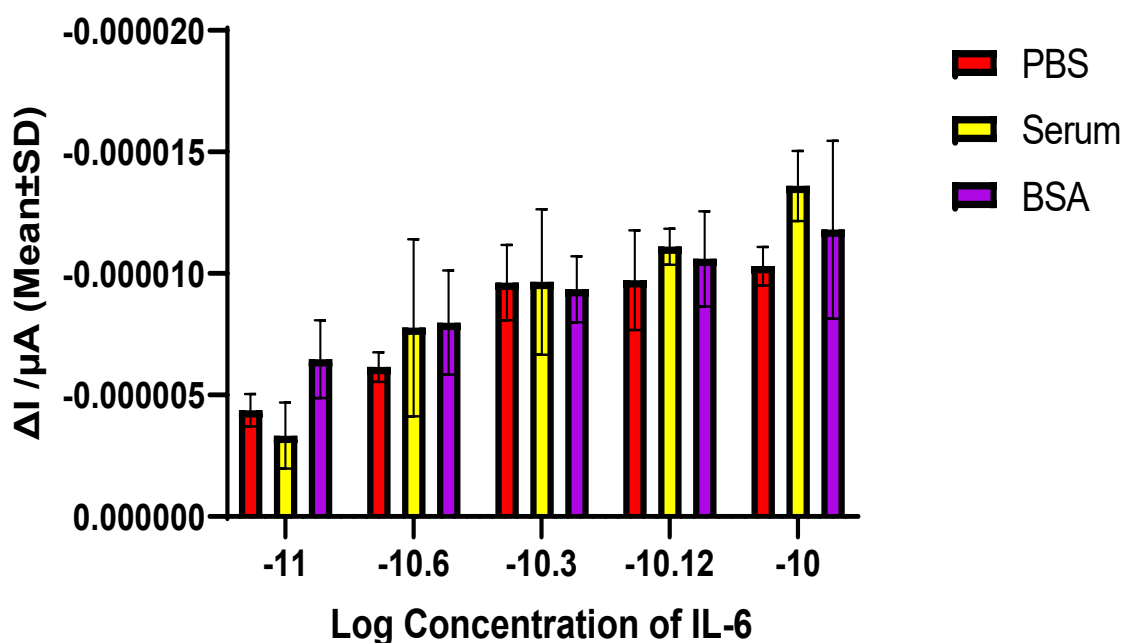


Figure 4.15. Change in peak current for IL-6 detection in PBS, 10% Serum and 10% BSA with three replicates for IL-6 antibody concentrations across 10 and 500 pg/mL. Two-way Anova analysis shown no significant difference in peak current change for IL-6 detection in PBS, 10% Serum and 10% BSA.

Chapter 5. Discussion and Conclusion

The aim of this Laser Scribed Graphene Electrode Biosensor (*LaserFlame*) study was to develop a prototype LSGE biosensor to detect inflammatory markers of inflamed immune cells, i.e. macrophages, for early diagnosis of inflammatory disease. To study the macrophage in different inflamed cell states, THP-1 monocytes were used as the immune effector cell model. The THP-1 monocytes were differentiated into macrophages (M0) and then polarised into classically activated macrophages (M1) responsible for pro-inflammatory responses, and alternatively activated macrophages (M2) responsible for anti-inflammatory responses.

The inflammatory cytokines secreted by different inflamed cell states were analysed with ELISA tests. Macrophage cell surface marker expression of different inflamed cell states were characterised by flow cytometry. A suitable inflammatory marker of classically activated macrophages (M1) responsible for the pro-inflammatory responses, IL-6, was chosen to be detected by the LSGE biosensor. The LSGE was functionalised with PBA and EDC:NHS that act as the linkers for the immobilisation of IL-6 antigen bioreceptor. The performance of the LSGE to detect IL-6 antibody was assessed by Cyclic Voltammetry and Differential Pulse Voltammetry with a commercial potentiostat on a three-electrode cell system with silver/silver chloride as the reference electrode, platinum wire as counter electrode and modified LSGE as the working electrode. Various concentrations of IL-6 antibody in PBS were tested and compared to ELISA results. The selectivity and specificity of the LSGE were assessed by testing the IL-6 antibody in the presence of interfering substances such as serum and serum albumin. Macrophage cells play a vital role in the immune system and response to the local microenvironment, (Ponzoni et al., 2018). To initiate this study, the THP-1 cell model employed required differentiation and polarisation into macrophage phenotypes with PMA used to differentiate the THP-1 monocytes into macrophages. After differentiation, the THP-1 monocytes in cell suspension started to adhere to the culture flask. Lipopolysaccharide (LPS) and Interferon Gamma (IFN- γ) were used to polarise the macrophages into the classically activated macrophage (M1). Interleukin 4 (IL-4) and Interleukin 13 (IL-13) were used to polarise macrophages into alternatively activated macrophages (M2) (Genin et al., 2015).

The M1 and M2 macrophage phenotypes were described as two extreme functional states by (Mantovani et al., 2002). Macrophages activated to classical activation states (M1 macrophage phenotype) for pro-inflammatory responses and to the alternatively activation state (M2 macrophage phenotype) for anti-inflammatory response. The M1 macrophage phenotype was characterised by the secretion of the pro-inflammatory cytokine, IL-6 and expression of surface marker CD80, found on various immune cells (Peach et al., 1995). The M2 macrophage phenotype was characterised by the secretion of fibronectin, limited secretion of pro-inflammatory cytokine such as IL-6 and the expression of mannose receptor, CD206.

5.1 ELISA

The polarisation of THP-1 macrophages to M1 and M2 phenotype macrophages was confirmed with ELISA technique. After polarisation with different stimuli, the medium used to culture THP-1 cells was collected and analysed with ELISA assays for IL-6, Fibronectin, IL-8, IL-12, IL-1 β and TGF- β ELISA.

According to literature, IL-6, IL-12, IL-1 β , IL-8 were pro-inflammatory cytokines secreted by M1 phenotype macrophages (Chanput, Mes and Wichers, 2014b) whereas TGF- β , (Atri, Guerfali and Laouini, 2018) and fibronectin (Genin et al., 2015) were associated with anti-inflammatory cytokine activities.

In the present study, ELISA results indicated that IL-6 was only secreted by the M1 macrophage phenotypes which were polarised by incubating with IFN- γ and LPS. The M2 macrophage phenotype, polarised with IL-4 and IL-13 did not secrete IL-6. This result was comparable to a study by (Jiménez-Uribe et al., 2019) and (Liu et al., 2018) show that LPS induced the secretion of IL-6.

Fibronectin was secreted in different levels by different phenotypes of activated THP-1 cells with the M2 phenotype noted in this present work, for the secretion of the highest level of fibronectin. This result concurred with (Genin et al., 2015) who showed mRNA expression of fibronectin by M2 macrophage phenotypes, differentiated by 150 nM PMA and polarised with 20 ng/mL of IL-4 and IL-13.

In the present study, ELISAs performed for IL-8, IL-12, IL-1 β and TGF- β did not detect any activity in THP-1 cells. (Chanput, 2012) and (Chanput et al., 2013) showed that LPS stimulated THP-1, M1 macrophage phenotypes secreted IL-8, IL-12 and IL-1 β detected by RT-PCR. (Długosz, Basalaj and Zawistowska-Deniziak, 2019) showed IL-12p70 secretion by ELISA with very low amounts (less than 5 pg/mL). (Liu et al., 2018) showed TGF- β was secreted by M2 macrophage phenotype with ELISA. The THP-1 cells were differentiated by 320 nM PMA for 6 hours and polarised by 20 ng/mL of IL-4 and IL-13 for 18 hours in their study (Liu et al., 2018). In this present study, lower concentrations of PMA (25 nM) were incubated with cells for 24 hours and a longer polarisation time of 72 hours which can potentially affect the expression of TGF- β .

5.2. Flow Cytometry

Flow cytometry analysis of forward scatter (FSC) indicated the size of the THP-1 cells and side scatter (SSC) indicated the granularity of the THP-1 cells. Both size and granularity of the THP-1 cells were increased after differentiation. This result was compatible with the literature stating the size and granularity of THP-1 macrophages were higher compared to monocytes (Forrester et al., 2018).

To further confirm the polarisation of macrophages into M1 and M2 phenotypes, the surface marker expression of macrophages after polarisation was analysed in this study. To analyse the surface marker expression, the activated THP-1 cells that were attached to the flask needed to be detached. Different detachment methods were tried which included physical detachment with cell scrapers and chemical detachment methods included trypsin and accutase. Of the different detachment methods employed in the present study, accutase worked best by generating the highest yield of viable cells.

Two surface markers were analysed which included CD80 and CD206. In this study, it was noted that CD80 was only expressed by M1 macrophage phenotype and CD206 only expressed by M2 macrophage phenotype. This result was comparable to literature (Forrester et al., 2018) who showed the expression of CD80 by M1 phenotype THP-1 cells and (Genin et al., 2015) who demonstrated the expression of CD206 by M2 macrophage phenotypes.

Besides playing a vital role in innate immunity, macrophages also act as antigen-presenting cells (APCs) to initiate T-cells by interacting with T-cell receptors. Macrophages process antigens to be presented to lymphocyte T cells through MHC-II molecules. CD80 was the main costimulatory molecule bound to CD28 or CD152 to promote T-cell activation (Jiménez-Urbe et al., 2019). It was reported by (Jiménez-Urbe et al., 2019) that there was a positive correlation between the CD80 expression and the secretion of IL-6. (Koorella et al., 2014) also reported that IL-6 stimulation can induce positive feedback to increase the expression of CD80 in dendritic cells.

While choosing a suitable detection inflammation marker to be biofunctionalised on to the LSGE, the inflammation markers of M1 phenotype THP-1 cells were selected instead of M2 phenotype THP-1 cells. M1 phenotype THP-1 cells were responsible for proinflammatory responses in the present study with IL-6 cytokine secreted only by M1 macrophage phenotypes which was deemed suitable as an inflammation marker to be biofunctionalized on to the LSGE.

5.3. Fabrication and Characterisation of LSGE

The electrochemical characteristics of graphene electrodes are very dependent on their morphology. The LSGE employed in this present study as the biosensing platform has high porosity which increases the surface area and offers a highly accessible electrochemical surface area (Vaughan et al., 2020), which was similar to an LSGE reported by (Fenzl et al., 2017). The results in this present work indicated a linear relationship between peak oxidation or reduction current and the square root of the scan rate which indicated that the LSGE surface structure was able to support rapid electron transfer.

5.4. LSGE Functionalisation

The bioreceptor antigen (anti-IL-6 antibody) can bind to the LSGE via carboxyl bonding and the surface of LSGE possesses some carboxylic groups (Fenzl et al., 2017). However, in the early stages of this present work, the peak current of DPV after the incubation of the antigen bioreceptor did not change which

indicated that the carboxylic groups on the LSGE surface were not enough to bind the bioreceptor. Hence, functionalisation steps with PBA were needed to attach more carboxylic groups on to the LSGE surface to facilitate binding of the bioreceptor.

Modification with 1-pyrenebutyric acid (PBA) has been widely used as a first step in functionalisation of graphene biosensors due to the presence of the pyrene group which enabled π - π stacking. (Hinnemo et al., 2017) and showed that in concentrated solutions, the PBA molecules stand up and stack horizontally with their edge contacting the graphene surface. This produced an LSGE surface densely populated with the carboxylic group in their work. After functionalisation with PBA, EDC/NHS coupling was performed. EDC reacted with the carboxylic group of PBA on the LSGE to form an active o-acylisourea intermediate. This intermediate was unstable and can fail to react with amine causing regeneration of the carboxyl group. Hence, EDC reactions always couple with NHS to improve and stabilise the o-acylisourea intermediate. The intermediate can be easily replaced by the primary amino group, which was the antigen bioreceptor, IL-6 antigen, in the present work. This allowed efficient conjugation of the carboxylic group on the LSGE surface to the antigen via the strong amide bond (Thermoscientific, 2012).

The LSGE functionalisation results were evaluated with Cyclic Voltammetry (CV) and Differential Pulse Voltammetry (DPV), two electrochemical techniques commonly used to investigate the reduction and oxidation of molecular species which in this study was the redox marker, ferricyanide ion $[\text{Fe}(\text{CN})_6]^{3-/4-}$. After PBA functionalisation, the LSGE surface was coated with the negatively charged carboxyl group (COO^-). The negatively charged carboxyl group inhibited the movement of redox marker $[\text{Fe}(\text{CN})_6]^{3-/4-}$ to the LSGE surface and reduced the peak current giving a smaller CV response. This was proved in the present work wherein, the cyclic voltammogram (figure 4.9) showed a peak current decrease from 120 μA of bare LSGE to 40.5 μA after PBA functionalisation.

After this, the LSGE was functionalised with EDC/NHS coupling to form an amide bond with the IL-6 antigen bioreceptor. Amide bonds were neutrally charged, so that the $[\text{Fe}(\text{CN})_6]^{3-/4-}$ can easily diffuse to the surface of the LSGE giving a larger

CV response. In the present work, this was proved by the increase of peak current from 40.5 μA after PBA functionalisation to 122 μA (figure 4.9) wherein the CV peak current of IL-6 antigen bioreceptor and IL-6 antibody were similar. Hence, DPV with higher sensitivity was used for the analysis of binding of IL-6 antibody to the IL-6 antigen bioreceptor. This result correlated well with other work published (Gao et al., 2013).

5.5. Optimisation for Modification of LSGE

The modification of the LSGE can be divided into three steps which were 1) PBA functionalisation, 2) EDC/NHS functionalisation and 3) IL-6 bioreceptor biofunctionalisation. The optimum concentration for each parameter of the biosensor was investigated.

To determine the optimum PBA concentration to functionalise the LSGE, various PBA concentrations ranging from 10 mM to 500 mM were used and CV was performed for each concentration (figure 4.10). An increase in PBA concentration resulted in increased negatively charged carboxyl groups present on the LSGE surface that hinder the movement of $[\text{Fe}(\text{CN})_6]^{3-/4-}$. Hence, an increase in PBA concentration further decreased the CV peak current from 10 mM to 250 mM PBA. Further increased concentrations to 500 mM PBA did not further decrease the CV peak current showing saturation behaviour. (Hinnemo et al., 2017) showed the optimum concentration of PBA on graphene to be 741 nM, however, their study was performed with pure graphene unlike the laser scribed graphene employed in the present study which could potentially affect changes in the peak current.

For EDC/NHS optimisation, three different concentrations suggested by different publications were used to determine the optimum concentration of EDC/NHS; (Sam et al., 2010) used 5 mM EDC:5 mM NHS and 400 mM EDC:100 mM NHS was used by (Thangamuthu, Santschi and Martin, 2018). (Fenzl et al., 2017) used 50 mM EDC: 50 mM NHS. (Thermoscientific, 2012) suggested that the EDC crosslinking was most efficient in acidic conditions with pH 4.5 but NHS ester crosslinking was more efficient at pH 7.2 to 8.5. EDC crosslinking had lower efficiency in neutral phosphate buffer but can be compensated by increasing the

amount of EDC. Hence, a final 75 mM EDC:50 mM NHS, where the EDC concentration was higher and dissolved in PBS was used in this present study.

To evaluate the best EDC/NHS concentration, the PBA modified LSGE was immersed in the EDC/NHS. The DPV was performed on the modified LSGE to ensure that the IL-6 antibody could be successfully detected (table 4.2). After the binding of the IL-6 antibody to the IL-6 antigen bioreceptor, the DPV peak current should decrease because the antibody bulk size would hinder the movement of redox marker $[\text{Fe}(\text{CN})_6]^{3-/4-}$ to the LSGE surface. Hence, a lower DPV peak current of antibody compared to antigen indicated successful binding of the antibody to antigen bioreceptor in the present work. The 75 mM EDC:50 mM NHS was the only concentration which decreased peak current and hence was selected for study.

To determine the best bioreceptor IL-6 antigen concentration to immobilise on the LSGE surface, the change in peak current before and after the immobilisation of the bioreceptor was measured (figure 4.11) which showed that 2.5 $\mu\text{g}/\text{mL}$ was the optimum IL-6 antigen bioreceptor concentration to use. The larger change of peak current indicated more IL-6 antigen present on the LSGE surface and hindered the movement of $[\text{Fe}(\text{CN})_6]^{3-/4-}$ to the LSGE surface which was desirable as more antigen bioreceptor available to bind and detect the antibody analyte would increase the LSGE's efficiency.

5.6. Calibration curve for IL-6 with LSGE

The interactions of IL-6 antibody with the LSGE bioreceptor (IL-6 antigen) were measured with DPV (figure 4.12 A). The calibration curve showed good linearity with R^2 of 0.974 across a linear range from 10 pg/mL to 500 pg/mL . This linear range was very similar to the Human IL-6 DuoSet ELISA by R&D System, UK with their ELISA linear range from 9.48 pg/mL to 600 pg/mL . A comparison plot was created to compare both methods with absorbances from the ELISA test on the x-axis and the change in peak current from LSGE biosensor on the y-axis for recombinant human IL-6 with concentration (Figure 4.13). The R^2 value indicated the LSGE biosensor was well comparable to more established ELISA detection methods for IL-6. A similar study by (Chikkaveeraiah et al., 2009) showed the

comparison plot for IL-6 detection with Single Wall Carbon Nanotube and ELISA with a comparable method slope of 0.975 R² value.

5.7. Specificity and Selectivity of LSGE

The change in peak current as the detection sensing platform in this present work was based on the specific binding of the IL-6 antibody (analyte) to the IL-6 antigen bioreceptor which was immobilised on to the LSGE surface that hindered the diffusion of the redox marker. However, non-specific binding of interfering substances, for example albumin or other proteins present in human blood, can potentially impede the diffusion as well giving false results. To study the effect of interference on analytes on the LSGE biosensor, IL-6 detection was examined in 10% serum and 10% BSA in PBS solutions (figure 4.14). Serum albumin, a constituent of blood, can potentially affect the accuracy of the detecting method.

The calibration curve of IL-6 in the presence of serum and BSA showed good linearity with no significant differences in peak current measured by LSGE biosensor in the three different media examined. This interference study was compatible to other IL-6 biosensors, for example works by (Lou et al., 2014) and (Chen et al., 2016) who showed specific detectability of IL-6 in ten-fold higher concentrations of BSA. The sensitivity of the LSGE for the detection of IL-6 antibody which was shown by the slope of the calibration curve was -6.49 μA per logarithmic concentration unit for PBS. The sensitivity increased for IL-6 antibody detection in the presence of 10 % serum to -9.25 μA per logarithmic concentration unit and decreased to -4.61 μA per logarithmic concentration unit in the presence of 10 % BSA. Hence, the presence of serum did not affect the sensitivity of the LSGE biosensor.

5.8. Future Work

Further studies can be done to expand upon work progressed in this novel study;

1. PCR could be performed to examine the gene expression of THP-1 cells in different inflamed states via Fibronectin, IL-8, IL-1 β , IL-12p70, and TGF- β gene expression detection.
2. The selectivity and sensitivity of the LSGE biosensor could be tested with IL-6 in whole blood samples which could evaluate the need to remove and save on sample preparation steps for testing (i.e. separation of serum for serology).
3. Multiplexing of bioreceptors for inflammation cytokines attached to the LSGE biosensor for simultaneous detection of different cytokines associated with different macrophage activation states involved in different diseases and states of disease.
4. Optimisation for the shape and size of LSGE biosensor could be progressed to assess how this attribute may affect the binding of IL-6 antibody and the possibility to expand the limits of detection to lower quantities e.g. 1 pg/mL of IL-6.

5.9. Conclusion

Macrophages act as the first line of defence in the immune system that has high plasticity and sensitivity to the local environment (Murray et al., 2014). This present study demonstrated that in the macrophage immune cell model, THP-1 monocytes can be differentiated into macrophages by PMA and polarised into different inflamed cell states, M1 and M2 macrophage phenotypes. LPS and IFN- γ activated the macrophages to M1 inflammatory phenotypes (Rawlings, Rosler and Harrison, 2004). IL-4 and IL-13 activated anti-inflammatory M2 macrophage phenotypes (Mantovani, 2014). M1 macrophage phenotype was characterised by the secretion of IL-6 and CD80 surface marker expression. M2 macrophage phenotype was characterised by the secretion of fibronectin and CD206 surface marker expression. IL-6 was chosen as the inflammatory cytokine to be detected by the LSGE Biosensor. A new novel approach to detect important inflammatory cytokines by LSGE modified sensors has been examined and a prototype developed.

The LSGE biosensor can serve as an electrochemical transducer in a complex bioanalytical sensing environment. The relatively simple fabrication step and universal functionalisation steps with PBA and EDC/NHS coupling reactions acted as linkers for immobilisation of the bioreceptor IL-6 antigen (Adachi and Nakamura, 2019). The IL-6 analyte levels of 10 pg/mL to 500 pg/mL in physiological buffer solutions containing typical interfering agents such as serum proteins were detected successfully using IL-6 antigen as the capture antibody bioreceptor to recognise the IL-6 target molecules. It was proved that the presence of serum and BSA did not affect the detection of IL-6 by this LSGE biosensor which indicated that this biosensor can potentially be used to test samples in serum or BSA without further treatment.

This novel LSGE biosensor has the potential to be a valuable time-saving, low-cost, point of care diagnostic tool for managing the risk of inflammatory diseases. This LSGE immunosensor suitable for future lab-on-chip diagnostic applications for early detection of inflammatory molecules could significantly improve the treatment and outcome of diseases induced by protracted inflammation. This LSGE biosensor was proved to be able to detect IL-6. Early detection of IL-6 can

potentially help to diagnose disease with IL-6 as biomarkers such as sepsis (Song et al., 2019), cardiovascular diseases (Held et al., 2017) and diagnosis of cancer in early-stage (Vainer, Dehlendorff and Johansen, 2018). This LSGE biosensor can also potentially be used to detect COVID-19 disease which studies showed IL-6 as an effective indicator for COVID-19 disease (Zhang et al., 2020; Sabaka et al., 2021),

Bibliography

- Adachi, T. and Nakamura, Y., 2019. *Aptamers: A review of their chemical properties and modifications for therapeutic application*. *Molecules*, Available at: </pmc/articles/PMC6930564/> [Accessed 12 Apr. 2021].
- Alahi, M.E.E. and Mukhopadhyay, S.C., 2017. *Detection methodologies for pathogen and toxins: A review*. *Sensors (Switzerland)*, .
- Anon, 2019. *1-Pyrenebutyric acid Structure - C₂₀H₁₆O₂ - Over 100 million chemical compounds* | *Mol-Instincts*. [online] Available at: <https://www.molinstincts.com/structure/1-Pyrenebutyric-acid-cstr-CT1001754497.html> [Accessed 8 Jul. 2021].
- Anon 2007. *Background*. [online] WHO. Available at: <http://www.fao.org/3/ac911e/ac911e04.htm> [Accessed 14 Apr. 2020].
- Anon 2019. *Normal and Diabetic Blood Sugar Level Ranges - Blood Sugar Levels for Diabetes*. [online] Available at: <https://www.diabetes.co.uk/diabetes_care/blood-sugar-level-ranges.html> [Accessed 12 Apr. 2021].
- Anon 2019. *Two Types of Macrophages: M1 and M2 Macrophages - Cusabio*. [online] cusabio. Available at: <https://www.cusabio.com/c-20938.html> [Accessed 3 Sep. 2020].
- Anon 2020. *Chronic Inflammation - Life Extension*. [online] Available at: <https://www.lifeextension.com/protocols/health-concerns/chronic-inflammation> [Accessed 14 Apr. 2020].
- Anon 2021. *Human IL-6 DuoSet ELISA DY206-05: R&D Systems*. [online] Systems, RnD. Available at: <https://www.rndsystems.com/products/human-il-6-duoset-elisa_dy206> [Accessed 8 Jul. 2021].
- Atri, C., Guerfali, F.Z. and Laouini, D., 2018. *Role of human macrophage polarization in inflammation during infectious diseases*. *International Journal of Molecular Sciences*
- Bai, Y., Xu, T. and Zhang, X., 2020. Graphene-based biosensors for detection of biomarkers. *Micromachines*, [online] 11(1). Available at: </pmc/articles/PMC7019259/?report=abstract> [Accessed 21 Jan. 2021].

- Batycka-Baran, A., Maj, J., Wolf, R. and Szepietowski, J.C., 2014. *The new insight into the role of antimicrobial proteins-alarmins in the immunopathogenesis of psoriasis. Journal of Immunology Research*, .
- Bhalla, N., Jolly, P., Formisano, N. and Estrela, P., 2016. Introduction to biosensors. *Essays in Biochemistry*, 60(1), pp.1–8.
- Bi, Y., Chen, J., Hu, F., Liu, J., Li, M. and Zhao, L., 2019. *M2 Macrophages as a Potential Target for Antiatherosclerosis. Neural Plasticity*.
- Cardoso, A.R., Marques, A.C., Santos, L., Carvalho, A.F., Costa, F.M., Martins, R., Sales, M.G.F. and Fortunato, E., 2019. Molecularly-imprinted chloramphenicol sensor with laser-induced graphene electrodes. *Biosensors and Bioelectronics*, 124–125, pp.167–175.
- Cavaillon, J.-M., 2011. The historical milestones in the understanding of leukocyte biology initiated by Elie Metchnikoff. *Journal of Leukocyte Biology*, [online] 90(3), pp.413–424. Available at: <<http://doi.wiley.com/10.1189/jlb.0211094>> [Accessed 24 Mar. 2020].
- Chanput, W., 2012. *Immunomodulating effects of food compounds : a study using the THP-1 cell line*. Wageningen University.
- Chanput, W., Mes, J.J., Savelkoul, H.F.J. and Wichers, H.J., 2013. Characterization of polarized THP-1 macrophages and polarizing ability of LPS and food compounds. *Food and Function*, [online] 4(2), pp.266–276. Available at: <<https://pubmed.ncbi.nlm.nih.gov/23135314/>> [Accessed 19 Apr. 2021].
- Chanput, W., Mes, J.J. and Wichers, H.J., 2014a. *THP-1 cell line: An in vitro cell model for immune modulation approach. International Immunopharmacology*, .
- Chanput, W., Mes, J.J. and Wichers, H.J., 2014b. *THP-1 cell line: An in vitro cell model for immune modulation approach. International Immunopharmacology*, .
- Chanput, W., Peters, V. and Wichers, H., 2015. THP-1 and U937 cells. In: *The Impact of Food Bioactives on Health: In Vitro and Ex Vivo Models*. Springer International Publishing. pp.147–159.
- Chen, H., Choo, T.K., Huang, J., Wang, Y., Liu, Y., Platt, M., Palaniappan, A., Liedberg, B. and Tok, A.I.Y., 2016. Label-free electronic detection of interleukin-6 using

- horizontally aligned carbon nanotubes. *Materials and Design*, 90, pp.852–857.
- Chikkaveeraiah, B. V., Bhirde, A., Malhotra, R., Patel, V., Gutkind, J.S. and Rusling, J.F., 2009. Single-wall carbon nanotube forest arrays for immunoelectrochemical measurement of four protein biomarkers for prostate cancer. *Analytical Chemistry*, 81(21), pp.9129–9134.
- Clark, E.R. and Clark, E.L., 1930. Relation of monocytes of the blood to the tissue macrophages. *American Journal of Anatomy*, 46(1), pp.149–185.
- Daghestani, H.N., Pieper, C.F. and Kraus, V.B., 2015. Soluble Macrophage Biomarkers Indicate Inflammatory Phenotypes in Patients With Knee Osteoarthritis.
- Damborský, P., Švitel, J. and Katrlík, J., 2016. Optical biosensors. *Essays in Biochemistry*, 60(1), pp.91–100.
- David F., Tyler E. J., L.M.S., 2013. *US9567642B2 - Methods and products related to targeted cancer therapy - Google Patents*. [online] Available at: <<https://patents.google.com/patent/US9567642>> [Accessed 30 Mar. 2020].
- Deng, C., Qu, F., Sun, H. and Yang, M., 2011. Sensitive electrochemical immunosensor based on enlarged and surface charged gold nanoparticles mediated electron transfer. *Sensors and Actuators, B: Chemical*, 160(1), pp.471–474.
- Długosz, E., Basałaj, K. and Zawistowska-Deniziak, A., 2019. Cytokine production and signalling in human THP-1 macrophages is dependent on *Toxocara canis* glycans. *Parasitology Research*, 118(10), pp.2925–2933.
- Domingo, 2010. *10 Semiconductors - conocimientos.com.ve: El grafano*. [online] Available at: <<http://conocimientossemiconductors.blogspot.com/2010/07/el-grafano.html>> [Accessed 8 Jul. 2021].
- Ebert, R.H. and Florey, H.W., n.d. *THE EXTRAVASCULAR DEVELOPMENT OF THE MONOCYTE OBSERVED IN VIVO*.
- Farooq, U., Yang, Q., Wajid Ullah, M. and Wang, S., 2019. Principle and Development of Phage-Based Biosensors. In: *Biosensors for Environmental Monitoring*.
- Fenzl, C., Nayak, P., Hirsch, T., Wolfbeis, O.S., Alshareef, H.N. and Baeumner, A.J., 2017. Laser-Scribed Graphene Electrodes for Aptamer-Based Biosensing. *ACS*

Sensors, 2(5), pp.616–620.

Fleit, H.B., 2014. Chronic Inflammation. In: *Pathobiology of Human Disease: A Dynamic Encyclopedia of Disease Mechanisms*. Elsevier Inc. pp.300–314.

Forrester, M.A., Wassall, H.J., Hall, L.S., Cao, H., Wilson, H.M., Barker, R.N. and Vickers, M.A., 2018. Similarities and differences in surface receptor expression by THP-1 monocytes and differentiated macrophages polarized using seven different conditioning regimens. *Cellular Immunology*, 332, pp.58–76.

G, R., R, V. den B. and P, D.B., 2005. Arginase-1 and Ym1 are markers for murine, but not human, alternatively activated myeloid cells. *Journal of immunology (Baltimore, Md. : 1950)*, 174(11), pp.6561–6562.

Gao, F., Zhang, X., Gao, F., Cai, X., Zheng, M., Jiang, S. and Wang, Q., 2013. Application of graphene-pyrenebutyric acid nanocomposite as probe oligonucleotide immobilization platform in a DNA biosensor. *Materials Science and Engineering C*, 33(7), pp.3851–3857.

Garg, M., Sharma, A.L. and Singh, S., 2021. Advancement in biosensors for inflammatory biomarkers of SARS-CoV-2 during 2019–2020. *Biosensors and Bioelectronics*, 171, p.112703.

Genin, M., Clement, F., Fattaccioli, A., Raes, M. and Michiels, C., 2015. M1 and M2 macrophages derived from THP-1 cells differentially modulate the response of cancer cells to etoposide. *BMC Cancer*, 15(1), p.577.

Gordon, S., 2003. *Alternative activation of macrophages*. *Nature Reviews Immunology*.

Grieshaber, D., Mackenzie, R., Vörös, J. and Reimhult, E., 2008. Electrochemical Biosensors-Sensor Principles and Architectures. *Sensors*, pp.1400–1458.

Hassani, S., Momtaz, S., Vakhshiteh, F., Maghsoudi, A.S., Ganjali, M.R., Norouzi, P. and Abdollahi, M., 2017. *Biosensors and their applications in detection of organophosphorus pesticides in the environment*. *Archives of Toxicology*, .

Heineman, W.R. and Jensen, W.B., 2006. Leland C. Clark Jr. (1918–2005). *Biosensors and Bioelectronics*, 21(8), pp.1403–1404.

Held, C., White, H.D., Stewart, R.A.H., Budaj, A., Cannon, C.P., Hochman, J.S., Koenig,

- W., Siegbahn, A., Steg, P.G., Soffer, J., Weaver, W.D., Östlund, O. and Wallentin, L., 2017. Inflammatory biomarkers interleukin-6 and c-reactive protein and outcomes in stable coronary heart disease: Experiences from the STABILITY (stabilization of atherosclerotic plaque by initiation of darapladib therapy) trial. *Journal of the American Heart Association*.
- Hinnemo, M., Zhao, J., Ahlberg, P., Hägglund, C., Djurberg, V., Scheicher, R.H., Zhang, S.L. and Zhang, Z. Bin, 2017. On Monolayer Formation of Pyrenebutyric Acid on Graphene. *Langmuir*, 33(15), pp.3588–3593.
- Hou, T., Huang, D., Zeng, R., Ye, Z. and Zhang, Y., 2015. Accuracy of serum interleukin (IL)-6 in sepsis diagnosis: A systematic review and meta-analysis. *International Journal of Clinical and Experimental Medicine*, pp.15238–15245.
- Huang, L., Su, J., Song, Y. and Ye, R., 2020. Laser-Induced Graphene: En Route to Smart Sensing. *Nano-Micro Letters*, pp.1–17.
- IHealthcareAnalyst, I., 2020. *Global Biosensor Devices Market \$27.1 Billion by 2027*. [online] iHealthcareAnalyst, Inc. Available at: <<https://www.ihealthcareanalyst.com/low-cost-non-invasive-medical-applications-biosensors-market/>> [Accessed 1 Jul. 2020].
- Italiani, P. and Boraschi, D., 2014. From Monocytes to M1/M2 Macrophages: Phenotypical vs. Functional Differentiation. *Frontiers in Immunology*, 5(OCT), p.514.
- Jiang, Z. and Zhu, L., 2016. *Update on the role of alternatively activated macrophages in asthma*. *Journal of Asthma and Allergy*
- Jiménez-Urbe, A.P., Valencia-Martínez, H., Carballo-Uicab, G., Vallejo-Castillo, L., Medina-Rivero, E., Chacón-Salinas, R., Pavón, L., Velasco-Velázquez, M.A., Mellado-Sánchez, G., Estrada-Parra, S. and Pérez-Tapia, S.M., 2019. CD80 expression correlates with IL-6 production in THP-1-like macrophages costimulated with LPS and dialyzable leukocyte extract (Transferon®). *Journal of Immunology Research*, 2019.
- Kazuo, T., Suzuki, Y., Yoshimura, K., Yasui, H., Karayama, M., Hozumi, H., Furuhashi, K., Enomoto, N., Fujisawa, T., Nakamura, Y., Inui, N., Yokomura, K. and Suda,

- T., 2019. Macrophage Mannose Receptor CD206 Predicts Prognosis in Community-acquired Pneumonia. *Scientific Reports*, 9(1), pp.1–10.
- Kelly, A., Grabiec, A.M. and Travis, M.A., 2018. Culture of human monocyte-derived macrophages. *Methods in Molecular Biology*, 1784, pp.1–11.
- Khan, M.A. and Mujahid, M., 2020. *Recent advances in electrochemical and optical biosensors designed for detection of Interleukin 6*. *Sensors (Switzerland)*, Available at: <<https://www.mdpi.com/1424-8220/20/3/646>> [Accessed 3 Apr. 2021].
- Khosravi, F., Loeian, S. and Panchapakesan, B., 2017. Ultrasensitive Label-Free Sensing of IL-6 Based on PASE Functionalized Carbon Nanotube Micro-Arrays with RNA-Aptamers as Molecular Recognition Elements. *Biosensors*, 7(4), p.17.
- Kim, Y.-J., Kim, Y., Novoselov, K. and Hong, B.H., 2015. Engineering electrical properties of graphene: chemical approaches. *2D Materials*, 2(4), p.042001.
- Kishimoto, T., 2010. IL-6: from its discovery to clinical applications. *International immunology*, 22(5), pp.347–52.
- Koorella, C., Nair, J.R., Murray, M.E., Carlson, L.M., Watkins, S.K. and Lee, K.P., 2014. Novel regulation of CD80/CD86-induced phosphatidylinositol 3-kinase signaling by NOTCH1 protein in interleukin-6 and indoleamine 2,3-dioxygenase production by dendritic cells. *Journal of Biological Chemistry*, 289(11), pp.7747–7762.
- Kozloski, G.A., 2019. Macrophage Markers. *Materials and Methods*, 9.
- Kumar, S., Ahlawat, W., Kumar, R. and Dilbaghi, N., 2015. *Graphene, carbon nanotubes, zinc oxide and gold as elite nanomaterials for fabrication of biosensors for healthcare*. *Biosensors and Bioelectronics*, .
- LC, C. and C, L., 1962. Electrode systems for continuous monitoring in cardiovascular surgery. *Annals of the New York Academy of Sciences*, 102(1), pp.29–45.
- Li, T. and Yang, M., 2011. Electrochemical sensor utilizing ferrocene loaded porous polyelectrolyte nanoparticles as label for the detection of protein biomarker IL-6. *Sensors and Actuators, B: Chemical*, 158(1), pp.361–365.
- Lin, J., Peng, Z., Liu, Y., Ruiz-Zepeda, F., Ye, R., Samuel, E.L.G., Yacaman, M.J.,

- Yakobson, B.I. and Tour, J.M., 2014. Laser-induced porous graphene films from commercial polymers. *Nature Communications*, p.5714.
- Lin, S., Feng, W., Miao, X., Zhang, X., Chen, S., Chen, Y., Wang, W. and Zhang, Y., 2018. A flexible and highly sensitive nonenzymatic glucose sensor based on DVD-laser scribed graphene substrate. *Biosensors and Bioelectronics*, 110, pp.89–96.
- Ling, C., Liu, X., Shen, Y., Chen, Z., Fan, J., Jiang, Y. and Meng, Q., 2018. Urinary CD80 excretion is a predictor of good outcome in children with primary nephrotic syndrome. *Pediatric Nephrology*, 33(7), pp.1183–1187.
- Liu, X., Yin, S., Chen, Y., Wu, Y., Zheng, W., Dong, H., Bai, Y., Qin, Y., Li, J., Feng, S. and Zhao, P., 2018a. LPS-induced proinflammatory cytokine expression in human airway epithelial cells and macrophages via NF- κ B, STAT3 or AP-1 activation. *Molecular Medicine Reports*, 17(4), pp.5484–5491.
- Liu, Y.C., Zou, X.B., Chai, Y.F. and Yao, Y.M., 2014. *Macrophage polarization in inflammatory diseases. International Journal of Biological Sciences*, .
- Liu, Z., Kuang, W., Zhou, Q. and Zhang, Y., 2018b. TGF- β 1 secreted by M2 phenotype macrophages enhances the stemness and migration of glioma cells via the SMAD2/3 signalling pathway. *International Journal of Molecular Medicine*, 42(6), pp.3395–3403.
- Lou, Y., He, T., Jiang, F., Shi, J.J. and Zhu, J.J., 2014. A competitive electrochemical immunosensor for the detection of human interleukin-6 based on the electrically heated carbon electrode and silver nanoparticles functionalized labels. *Talanta*, 122, pp.135–139.
- Mantovani, A., Sozzani, S., Locati, M., Allavena, P. and Sica, A., 2002. *Macrophage polarization: Tumor-associated macrophages as a paradigm for polarized M2 mononuclear phagocytes. Trends in Immunology*.
- Mantovani, S.K.B. and A., 2014. *Macrophage Biology and Role in the Pathology of Disease*. Springer New York Heidelberg Dordrecht London.
- Mbongue, J., Nicholas, D., Firek, A. and Langridge, W., 2014. *The role of dendritic cells in tissue-specific autoimmunity. Journal of Immunology Research*, .

- Medina, K.L., 2016. Overview of the immune system. In: *Handbook of Clinical Neurology*. Elsevier.pp.61–76.
- Mehrotra, P., 2016. *Biosensors and their applications - A review*. *Journal of Oral Biology and Craniofacial Research*, .
- Mills, C.D., Kincaid, K., Alt, J.M., Heilman, M.J. and Hill, A.M., 2000. M-1/M-2 Macrophages and the Th1/Th2 Paradigm. *The Journal of Immunology*, 164(12), pp.6166–6173.
- Mohammed Asef Iqbal, S.G.G. and H.S.S., 2012. *A Review on Electrochemical Biosensors: Principles and Applications*.
- Moore, K.J., Sheedy, F.J. and Fisher, E.A., 2013. *Macrophages in atherosclerosis: A dynamic balance*. *Nature Reviews Immunology*, .
- MouseDoctor, 2013. *IL-6 as a Biomarker in MS – Multiple Sclerosis Research Blog*. [online] Available at: <<https://multiple-sclerosis-research.org/2013/09/il-6-as-a-biomarker-in-ms/>> [Accessed 4 Apr. 2021].
- Murray, P.J., Allen, J.E., Biswas, S.K., Fisher, E.A., Gilroy, D.W., Goerdts, S., Gordon, S., Hamilton, J.A., Ivashkiv, L.B., Lawrence, T., Locati, M., Mantovani, A., Martinez, F.O., Mege, J.L., Mosser, D.M., Natoli, G., Saeij, J.P., Schultze, J.L., Shirey, K.A., Sica, A., Suttles, J., Udalova, I., VanGinderachter, J.A., Vogel, S.N. and Wynn, T.A., 2014. Macrophage Activation and Polarization: Nomenclature and Experimental Guidelines. *Immunity*, 41(1), pp.14–20.
- Nathan, C.F., Murray, H.W., Wlebe, I.E. and Rubin, B.Y., 1983. Identification of interferon- γ , as the lymphokine that activates human macrophage oxidative metabolism and antimicrobial activity. *Journal of Experimental Medicine*, 158(3), pp.670–689.
- National Center for Biotechnology Information, 1998. The p53 tumor suppressor protein. In: *Genes and Disease*. [online] National Center for Biotechnology Information (US). Available at: <<https://www.ncbi.nlm.nih.gov/books/NBK22268/>> [Accessed 8 Jul. 2021].
- Nolan, A., Kobayashi, H., Naveed, B., Kelly, A., Hoshino, Y., Hoshino, S., Karulf, M.R., Rom, W.N., Weiden, M.D. and Gold, J.A., 2009. Differential Role for CD80 and

CD86 in the Regulation of the Innate Immune Response in Murine Polymicrobial Sepsis. *PLoS ONE*, 4(8), p.e6600.

Ogi, H., 2013. *Wireless-electrodeless quartz-crystal-microbalance biosensors for studying interactions among biomolecules: A review. Proceedings of the Japan Academy Series B: Physical and Biological Sciences*, .

Pahwa R, Goyal A, Bansal P, et al., 2020. Chronic Inflammation. In: *Pathobiology of Human Disease: A Dynamic Encyclopedia of Disease Mechanisms*. Elsevier Inc.

Parisi, L., Toffoli, A., Ghezzi, B., Mozzoni, B., Lumetti, S. and Macaluso, G.M., 2020. A glance on the role of fibronectin in controlling cell response at biomaterial interface. *Japanese Dental Science Review*, 56(1), pp.50–55.

Parkin, J. and Cohen, B., 2001. *An overview of the immune system. Lancet*.

Patricia, C., 2004. Development of immunodetection assays for penicillins and sulfonamides in food of animal origin. *Detection of penicillins and sulphonamides using ELISA*.

Peach, R.J., Rgen Bajorath, J., Naemura, J., Leytze, G., Greene, J., Aruffo, A. and Linsley, P.S., 1995. *Both Extracellular Immunoglobulin-like Domains of CD80 Contain Residues Critical for Binding T Cell Surface Receptors CTLA-4 and CD28**.

Peng, J., Feng, L.-N., Ren, Z.-J., Jiang, L.-P. and Zhu, J.-J., 2011. Synthesis of Silver Nanoparticle-Hollow Titanium Phosphate Sphere Hybrid as a Label for Ultrasensitive Electrochemical Detection of Human Interleukin-6. *Small*, 7(20), pp.2921–2928.

Ponzoni, M., Pastorino, F., Di Paolo, D., Perri, P. and Brignole, C., 2018. *Targeting macrophages as a potential therapeutic intervention: Impact on inflammatory diseases and cancer. International Journal of Molecular Sciences*, .

Prabhakaran, A. and Nayak, P., 2020. Surface Engineering of Laser-Scribed Graphene Sensor Enables Non-Enzymatic Glucose Detection in Human Body Fluids. *ACS Applied Nano Materials*, 3(1), pp.391–398.

Prakrankamanant, P., 2014. *Quartz Crystal Microbalance Biosensors: Prospects for Point-of-Care Diagnostics. J Med Assoc Thai*, .

- Pupim Ferreira, A.A., Venturini, C., Souza Castilho, M. de, Canaverolo, N., Vinicius, M., dos Santos, G.P., Sadao, C., Vicente, A. and Yamanak, H., 2013. Amperometric Biosensor for Diagnosis of Disease. In: *State of the Art in Biosensors - Environmental and Medical Applications*. InTech.
- Qin, Z., 2012. *The use of THP-1 cells as a model for mimicking the function and regulation of monocytes and macrophages in the vasculature. Atherosclerosis*, .
- Rawlings, J.S., Rosler, K.M. and Harrison, D.A., 2004. The JAK/STAT signaling pathway. *Journal of Cell Science*, 117, pp.1281–1283.
- Ridker, P.M., 2009. *C-Reactive protein: Eighty years from discovery to emergence as a major risk marker for cardiovascular disease. Clinical Chemistry*.
- Rocchitta, G., Spanu, A., Babudieri, S., Latte, G., Madeddu, G., Galleri, G., Nuvoli, S., Bagella, P., Demartis, M.I., Fiore, V., Manetti, R. and Serra, P.A., 2016. Enzyme Biosensors for Biomedical Applications: Strategies for Safeguarding Analytical Performances in Biological Fluids.
- Russell, C., Ward, A.C., Vezza, V., Hoskisson, P., Alcorn, D., Steenson, D.P. and Corrigan, D.K., 2019. Development of a needle shaped microelectrode for electrochemical detection of the sepsis biomarker interleukin-6 (IL-6) in real time. *Biosensors and Bioelectronics*, 126, pp.806–814.
- Sabaka, P., Koščálová, A., Straka, I., Hodosy, J., Lipták, R., Kmotorková, B., Kachlíková, M. and Kušnírová, A., 2021. Role of interleukin 6 as a predictive factor for a severe course of Covid-19: retrospective data analysis of patients from a long-term care facility during Covid-19 outbreak. *BMC Infectious Diseases* 2021 21:1, 21(1), pp.1–8.
- Salvo, P., Dini, V., Kirchhain, A., Janowska, A., Oranges, T., Chiricozzi, A., Lomonaco, T., Di Francesco, F. and Romanelli, M., 2017. *Sensors and biosensors for C-reactive protein, temperature and pH, and their applications for monitoring wound healing: A review. Sensors (Switzerland)*, .
- Sam, S., Touahir, L., Salvador Andresa, J., Allongue, P., Chazalviel, J.N., Gouget-Laemmel, A.C., De Villeneuve, C.H., Moraillon, A., Ozanam, F., Gabouze, N. and Djebbar, S., 2010. Semiquantitative study of the EDC/NHS activation of acid

- terminal groups at modified porous silicon surfaces. *Langmuir*, 26(2), pp.809–814.
- Schneemann, M. and Schoeden, G., 2007. Macrophage biology and immunology: man is not a mouse. *Journal of Leukocyte Biology*, 81(3), pp.579–579.
- Sciences, E.L., 2020. *COVID-19 and the Cytokine Storm the crucial role of IL-6 - Enzo Life Sciences*. [online] Available at: <<https://www.enzolifesciences.com/science-center/technotes/2020/april/covid-19-and-the-cytokine-storm-the-crucial-role-of-il-6/>> [Accessed 15 Jul. 2020].
- Sharpe, M. and Mount, N., 2015. *Genetically modified T cells in cancer therapy: Opportunities and challenges. DMM Disease Models and Mechanisms*, .
- Sharrock, J., 2019. Natural Killer Cells and Their Role in Immunity - European Medical Journal. *EMJ Allergy & Immunology*.
- SJ, U. and GP, H., 1967. Reagentless substrate analysis with immobilized enzymes. *Science (New York, N.Y.)*, 158(3798), pp.270–272.
- Song, J., Park, D.W., Moon, S., Cho, H.J., Park, J.H., Seok, H. and Choi, W.S., 2019. Diagnostic and prognostic value of interleukin-6, pentraxin 3, and procalcitonin levels among sepsis and septic shock patients: A prospective controlled study according to the Sepsis-3 definitions. *BMC Infectious Diseases*, 19(1), p.968.
- Stone, W.L., Basit, H. and Burns, B., 2020. Pathology, Inflammation. *Nephrology Dialysis Transplantation*, 29(suppl 3), pp.iii25–iii26.
- Suzuki, Y., Shirai, M., Asada, K., Yasui, H., Karayama, M., Hozumi, H., Furuhashi, K., Enomoto, N., Fujisawa, T., Nakamura, Y., Inui, N., Shirai, T., Hayakawa, H. and Suda, T., 2018. Macrophage mannose receptor, CD206, predict prognosis in patients with pulmonary tuberculosis. *Scientific Reports*, 8(1), pp.1–9.
- Tanaka, T., Narazaki, M. and Kishimoto, T., 2014. Il-6 in inflammation, Immunity, And disease. *Cold Spring Harbor Perspectives in Biology*, 6(10).
- Tarique, A.A., Logan, J., Thomas, E., Holt, P.G., Sly, P.D. and Fantino, E., 2015. Phenotypic, functional, and plasticity features of classical and alternatively activated human macrophages. *American Journal of Respiratory Cell and Molecular Biology*, 53(5), pp.676–688.

- TAS, F., BILGIN, E., KARABULUT, S., TASTEKIN, D. and DURANYILDIZ, D., 2016. Levels of serum fibronectin as a biomarker in gastric cancer patients: Correlation with clinical diagnosis and outcome. *Molecular and Clinical Oncology*, 4(4), pp.655–659.
- Tehrani, F. and Bavarian, B., 2016. Facile and scalable disposable sensor based on laser engraved graphene for electrochemical detection of glucose. *Scientific Reports*, 6(1), pp.1–10.
- Tertis, M., Leva, P.I., Bogdan, D., Suci, M., Graur, F. and Cristea, C., 2019. Impedimetric aptasensor for the label-free and selective detection of Interleukin-6 for colorectal cancer screening. *Biosensors and Bioelectronics*, 137, pp.123–132.
- Thangamuthu, M., Santschi, C. and Martin, O.J.F., 2018. Label-free electrochemical immunoassay for C-reactive protein. *Biosensors*, 8(2).
- ThermoFisher, 2012. *Thermo Scientific Crosslinking Technical Handbook*. [online] Available at: <<https://tools.thermofisher.com/content/sfs/brochures/1602163-Crosslinking-Reagents-Handbook.pdf>> [Accessed 6 Apr. 2021].
- Thomas A. Wynn, Ajay Chawla, and J.W.P., 2014. Origins and Hallmarks of Macrophages: Development, Homeostasis, and Disease. *PMC*.
- Tsuchiya, S., Yamabe, M., Yamaguchi, Y., Kobayashi, Y., Konno, T., Tada, K. and Kobayashi, Y., 1980. *Establishment and characterization of a human acute monocytic leukemia cell line (THP-1)*.
- Vainer, N., Dehlendorff, C. and Johansen, J.S., 2018. *Systematic literature review of IL-6 as a biomarker or treatment target in patients with gastric, bile duct, pancreatic and colorectal cancer. Oncotarget*, .
- Vanegas, D., Patiño, L., Mendez, C., Oliveira, D., Torres, A., Gomes, C. and McLamore, E., 2018. Laser Scribed Graphene Biosensor for Detection of Biogenic Amines in Food Samples Using Locally Sourced Materials. *Biosensors*, 8(2), p.42.
- Vaughan, E., Iacopino, D., Larrigy, C., Burke, M., Sygellou, L., Quinn, A.J. and Galiotis, C., 2020. Visible laser scribing fabrication of porous graphitic carbon electrodes: Morphologies, electrochemical properties, and applications as disposable sensor

- platforms. *ACS Applied Electronic Materials*, 2(10), pp.3279–3288.
- Vijayan, V., Pradhan, P., Braud, L., Fuchs, H.R., Gueler, F., Motterlini, R., Foresti, R. and Immenschuh, S., 2019. Human and murine macrophages exhibit differential metabolic responses to lipopolysaccharide - A divergent role for glycolysis. *Redox Biology*, 22, p.101147.
- Wang, C., Yu, X., Cao, Q., Wang, Y., Zheng, G., Tan, T.K., Zhao, H., Zhao, Y., Wang, Y. and Harris, D.C., 2013. Characterization of murine macrophages from bone marrow, spleen and peritoneum. *BMC Immunology* 2013 14:1, 14(1), pp.1–10.
- Wang, G., Huang, H., Wang, B., Zhang, X. and Wang, L., 2012. A supersandwich multienzyme–DNA label based electrochemical immunosensor. *Chemical Communications*, 48(5), pp.720–722.
- Wang, G., Huang, H., Zhang, G., Zhang, X., Fang, B. and Wang, L., 2011. Dual amplification strategy for the fabrication of highly sensitive interleukin-6 amperometric immunosensor based on poly-dopamine. *Langmuir*,
- Wang, W., Mai, Z., Chen, Y., Wang, J., Li, L., Su, Q., Li, X. and Hong, X., 2017. A label-free fiber optic SPR biosensor for specific detection of C-reactive protein. *Scientific Reports*, 7(1), pp.1–8.
- WK, L., CA, V., WT, H., HW, N., FW, V., GJ, W. and CE, H., 1999. C-reactive protein as a cardiovascular risk factor: more than an epiphenomenon? *Circulation*, 100(1), pp.96–102.
- WS, T. and T, F., 1930. SEROLOGICAL REACTIONS IN PNEUMONIA WITH A NON-PROTEIN SOMATIC FRACTION OF PNEUMOCOCCUS. *The Journal of experimental medicine*, 52(4), pp.561–571.
- Xu, G., Jarjes, Z.A., Desprez, V., Kilmartin, P.A. and Travas-Sejdic, J., 2018. Sensitive, selective, disposable electrochemical dopamine sensor based on PEDOT-modified laser scribed graphene. *Biosensors and Bioelectronics*, 107, pp.184–191.
- Yang, T., Wang, S., Jin, H., Bao, W., Huang, S. and Wang, J., 2013. An electrochemical impedance sensor for the label-free ultrasensitive detection of interleukin-6 antigen. *Sensors and Actuators, B: Chemical*, 178, pp.310–315.

- Zasłona, Z., Przybranowski, S., Wilke, C., van Rooijen, N., Teitz-Tennenbaum, S., Osterholzer, J.J., Wilkinson, J.E., Moore, B.B. and Peters-Golden, M., 2014. Resident Alveolar Macrophages Suppress, whereas Recruited Monocytes Promote, Allergic Lung Inflammation in Murine Models of Asthma. *The Journal of Immunology*, 193(8), pp.4245–4253.
- Zhang, G., 2009. Nanostructure-Enhanced Surface Acoustic Waves Biosensor and Its Computational Modeling. *Journal of Sensors*.
- Zhang, J., Hao, Y., Ou, W., Ming, F., Liang, G., Qian, Y., Cai, Q., Dong, S., Hu, S., Wang, W. and Wei, S., 2020. Serum interleukin-6 is an indicator for severity in 901 patients with SARS-CoV-2 infection: a cohort study. *Journal of Translational Medicine* 2020 18:1, 18(1), pp.1–8.
- Zhou, Y., Fang, Y. and Ramasamy, R., 2019. Non-Covalent Functionalization of Carbon Nanotubes for Electrochemical Biosensor Development. *Sensors*, 19(2), p.392.
- Zhuang, W.R., Wang, Y., Cui, P.F., Xing, L., Lee, J., Kim, D., Jiang, H.L. and Oh, Y.K., 2019. Applications of π - π stacking interactions in the design of drug-delivery systems. *Journal of Controlled Release*, 294, pp.311–326.